Nuclear Magnetic Resonance Studies of the Conformational Preferences in 3,5-dichloro-2-hydroxythiophenol, and the Rotational Barrier in 2,6-difluoroisopropylbenzene

by

Richard P. N. Veregin

A Thesis Submitted to
the Faculty of Graduate Studies and Research
of the University of Manitoba
in partial fulfillment
of the requirements of the degree
Master of Science

Winnipeg, Manitoba

March, 1982

NUCLEAR MAGNETIC RESONANCE STUDIES OF THE CONFORMATIONAL PREFERENCES IN 3,5-DICHLORO-2-HYDROXYTHIOPHENOL, AND THE ROTATIONAL BARRIER IN 2,6-DIFLUOROISOPROPYLBENZENE

BY

RICHARD P.N. VEREGIN

A thesis submitted to the Faculty of Graduate Studies of the University of Manitoba in partial fulfillment of the requirements of the degree of

MASTER OF SCIENCE

Abstract

This thesis describes studies of the conformational preferences in 3,5-dichloro-2-hydroxythiophenol, and the rotational barrier in 2,6-difluoroisopropylbenzene, using high-resolution nuclear magnetic resonance.

The long-range spin-spin coupling constants for the sidechain protons in 3,5-dichloro-2-hydroxythiophenol show that the compound exists as a mixture of three conformers in CCl_4 solution at 305 K. The conformer, in which the S-H bond is held roughly perpendicular to the ring plane by an O-H···3p hydrogen bond, is 13 % abundant. The other two conformers, of roughly equal proportions, contain an O-H···Cl hydrogen bond. One of these has the S-H bond cis to the OH group, the other has it trans. The chemical shifts of the S-H proton and of H-6 are in agreement with these conclusions. The free energy preference of the O-H···Cl over the O-H···S bond is 1140 ± 100 cal/mole at 305 K. The five-bond coupling between the sidechain protons is negative and very likely involves proximate interactions via lone pairs on either or both sulfur and oxygen.

Dynamic fluorine nmr measurements on 2,6-difluoroisopropylbenzene in solution, between 140 and 200 K, give the free energy, enthalpy and entropy of activation for the internal rotation of the isopropyl group. The ground state conformer has the α C-H bond in the plane of the ring, and the transition state conformer has this bond in a plane perpendicular to the ring. A purely empirical correlation, relating the barrier to internal rotation in α,α,2,6-tetrasubstituted toluenes with the van der Waals volumes and separations of the α and ortho

substituents, is found. It is concluded that the rotational barriers in these compounds are dominated by steric interactions between the α and ortho substituents.

The long-range six-bond coupling between the α proton of the sidechain and the para ring proton in 2,6-difluoroisopropylbenzene gives the two-fold potential energy barrier in acetone-d_6 at 305 K. This barrier is in good agreement with that determined by the dynamic nmr method.

In isopropylbenzenes, the five-bond coupling between the methyl protons and the fluorine nucleus, and the four-bond coupling between the α C-H proton and the fluorine nucleus, are small and positive when the nuclei involved in the coupling are proximate, and are likely dominated by a through-space mechanism. The four-bond coupling is small and negative when the C-H bond lies trans to the C-F bond, and may be dominated by a σ-mechanism.

Acknowledgements

I wish to thank Dr. T. Schaefer for his encouragement, guidance, and thoughtful criticism relating to this study, and to other matters.

I also wish to thank Rudy Sebastian and Kirk Marat for their invaluable contributions to this work. The work of Dr. J. Charlton and his coworkers, performing a synthesis in this study, was greatly appreciated. The assistance of Dr. D. Mckinnon with a synthesis in this study is also gratefully acknowledged.

I extend my thanks to my colleagues for many interesting discussions, sometimes related to this work. The continued support of my family and of Alison Connor has helped me pursue my studies.

Finally, I thank the Natural Sciences and Engineering Research Council for a Postgraduate Scholarship.

Table of Contents

Table of Contents (continued)

Table of Contents (continued)

List of Figures

List of Figures (continued)

List of Figures (continued)

List of Tables

Chapter I

Introduction

Many molecules exist as a mixture of conformational isomers, conformers, that can be interconverted by internal rotations about chemical bonds. These rotations are often hindered, involving changes in the internal energy of the molecule. Associated with the rotation is the free energy barrier hindering rotation, $\Delta G^{\dagger}$, and the free energy difference between the two stable isomers A and B, ΔG°, given by

$$\Delta G^{\circ} = -RT \ln K \qquad (1)$$

K is the equilibrium constant between the two isomers. From the temperature dependence of the free energies their respective enthalpies and entropies can be calculated,

$$\Delta G^{\circ} = \Delta H^{\circ} - T \Delta S^{\circ} \qquad (2)$$

$$\Delta G^{\dagger} = \Delta H^{\dagger} - T \Delta S^{\dagger} \qquad (3)$$

The energy differences between stable isomers, and the barriers to internal rotation have been determined by a variety of techniques, including measurements of entropy and heat capacity, electron diffraction, neutron scattering, dipole moment measurements, ultrasonic and dielectric absorption measurements, as well as by infrared, Raman, microwave, electron spin resonance and nuclear magnetic resonance (nmr) spectroscopy. These various methods have been discussed and compared in a number of articles.[1]

The following pages are restricted to the application of a few specific nmr techniques to studies of rotational isomerism about bonds between the sidechain and the benzene ring in benzene derivatives. Chapter

I.A describes the application of the stereospecific coupling constant, ^5J_m, to the calculation of conformer equilibrium constants. Chapter I.B describes the application of ^6J_p, and Chapter I.C the application of dynamic nuclear magnetic resonance (dnmr), to the calculation of barriers to internal rotation.

This thesis describes proton magnetic resonance studies of the conformational equilibria in 3,5-dichloro-2-hydroxythiophenol, and proton and fluorine magnetic resonance studies of the internal rotational barrier in 2,6-difluoroisopropylbenzene.

A. Determination of Conformational Equilibria Using ^5J_m

Spin-spin coupling constants have proven valuable in the determination of conformational equilibria. In benzene derivatives the stereospecific coupling, ^5J_m, over the all-trans five-bond path between the α-proton of the sidechain and a meta ring proton, may indicate the relative populations of cis and trans conformers (see Figure 1). Note that non-planar conformations may also be significantly populated near room temperature for certain sidechains. The barrier to internal rotation of the hydroxyl sidechain in phenol is 3.4 ± 0.2 kcal/mole (1 cal = 4.184 joule),[9] while that of the sulfhydryl sidechain in thiophenol is only about 0.8 kcal/mole.[10] Thus for the hydroxyl sidechain only planar conformations are considered to be significantly populated near room temperature. For a sulfhydryl sidechain non-planar conformations need to be taken into account, as has been observed.[11] Similar considerations apply to other sidechains.

One of the first conformational deductions from this stereospecific coupling was the determination of the most stable isomers in 3-nitro and 5-nitro 2-hydroxybenzaldehyde.[2] Since that time Schaefer and coworkers have determined cis-trans equilibrium constants, and have made other conformational deductions for a large number of molecules. These studies applied this stereospecific coupling to a wide variety of sidechains, including OH,[3] SH,[3f,g,23,24] CHO,[5] $CHCl_2$,[6] $CHBr_2$,[7] CHI_2,[8] and $CH(CH_3)_2$.[3h]

Rowbotham and Schaefer used the stereospecific coupling to a phenolic proton to determine the cis-trans equilibria in a series of

Figure 1

planar ortho conformers of a benzene derivative

a the cis conformer

b the trans conformer

The all-trans path of the stereospecific coupling over five bonds, $^{5}J_{m}$, is illustrated by the bold line.

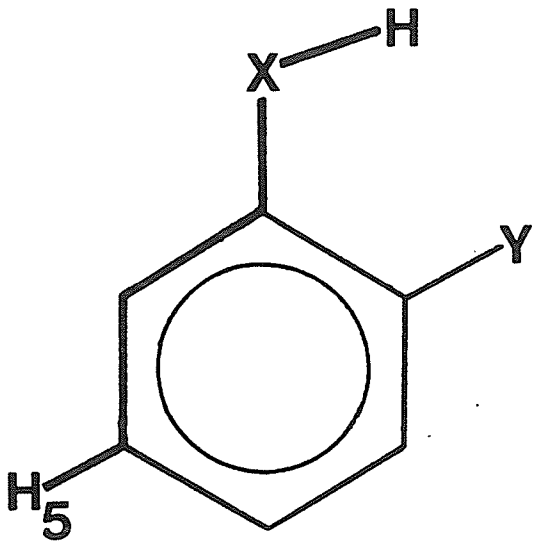

a

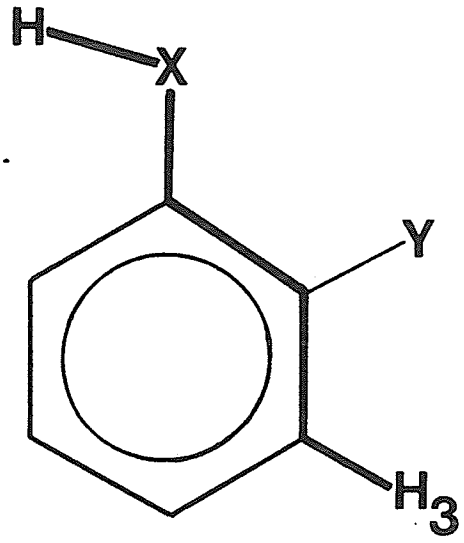

b

2,4-dihalo and 2,4,6-trihalo phenols in carbon tetrachloride solution.[3b] The results for the dihalophenols showed that neither non-planar conformations, nor cis-trans dimers need to be considered when the solute concentrations are less than 6 mole %.

Using these results, the asymmetric 2,4,6-trihalophenols yielded the order of hydrogen bond strengths, Cl ≈ Br > F > I, for the hydrogen bond between the phenolic proton and the ortho halogen atom. It was assumed that the free energy difference between conformers was solely due to the differences in the hydrogen bond strength to the two ortho halogens. It was also assumed that, for any particular molecule, the proportionality constant, J_t, between the observed all-trans coupling constant for a conformer and the population of that conformer was identical to that for the other conformer. Thus writing the equilibrium constant in mole fraction units gives,

$$K = \frac{X_5}{X_3} = \frac{X_5\, J_t}{X_3\, J_t} = \frac{J_5}{J_3} \qquad (4)$$

X_5 and X_3 are the mole fractions of conformers a and b respectively, and J_5 and J_3 are the observed coupling constants to the protons at positions 5 and 3 respectively, in Figure 1. Using (1) and (4) Rowbotham and Schaefer calculated a set of internally consistent free energy differences between the halogens.[3b] The entropy differences in these compounds were suggested to be negligible.

Further competition experiments placed the trifluoromethyl

group as forming a much weaker hydrogen bond than iodine in 2,4,6-trisubstituted phenols.[3d] Relative to iodine the free energy differences were -460 ± 60 for Cl and Br, -75 ± 20 for F, and +1230 ± 200 cal/mole for CF_3 in carbon tetrachloride solution.

The usefulness of this coupling in the determination of equilibria is limited by the accuracy with which J_5 and J_3 in (4) can be measured. Since J_t is of the order of 1 Hz, reliable results require that the free energy difference between conformers cannot be greater than about 1500 cal/mole, and thus the technique is applicable to energy differences between 0 and 1500 cal/mole. The method also requires the observation of both meta couplings, unless the sum of the two meta couplings can be deduced from other related molecules.

Further discussion of this coupling is presented in Chapter II.

B. Determination of Internal Rotational Barriers Using ^6J_p

The six-bond coupling between the α-proton of the sidechain and the para ring proton, ^6J_p, in benzene derivatives has proven useful in the deduction of conformations, and in the determination of internal rotational barriers. This coupling has a maximum magnitude when the α-proton of the sidechain lies in a plane perpendicular to the plane of the benzene ring, and vanishes when the α-proton is in the plane of the ring. The coupling can be expressed as,

$$^6J_p = {}^6J_{90} \langle \sin^2\theta \rangle \qquad (5)$$

where $^6J_{90}$ is the maximum magnitude of the six-bond coupling, and $\langle \sin^2\theta \rangle$ is the expectation value of $\sin^2\theta$. θ is the dihedral angle shown in Figure 2. This angle is zero when the α-proton is in the plane of the ring. If the value of $^6J_{90}$ is known or can be deduced, then a measurement of the coupling over six bonds determines $\langle \sin^2\theta \rangle$, which can be related to the internal rotational barrier and to the preferred conformations of the sidechain. The barrier determined in this way is the two-fold potential energy barrier, V_2, which is often taken to be equivalent to $\Delta H^\dagger$(see Appendix), and thus can be related to the free energy barrier $\Delta G^\dagger$ by (3).

In practice this method — known as the J method — is presently restricted to benzene derivatives containing sidechains with two-fold barriers to internal rotation in the range of 0.2 to 3.0 kcal/mole.

Figure 2

definition of the dihedral angle for the six-bond coupling, $^{6}J_{p}$

The dihedral angle is defined by $H_{\alpha}-C_{\alpha}-C_{1}-C_{2}$.

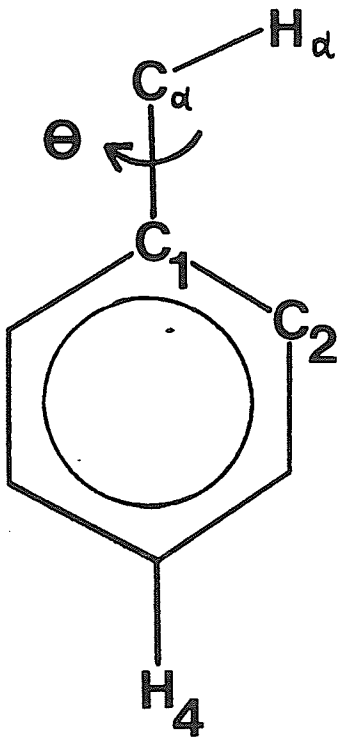

$\theta = 0^\circ$

The use of the J method has been recently reviewed.[1L] Using this method the barrier to internal rotation in phenylethane was determined to be 1.15 ± 0.20 kcal/mole about the exocyclic carbon-carbon bond, with the preferred conformation having the methyl group perpendicular to the ring.[14] These results agreed with microwave deductions,[15] and the barrier of 1.16 kcal/mole from heat capacity measurements.[16] Similarly, the barriers in isopropylbenzene,[17] phenylcyclopropane,[18] and phenylcyclohexane[19] were determined to be 1.77 ± 0.2, 1.9 ± 0.3, and 1.95 kcal/mole respectively, with the α-proton of the sidechain in the ring plane in the minimum energy conformation. These values compare well with the barrier of 2.13 kcal/mole measured for the trityl radical.[20] The similarity of these barriers suggests that their origin is in steric interactions. If a 1,3-dithiane ring replaces the cyclohexane ring the barrier is changed only slightly, while replacement by a 1,3-dioxane ring gives a barrier of only 0.4 ± 0.2 kcal/mole.[19] Thus the steric requirements of CH_3 and CH_2 groups, and sulfur atoms are similar, while those of oxygen atoms are considerably lower.

Application of the J method to benzylic sidechains, CH_2X, containing various substituents X, showed that the magnitude of the barriers increased with increasing size of the heteroatom.[1L] Barriers increased in the order $AsMe_2 > NMe_2$; SeH > SH > OH ; I ≥ Br > Cl for the substituent X.

Similarly, for benzalic sidechains, CHX_2, the barriers to internal rotation were found to increase with increasing size of the substituent X, in the order Br > Cl > F.[21]

Barriers to internal rotation about the exocyclic bond to an α-heteroatom in the sidechain have also been measured by this method. Barriers in phenyldimethyl and phenyldichloro silanes[22] are substantially lower than those in the analogous benzal compounds, although the minimum energy conformation is the same. The sidechains in phenol, benzenethiol, and benzeneselenol prefer a planar conformation, with barriers of 3.4 ± 0.2,[9] 1.1 ± 0.2[10b] and 0.35 ± 0.25 kcal/mole,[13] the latter two calculated by the J method. The decrease may be attributed to a progressive loss of lone-pair to π-electron conjugation.

Recent work using both the six-bond *para* coupling and the five-bond stereospecific *meta* coupling has determined conformational equilibria and barriers to internal rotation in thiophenol derivatives.[3f,23,24] In general the sulfhydryl proton prefers the benzene ring plane, with a value of V_2 ranging from about 2 to 4 kcal/mole. However, in 2-hydroxythiophenol the S-H bond lies in a plane perpendicular to the ring.[3g] This is interpreted as due to the formation of a hydrogen bond between the polar *ortho* O-H bond and the directional mainly 3p lone-pair on sulfur, forcing the S-H bond out of plane.

The six-bond coupling from the α-proton of a sidechain to the *para* ring proton will be discussed further in Chapter II.

C. The Application of DNMR to Internal Rotation

The first detailed kinetic study of hindered rotation using dynamic nuclear magnetic resonance spectroscopy (dnmr) was done by Newmark and Sederholm on several halogenated ethanes.[25] Since that time the dnmr method has found wide use in the determination of barriers to internal rotation.[1g]

Internal rotation about a bond interconverts the stable conformers of a molecule. If a magnetic nucleus has different magnetic environments in these conformers, then the rotation between the conformers exchanges the nucleus between magnetically non-equivalent positions, or sites, in the molecule. If the rate of this exchange is of the order of the chemical shift difference for this nucleus in two of these sites, then the shape of the nmr absorption signal for the nucleus will be affected. The dnmr method relates the shape of the nmr signal to the rate of exchange. From the rate constant for the exchange, absolute reaction rate theory (see Appendix) gives the free energy barrier to internal rotation,

$$\Delta G^{\dagger} = -RT \ln \frac{k_r h}{kT} \qquad (6)$$

k_r is the rate constant for the exchange, and other symbols have their usual meanings. The other thermodynamic parameters can then be determined from the temperature dependence of the rate constant using (3). The dnmr method is applicable to barriers from approximately 8 to 30 kcal/mole, although a barrier of 4.2 kcal/mole has been determined from dnmr spectra measured at 90 K.[26]

Compared to the situation for sp^3-sp^3 and sp^2-sp^2 bonds, little work has been done on rotation about sp^2-sp^3 bonds. A number of workers have studied rotation about the dihalomethyl-aryl bond in α,α,2,6-tetrasubstituted toluene derivatives (see Figure 3). The minimum energy conformation for these molecules is known to have the α-proton of the sidechain eclipsing one of the ortho-aryl substituents. The experimental and theoretical evidence for this ground state will be presented in Chapter II.F.

Mannschreck and Ernst have determined conformations and free energy barriers in a number of symmetrically and asymmetrically substituted benzal compounds.[27] In asymmetrically ring-substituted isopropylbenzenes the preferred conformation was found to have the α-proton eclipsing the substituent with larger van der Waals radius, the order of preference being Br > CH_3 > Cl. The free energy barriers to internal rotation increased with increasing size of the ortho-ring substituents. However, the barrier of 13.9 kcal/mole in 2,6-dimethylbenzal chloride was larger than that of 12.8 kcal/mole in 2,6-dimethylisopropylbenzene, suggesting the ortho ring chlorine causes a larger steric hinderance than an ortho ring CH_3.

These, as well as their other results do suggest that the barriers in these compounds are mainly steric in nature. Such barriers are a result of the potential energy change due to non-bonded interactions, bond stretching, interbond angle bending, and torsional strain. The order

Figure 3

α,α,2,6-tetrasubstituted toluene in a minimum energy conformation

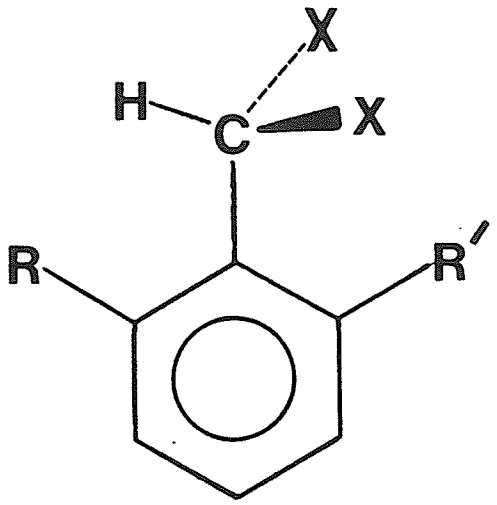
X
H
C
X
R
R'

of increasing steric requirements of the substituents is Cl ≃ CH_3 < Br, from their data. The placement of the CH_3 substituent is not certain.

Nilsson and coworkers measured free energy barriers for rotation of neopentyl sidechains in 2,4,6-trisubstituted 1,3,5-trineopentylbenzenes.[28] These predominantly steric barriers increased monotonically with the van der Waals volume (estimated by Bondi[29]) of the ortho substituents, in the order H < F < Cl < CH_3 < Br < I. The CH_3 substituent deviated slightly from this smooth curve. They attributed this deviation to their assumption that the CH_3 group is approximately cylindrically symmetric, which ignores the possibility of "gear effects" due to the "three-pronged" nature of CH_3.

A later statistical evaluation of the work of Nilsson and of others, shows that the correlations between free energy barriers and steric parameters are generally successful for substituents in both aromatic rings and attached to aliphatic carbon atoms, provided that there are at least 4 data points.[30] It was also found that the methyl group behaved as a symmetrical substituent, as did the tertiary-butyl group, which should be even more susceptible to gear effects.

Peeling measured free energy barriers, and in some cases barrier enthlapies and entropies for a number of symmetrical 2,6-dihalobenzal halides.[6,7,8,31] The barriers increased with increasing van der Waals volume of the halogens.[32] The barrier could be expressed by the empirical relation

$$\Delta G^{\ddagger} = -213.56\ S^{-1} + 30.414 \quad \text{kcal/mole} \qquad (7)$$

with an average deviation of 0.2 kcal/mole from the experimental values. The quantity S is the sum of the van der Waals volumes of the α and ortho substituents, multiplied by the difference in the internuclear separations between the α and ortho substituents for the ground state and the transition state. This type of relation might be expected for barriers due mainly to steric hinderance, which depend on the effective sizes of the substituents and on their separation in the ground and transition states.

Chapter II

Theoretical and Experimental Considerations

A. Calculation of Coupling Constants

Ramsey and Purcell proposed that the mechanism of the isotropic nuclear spin-spin coupling arose from the interaction between nuclear spins, transmitted via the magnetic polarization of the molecular electrons.[33] Considerable attention has been directed to the calculation of these coupling constants since this time, and a number of reviews have appeared.[34]

Ramsey described the coupling interaction Hamiltonian in terms of an orbital-dipole interaction between the electron orbital and the nuclear spin moments, a dipole-dipole interaction between the electron and nuclear spin moments, and the Fermi contact interaction between the electron and nuclear spin moments.[35] Since the couplings between protons and those of other light nuclei are dominated by the contact interaction, most calculations approximate the coupling Hamiltonian by the Fermi contact term alone. Fortuitously, this term has the easiest matrix elements to evaluate.

As the nuclear spin-spin coupling constants are a second-order property, they must be treated either variationally or by perturbation theory. Although variational calculations have been successful for small molecules,[36] perturbation theory is much less difficult to apply to larger systems, and thus the latter has been used in most studies.

Using second-order perturbation theory, the contact contribution to the coupling between the nuclei A and B can be calculated,

$$J_{AB} = \frac{-2}{3h} (16\pi\beta\hbar/3)^2 \gamma_A \gamma_B \sum_{n=1}^{\infty} \sum_{k}^{N} \sum_{j}^{N} \frac{\langle 0|\delta(\vec{r}_{kA})\hat{\vec{S}}_k|n\rangle\langle n|\delta(\vec{r}_{jB})\hat{\vec{S}}_j|0\rangle}{E_n - E_o} \qquad (8)$$

The symbols $|0\rangle$ and $|n\rangle$ represent the ground and excited state wavefunctions, with energies E_o and E_n respectively. The summation on n is over all discrete and continuum excited states, and summations on j and k are over all electrons. The Dirac delta function, δ, represents the "contact" between nucleus A and electron k. The symbols β, γ and $\hat{\vec{S}}$ represent the Bohr magneton, the nuclear gyromagnetic ratio and the electron spin moment operator, with other symbols having their usual meanings.

Assuming the approximation of an average excitation energy, and applying the closure approximation, which assumes the set of excited state wavefunctions is complete, leads to the expression

$$J_{AB} = \frac{-2}{3h} (16\pi\beta\hbar/3)^2 \frac{\gamma_A \gamma_B}{\Delta E} \sum_{k}^{N} \sum_{j}^{N} \langle 0|\delta(\vec{r}_{kA})\delta(\vec{r}_{jB})\hat{\vec{S}}_k \hat{\vec{S}}_j|0\rangle \qquad (9)$$

As this expression requires only the ground state wavefunction, it is much less formidable to evaluate than (8).

Using the valence bond approach, Barfield developed a method involving an explicit summation over a finite set of triplet state wavefunctions (VB SOS), and thus avoided the average energy approximation.[37] Despite criticism,[38] this method was presumed to be no more hazardous than the above average energy approximation.

Pople, McIver and Ostlund have proposed a general method of describing physical properties which are dependent on electronic structure.[39] It involved the calculation of unrestricted, self-consistent, single-determinantal molecular orbital wavefunctions in the presence of a small, finite perturbation. The Hamiltonian in the presence of this perturbation is

$$\hat{H}(\lambda) = \hat{H}_o + \sum_r \lambda_r \hat{H}'_r \tag{10}$$

where the λ are independent parameters. For a second-order property, such as a coupling constant, they showed that the Hellmann-Feynman theorem gives the expression

$$\left.\frac{\partial^2 E(\lambda)}{\partial\lambda_s \partial\lambda_r}\right|_{\lambda=0} = \left.\frac{\partial}{\partial\lambda} \langle\Psi(\lambda_s)|\hat{H}'_r|\Psi(\lambda_s)\rangle\right|_{\lambda_s=0} \tag{11}$$

where E is the interaction energy for the second-order property, and the symbol $\Psi(\lambda_s)$ indicates that the wavefunction Ψ has all λ, except λ_s, set to zero.

To calculate the coupling constant between two nuclear moments A and B, it is convenient to consider them oriented along the z-axis. Taking only the Fermi contact term into account, the Hamiltonian (10) becomes[40]

$$\hat{H}(\mu_A, \mu_B) = \hat{H}_o + \mu_A \hat{H}'_A + \mu_B \hat{H}'_B \tag{12}$$

where μ_r is the nuclear magnetic moment of nucleus r, and where

$$\hat{H}'_r = \frac{16\pi\beta}{3} \sum_k^N \delta(\vec{r}_{kr}) \hat{S}_{zk} \tag{13}$$

$\hat{S}_{zk}$ is the operator for the z-component of the spin angular moment of electron k. From (11) the reduced coupling constant is

$$K_{AB} = \frac{\partial}{\partial \mu_B} \langle \Psi(\mu_B) | \hat{H}'_A | \Psi(\mu_B) \rangle \Big|_{\mu_B = 0} \tag{14}$$

which is related to the coupling constant by, $J_{AB} = \hbar/2\pi \ \gamma_A \ \gamma_B \ K_{AB}$. The wavefunction $\Psi(\mu_B)$ can be calculated using the Hamiltonian

$$\hat{H}(\mu_B) = \hat{H}_o + \mu_B \hat{H}'_B \tag{15}$$

For unrestricted self-consistent molecular orbitals, using linear combinations of atomic orbitals in any basis and at any level of approximation,

$$K_{AB} = \frac{8\pi\beta}{3} \sum_\mu \sum_\nu \int \phi_\mu \ \delta(\vec{r}_A) \phi_\nu \ d\tau \left[\frac{\partial}{\partial \mu_B} \rho_{\mu\nu} (\mu_B) \right]_{\mu_B = 0} \tag{16}$$

The summations extend over all atomic orbitals, and $\rho_{\mu\nu}(\mu_B)$ is an element of the spin density matrix defined by

$$\underline{\rho} = \underline{P}^{\alpha} - \underline{P}^{\beta} \tag{17}$$

$\underline{P}^{\alpha}$ and $\underline{P}^{\beta}$ are the density matrices for the α and β spins. In the unrestricted SCF equations, the presence of the perturbation only changes the one-electron core part of the Fock matrices, which now

include the perturbation

$$\pm \frac{8\pi}{3} \beta\mu_B \int \phi_\mu \, \delta(\vec{r}_B)\phi_\nu \, d\tau \tag{18}$$

in the matrices for the α and β spins respectively.

Although accurate calculations for small molecules using the above LCAO-SCF approach have been made, without further approximation computational difficulties limit its usefulness for larger molecules. In the CNDO[41,42] approximation of SCF-MO theory the essential features are the use of a valence basis set, the use of a semi-empirical approach to the calculation of parameters, and the neglect of the overlap distributions $\phi_\mu\phi_\nu$ if μ and ν are different. The INDO[41,43] approach to SCF-MO theory is similar to CNDO, except that the overlap distribution for the one atomic-center exchange integrals is not neglected. In the INDO approximation the integrals in (16) and (18) become

$$\int \phi_\mu \, \delta(\vec{r}_r)\phi_\nu \, d\tau = s_r^2(0) \tag{19}$$

where $s_r^2(0)$ is the density of the valence s orbital at nucleus r. The perturbation in (18) becomes a constant, $\pm h_B$

$$h_B = \frac{8\pi}{3}\beta \, \mu_B \, s_B^2(0) \tag{20}$$

The reduced coupling constant from (16) becomes

$$K_{AB} = \left[\frac{8\pi\beta}{3}\right]^2 s_A^2(0) \, s_B^2(0)\left[\frac{\partial}{\partial h_B} \rho_{s_A s_B}(h_B)\right] h_B = 0 \tag{21}$$

Thus the coupling constant is directly proportional to the derivative, with respect to the perturbation on atom B, of the diagonal element of the spin-density matrix, ρ, corresponding to the valence s s-orbital of atom A. Using the method of finite differences,[39] the reduced coupling constant may be approximated by

$$K_{AB} = \left[\frac{8\pi\beta}{3}\right]^2 s_A^2(0)\, s_B^2(0)\, \frac{\rho_{s_A s_A}(h_B)}{h_B} \qquad (22)$$

Using the optimum value of h_B, which was found to be approximately 10^{-3}, equation (22) was shown to introduce a negligible error in the calculation of coupling constants.

These methods, CNDO-FPT and especially INDO-FPT, have recently proved popular for the calculation of coupling constants.[34]

B. Mechanisms of Nuclear Spin-spin coupling

It has been found convenient to separate nuclear spin-spin couplings into contributions from various mechanisms.[34] The separation into the σ-mechanism, the π-mechanism, and the through-space mechanism is commonly made.

In the σ-mechanism the coupling is transmitted by the σ-bond framework, although the interaction does not necessarily pass through the intervening σ-bonds. The three-bond vicinal proton-proton coupling in the H-C-C-H fragment, for example, may contain σ-contributions from the direct interaction of the electrons in the two C-H bonds.

The π-mechanism[58] involves transmission by the π-electron system. Since the nuclei are located at the nodes of the π-orbitals, the π-mechanism must involve the spin polarization of the σ-electrons, known as the σ-π interaction.[62] This follows as the contact contribution, which measures spin density at the coupled nuclei, vanishes for p-orbitals.

The through-space, or proximate coupling mechanism involves the transmission of the coupling via the direct overlap of the electron distributions of the two atoms, non-bonded but spatially proximate, containing the coupled nuclei.[34,54,105]

C. The Stereospecific ^5J_m Coupling

The stereospecific coupling over five bonds between the α-proton of the sidechain and the meta protons of aromatic rings has been studied extensively.[34,55]

An early study of some ortho-substituted benzaldehydes showed a splitting between the aldehydic proton and the meta ring proton most distant from it.[44] Observations of benzaldehydes in which the conformation of the aldehyde group was fixed usually showed a splitting of 0.7 Hz to the meta proton over the all-trans path, while the nearer meta proton was not coupled.[45] Similarly, a splitting of 0.60 Hz was observed from the aldehydic proton to the 3 position and to the 5 position, respectively, in 5-nitro and 3-nitro 2-hydroxybenzaldehyde.[2] Double irradiation experiments have shown ^5J_m to be positive in a number of aromatic aldehydes.[47]

Forsen, Akermark and Alm were unable to observe a meta coupling from the methyl protons in 2-hydroxyacetophenone, which they compared to the 0.7 Hz splitting that they observed from the aldehydic proton in benzaldehyde.[48] According to the "methyl replacement" technique,[49] the π-component of a coupling is unchanged in magnitude, although changed in sign, when a proton involved in the coupling is replaced by a methyl group. The absence of a coupling in 2-hydroxyacetophenone suggests that the stereospecific coupling is dominated by the σ-mechanism, and that the π-contribution is negligible.

Early work suggested that the hydroxyl group also exhibited the stereospecific coupling.[2,47c,48] A coupling over the all-trans

path was observed in methyl salicylate,[50] and couplings of 0.62 and 0.13 Hz were observed to the meta protons in the 4 and 6 positions, respectively, of 2-hydroxy-3-methoxybenzaldehyde.[51] Double irradiation experiments found this coupling to be positive.

Further evidence for the stereospecificity of ^5J_m has been obtained for a large number of molecules with various sidechains and aromatic rings.[5,52] Many of these studies include molecular orbital calculations, which in general predict a small, positive stereospecific coupling over the all-trans path, and a negligible coupling to the near meta proton. These INDO and CNDO/2 calculations, however, overestimate the magnitude of the coupling, with the CNDO/2 calculations giving the better agreement with experiment.

The coupling $^5J_m^{CH,H}$, from the methyl group to the meta ring proton in toluene, was separated into its σ and π contributions by Wasylishen and Schaefer.[12] They were able to show that the all-trans coupling is dominated by the σ-mechanism. They expressed the π-contribution to $^5J_m^{CH,H}$ as

$$J^{\pi} = J^{\pi}_{90} \sin^2\theta \qquad (23)$$

where J^{π}_{90} is the maximum value of the coupling when θ is 90 , with a value of 0.38 Hz in this case. The dihedral angle θ is defined in Figure 2.

Equation (23) can be rationalized by a π-mechanism[58] transmitted via hyperconjugation[49,61] between the π-orbital of the methyl group and the π-orbitals of the aromatic ring, and via the σ-π interaction[62] from

the aromatic π-orbitals to the meta aromatic ring proton. The methyl group π-orbital is a group orbital, constructed from the three methyl protons,[57] which has approximately the symmetry of a 2p π-orbital, and thus can interact strongly with the aromatic π-orbitals. For this type of π-mechanism, the overlap of the methyl π-orbital and the adjacent aromatic π-orbital, and thus the magnitude of the coupling, is expected to be proportional to the square of the sine of the dihedral angle, θ.[55,59] This overlap is a maximum at a dihedral angle of 90°, when a methyl group C-H bond lies in a plane perpendicular to the aromatic ring. Equation (23) is analogous to the McConnell-Heller equation, which has been established for the hyperfine interaction of methyl protons with unpaired spin density on adjacent π-orbitals in ESR spectroscopy.[59a,d,60]

Wasylishen and Schaefer subtracted the π-contribution in (23) from the angle dependance of the coupling calculated using INDO-FPT molecular orbital theory.[12] The remaining coupling obeys closely the square of the sine of one-half the dihedral angle, a function with twice the period of that for the π-contribution to the coupling, and was attributed to a dominant σ-contribution.

On the basis of these results one might write the coupling between the methyl protons and the meta ring proton as the sum of the σ and π contributions,

$$^{5}J_{m}^{CH,H} = 0.38 \sin^2\theta + 0.60 \sin^2(\theta/2) \qquad (24)$$

By analogy with these results for toluene, a similar relation may apply to the other sidechains and aromatic systems in which this stereospecific coupling has been observed. In the case of sidechains where only planar conformations are significantly populated, (24) predicts a small π-contribution to the coupling, with a σ-contribution that is stereospecific over the all-trans path. The coupling will have its maximum value for the all-trans orientation of bonds, and will be zero for the other planar orientation.

D. The ^6J_p Coupling

The six-bond coupling between the α-proton of a sidechain and the para proton of an aromatic ring has been quite widely studied.[1L,34,55]

Hoffman observed a splitting of 0.62 ± 0.6 Hz from the para and ortho ring protons to the methyl protons in mesitylene.[49] He attributed these couplings to the π-mechanism, transmitted by hyperconjugation. The π-contribution to the six-bond coupling from the methyl protons to the para ring proton, $^6J_p^{CH,H}$, can then be expressed by (23), as has been described in the preceeding section.

Dewar and Fahey supported this π-electron mechanism for the coupling with nmr studies on aromatic systems where the α-proton of the sidechain was in a locked conformation.[59c] In acenaphthylene, where the α-protons lie in the plane of the naphthylene ring, θ is 0°, and the six-bond coupling is not observed. This agrees with the prediction of (23), if the coupling were transmitted solely by a π-electron mechanism. In acenaphthene, θ is approximately 25° and the six-bond coupling is ± 0.5 Hz, which compares fairly well with the value of -0.3 Hz that they calculated for the π-electron mechanism.

Similarly, the six-bond coupling from the α-proton to the para ring proton in some benzal compounds[7,8,31,52a] and in

phenol[63] is zero within experimental error.* In these compounds the ground state conformation has the α-proton in the aromatic ring plane, and a barrier to rotation large enough so that out of plane conformations are not significantly populated. These studies suggest a negligible σ-contribution to this π-electron dominated coupling.

Simple molecular orbital theory predicts that the π-electron contribution to the ring proton-methyl proton coupling is proportional to the square of the mobile bond order between the carbon atoms bonded to the methyl group and to the ring proton.[58,59a,c,68] Blears, Danyluk and Schaefer found a linear relationship between the square of the mobile bond order and the observed proton-methyl proton coupling in four aromatic and allylic compounds.[69] This suggests that the couplings are transmitted by a π-electron mechanism.

The change in sign expected for a π-electron dominated coupling, according to the methyl group replacement technique, was observed by Kotowycz and Schaefer in a toluene derivative.[64] They found the sign of the six-bond methyl proton-ring proton coupling, $^{6}J_{p}^{CH_3,H}$, was negative, opposite to that for the five-bond para proton-proton coupling, $^{5}J_{p}^{H,H}$. MacDonald and Reynolds determined the six-bond methyl to ring proton coupling, $^{6}J_{p}^{CH_3,H}$, and the seven-bond methyl to methyl proton coupling, $^{7}J_{p}^{CH_3,CH_3}$, in substituted xylenes. They found that $^{6}J_{p}^{CH_3,H}$ was

---

* $^{6}J_{p}^{OH,H}$ was less than 0.03 Hz in magnitude in phenol, as determined by decoupling experiments.

-0.61 ± 0.03 Hz and -0.57 ± 0.03 Hz, and $^{7}J_{p}^{CH_3,CH_3}$ was +0.62 ± 0.03 Hz.[65] These results agree well, within experimental error, with a dominant π-mechanism, and a negligible σ-contribution.

Using VB SOS calculations,[37] Barfield and Chakrabarti determined that the π-contributions to the five-bond proton-proton coupling in benzene and the seven-bond methyl-methyl proton coupling in para-xylene were +0.65 and +0.63 respectively.[37b] These calculations agree, within experimental error, with those measured by MacDonald and Reynolds.[65] From their studies of a number of aromatic compounds Barfield and Chakrabarti[37b] concluded that $^{5}J_{p}^{H,H}$, $^{6}J_{p}^{CH_3,H}$ and $^{7}J_{p}^{CH_3,CH_3}$ are dominated by the π-electron, σ-π configuration interaction.

Wasylishen and Schaefer calculated $^{6}J_{p}^{CH_3,H}$ in toluene and $^{7}J_{p}^{CH_3,CH_3}$ in para-xylene using INDO-FPT molecular orbital theory. They calculated the six-bond coupling from an α-proton to the para ring proton in toluene as a function of the dihedral angle defined in Figure 2, and found that the coupling followed a $\sin^2\theta$ dependence very closely. Assuming that the INDO values for a 90° dihedral angle were solely due to a π-mechanism, and assuming free rotation for the methyl group to give $\langle \sin^2\theta \rangle = 1/2$, they estimated the rotationally averaged coupling, $\langle J^{\pi} \rangle$, for this mechanism as

$$\langle J^{\pi} \rangle = \frac{1}{2} J^{\pi}_{90} \qquad (25)$$

from (23). In toluene $\langle {}^{6}J_{p}^{\pi}(CH_3,H) \rangle$ was calculated to be -0.61, and in para-xylene $\langle {}^{7}J_{p}^{\pi}(CH_3,CH_3) \rangle$ to be 0.72, which compare well with the experimental values of -0.62 ± 0.02 Hz[70] and +0.62 ± 0.03 Hz[65]

respectively. Assuming free rotation of the methyl group, they also calculated the average INDO value for $^{6}J_{p}^{CH_3,H}$ in toluene as -0.64, which is very similar to $\langle {}^{6}J_{p}^{\pi}(CH_3,H)\rangle$. This indicates an almost pure π-electron mechanism for the coupling.

Rowbotham and coworkers applied SCF-FPT-MO calculations to $^{6}J_{p}^{CH_3,H}$ in benzal fluoride.[31] The value of this coupling from INDO calculations followed a $\sin^2\theta$ curve, while CNDO/2 calculations gave approximately zero couplings for all conformations. As the major difference between INDO and CNDO/2 calculations is that the latter neglects the one-centre exchange integrals, the σ-π interaction for transmission of spin-spin coupling is not operative in CNDO/2 calculations. Thus the difference in the value of the coupling in INDO and CNDO/2 calculations indicates dominant π-contribution to this coupling. However, the magnitude of the contribution is overestimated for benzal fluoride. The INDO and CNDO/2 results also support the $\sin^2\theta$ dependence of $^{6}J_{p}^{CH_3,H}$.

A recent study has applied partially restricted molecular orbital orbitals (PRMO) in the INDO-FPT method to the evaluation of transmission mechanisms of spin-spin coupling.[71] In INDO-FPT calculations the finite perturbation by a nuclear magnetic moment introduces an uneven spin distribution, which must be accomodated by utilizing spin-unrestricted SCF-MO wavefunctions. In the PRMO method unrestricted calculations are done on σ-electrons and restricted calculations on π-electrons. Subtraction of the PRMO values for a coupling from INDO-FPT values gives the π-contribution to the coupling. For the π-contribution to $^{6}J_{p}^{CH_3,H}$

in toluene using the PRMO method, Engelmann and coworkers found a $\sin^2\theta$ dependence and an average value of -0.57 Hz,[71] in good agreement with the experimental value of -0.62 ± 0.02 Hz[70] and a number of previous theoretical calculations.[71]

E. Dynamic Nuclear Magnetic Resonance

1. Classical Lineshape Theory

Theoretical expressions for the nmr spectral lineshape as a function of the rate of chemical exchange have been derived using classical calculations. A number of reviews have appeared.[72]

Although discrete spin states in a magnetic field can only be explained by quantum theory, Bloch described the nmr phenomenon by a set of classical equations[73] which provide an adequate description in the absence of nuclear spin-spin coupling. Gutowsky and coworkers derived expressions for nmr lineshapes in the presence of chemical exchange by modifying the Bloch equations.[74] For an exchange between two sites A and B, with populations p_A and p_B and chemical shifts of $\delta\omega/2$ and $-\delta\omega/2$ from their weighted average frequency ω_o, they found that the total macroscopic magnetization in the x-y plane is given by

$$G = \frac{i\ \gamma H_1\ M_o\left[(\tau_A + \tau_B) + \tau_A\ \tau_B(\alpha_A\ p_B + \alpha_B\ p_A)\right]}{(1 + \alpha_A \tau_A)(1 + \alpha_B\ \tau_B) - 1} \qquad (26)$$

The average lifetime at site A is $\tau_A = 1/k_{A\rightarrow B} = \tau/p_B$, and at site B is $\tau_B = 1/k_{B\rightarrow A} = \tau/p_A$, where the preexchange lifetime is $\tau = \tau_A\ \tau_B/(\tau_A + \tau_B)$. $k_{M\rightarrow N}$ is the rate constant for the exchange from site M to site N, H_1 is the strength of the applied rf field of frequency ω, and M_o is the static macroscopic nuclear magnetization at thermal equilibrium. The definitions $\alpha_A = (1/T_{2A}) - i(\Delta\omega + \delta\omega/2)$ and $\alpha_B = (1/T_{2B}) - i(\Delta\omega + \delta\omega/2)$ have been made, with $\Delta\omega = \omega_o - \omega$. T_2 is the effective transverse relaxation time of the magnetic nucleus in sites A and B, and can be related to the inverse of the linewidth of the nmr resonance in the absence of chemical exchange. The nmr absorption signal

is given by the imaginary part of the x-y magnetization

$$Y = \mathrm{Im}(G) \tag{27}$$

The shape of the nmr signal is determined by $\delta\omega$, T_2, τ_A, τ_B, p_A and p_B, as described by (26) and (27). For slow exchange rates, where τ is much greater than $1/\delta\omega$, two nmr signals are observed. As τ decreases the separation of the signals decreases and the signals broaden. For fast exchange rates, where τ is much less than $1/\delta\omega$, a single nmr absorption signal is observed at a frequency of ω_o. The point at which the two separate signals merge into one is known as coalescence.

McConnell derived the same equation in a much simpler manner, by including in the Bloch equations terms taking into account the chemical exchange.[75] His formulation can be easily extended to the exchange between unequally populated sites, and to multi-site exchange processes. For the exchange among n sites, each with a population p_j, it is necessary to solve n coupled equations for G_j

$$-\left[i(\omega_j - \omega) + \frac{1}{T_{2j}}\right]G_j + \sum_{k\neq j}\left[p_j \frac{G_k}{\tau'_{jk}} - p_k \frac{G_j}{\tau'_{jk}}\right] = -i\gamma H_1 M_o p_j \tag{28}$$

$$j,k = 1,2,3\ldots n$$

where ω_j, T_{2j} and p_j are the frequency in absence of exchange, the effective transverse relaxation time, and the population of site j respectively. Since the exchange is at equilibrium

$p_k \tau_{jk} = p_j \tau_{kj} = \tau'_{jk} = \tau'_{kj}$, where $\tau_{kj} = 1/k_{k\to j}$. The total x-y magnetization is given by

$$G = \sum_{j}^{n} G_j \qquad (29)$$

where the summation is over all n sites j. The nmr absorption signal is then found from (27). Equation (28) can be conveniently expressed in matrix form to be solved by matrix methods. Reeves and coworkers have developed a matrix formulation of this type for many-site exchange, and adapted it to computer calculation.[76] Equivalent equations have also been developed[77] based on Anderson's stochastic theory of random Markovian modulation.[78]

2. Rate Constant Determination from NMR lineshapes

The nmr lineshape in the presence of exchange depends on the lifetimes of the nuclei at each site. The lineshape also depends on the populations, chemical shifts, and the effective transverse relaxation times for the nuclei at each site in the absence of exchange. Since these latter parameters may not be determinable in exchange-broadened spectra, it may be necessary to find their values, and the temperature dependence of the values, from spectra that are not exchange broadened. This is followed by extrapolation or interpolation to the temperature region where exchange broadening occurs. The nmr lineshapes can then be calculated from (26) or (28) as a function of the preexchange lifetime τ, which is related to the rate constant for the exchange. The complete calculated and observed lineshapes can then be compared to determine the best value of τ.

Although the rate constant may be determined to a precision of less than ± 6 %, this method may be subject to serious systematic errors.[72a,c,79] Often these errors arise from the neglect of the temperature dependence of the chemical shifts, the linewidths and the transverse relaxation time, as well as from improper temperature calibration.[1h]

The accuracy of the dnmr method can be evaluated by comparison with results from other methods. Spin-echo nmr methods[79a,80] are usually only in moderate agreement with the dnmr method. Excellent agreement with the results of double resonance nmr[81] and with kinetic equilibration methods[82] has been obtained. These results provide a sound basis for the dnmr total lineshape analysis method.

F. The Shape of the Potential Barrier to Internal Rotation in α,α,2,6-tetrasubstituted Toluenes

Classical semi-empirical molecular mechanics calculations based on Westheimer's method[83] have been used by a number of workers to determine the conformational energies for internal rotation in some α,α,2,6-tetrasubstituted toluenes. These calculations make use of a 6-12 Lennard-Jones potential for non-bonded interactions, and allow for some bond length stretching and bond angle bending during the rotation.

Calculations by Ernst and coworkers predict that the shape of the potential barrier in some 2,6-disubstituted isopropylbenzene derivatives and α,α,2,6-tetrahalogenated toluene derivatives is that shown in Figure 4.[27a,b,7,8 32] These calculations find that the ground state conformation has the α-proton in the benzene plane, 1, and the maximum energy conformation for the transition state has the α C-H bond in a plane perpendicular to the benzene plane, 3.

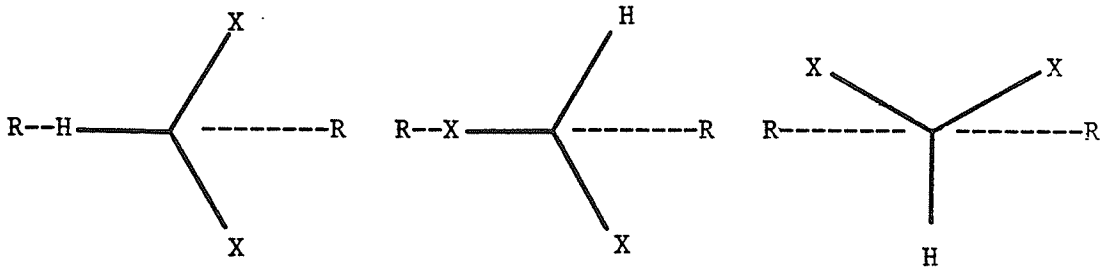

1 2 3

Figure 4

potential energy barrier calculated by Ernst's method for α,α,2,6-tetrasubstituted toluenes as a function of the dihedral angle (defined in Figure 2)

The designations 1 and 3 refer to the conformations given in the text.

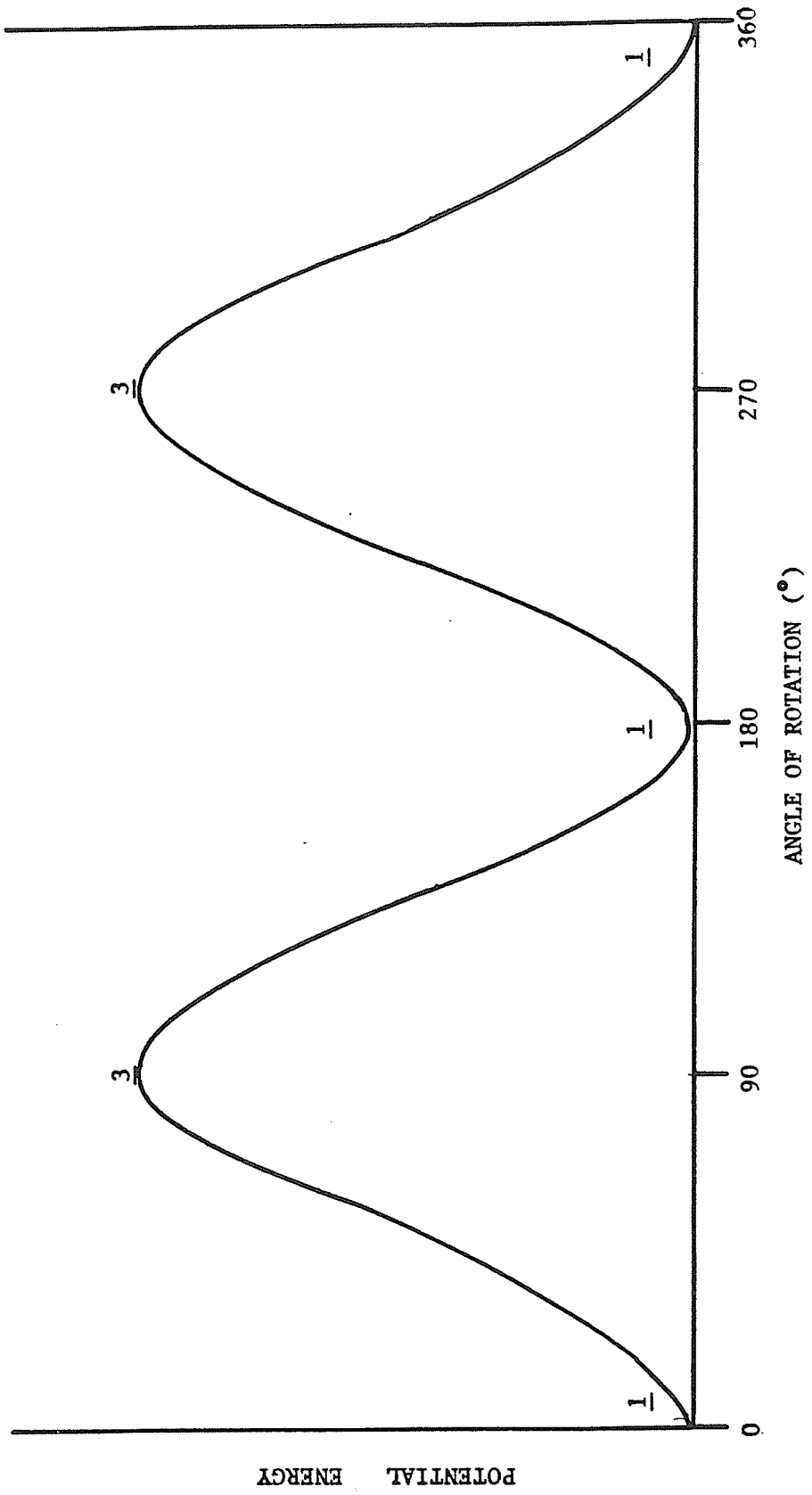
POTENTIAL ENERGY
0
90
180
270
360
ANGLE OF ROTATION (°)
1
3
1
3
1

However, calculations by Barber and Schaefer, using either a modified Buckingham potential or a van der Waals potential and a fixed molecular geometry during the internal rotation, predicted local maxima for conformations 2 and 3, with conformation 2 having the maximum potential energy. Conformation 1 was again predicted to be the ground state.[85] Although the calculations of Ernst and coworkers[27b] are preferred, as they take the flexibility of bond lengths and bond angles into account, Ernst's calculations also make approximations that may affect the shape of the barrier.[27b,32]

The available evidence does suggest that the barrier shape predicted by Ernst is the correct one. Both calculations predict that 1 is the ground state conformation. This is consistent with the zero value of the six-bond coupling between the α-proton and the para ring proton in the low temperature spectrum of 2,6-dichlorobenzal chloride,[52a] and with the downfield shift of the methine proton due to the magnetic anisotropy of the benzene ring in this compound[52a] and in 1,3,5-trimethyl-2-isopropylbenzene.[86] For the α,α,2,6-tetrasubstituted toluenes studied, Ernst's method produced calculated barrier heights that agree well with experimental measurements,[27a,b,7,8,32] while Barber's calculations are qualitative only. Furthermore, the former calculations reproduce the energy differences between the two ground state conformers in some asymmetrical 2,6-disubstituted isopropylbenzenes.[27b]

Further support for the barrier shape determined by Ernst's classical calculations comes from studies of rotational barriers in α,α′-halogenated xylyl compounds.[8] The barriers to rotation in the

xylyl compounds 4, 5 and 6 have been measured, and compared to those in the benzal compounds 7, 8 and 9.[7] It has been fairly well

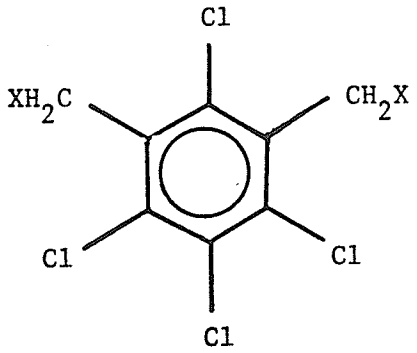

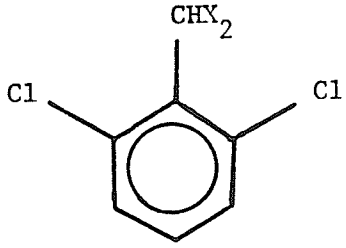

4 : X=Cl

5 : X=Br

6 : X=I

7 : X=Cl

8 : X=Br

9 : X=I

established that the ground state conformation of the xylyl compounds 4, 5 and 6 has the C-X bond perpendicular to the benzene ring plane, as in 10.[87] Clearly, the maximum energy transition state has a C-X bond which eclipses a C-Cl bond in the ring, as in 11. If Barber's

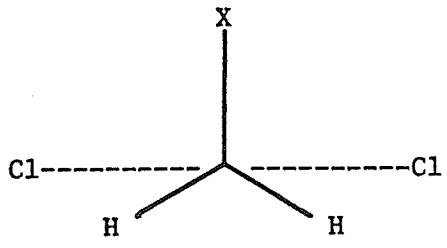

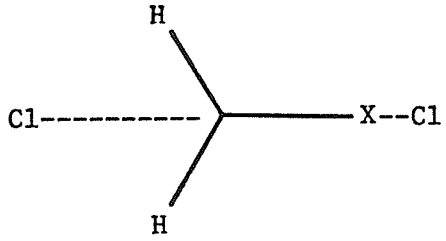

10

11

calculations are correct, 2 is the maximum energy conformation for benzal compounds. Then comparing conformations 1 and 2 with 10 and 11 suggests that the barriers to internal rotation in the xylyl compounds 4, 5 and 6 should be approximately equal to the barriers in the benzal compounds 7, 8 and 9 respectively. If Ernst's calculations are correct, then 3 is of higher energy than 2 in benzal halides. Comparing conformations 1, 2 and 3 with 10 and 11 suggests that the barriers in the xylyl compounds should be considerably lower than in the corresponding benzal compounds. Experimentally, the rotational barriers for 4, 5 and 6 are only about 60 % of the corresponding barriers in 7, 8 and 9,[8] supporting the curve predicted by Ernst.

The available evidence strongly suggests that the potential energy barrier in α,α,2,6-tetrasubstituted toluenes is that calculated by Ernst and shown in Figure 4.

Chapter III

The Three Conformations of 3,5-dichloro-2-hydroxythiophenol

A. Introduction to the Problem

The perpendicular conformation of the sulfhydryl proton in 2-hydroxythiophenol, 12 (X=H), has been deduced from nmr spin-spin couplings in dilute CCl_4 solution at 305 K.[3g] This conformational preference has been attributed to the formation of a hydrogen bond between the directional mainly 3p lone-pair on sulfur and the ortho O-H bond, which forces the S-H bond into a plane perpendicular to the benzene ring plane. The free energy preference of 12 (X=H) over the likely planar forms was at least 2 kcal/mole (1 cal = 4.184 joule), agreeing semiquantitatively with STO-3G calculations and with Schroeder-Lippencott potential functions.[88] However, the strength of the O-H··· S bond could not be measured.

The intent of the present work was to determine the conformational preferences for 3,5-dichloro-2-hydroxythiophenol using stereospecific long-range nmr coupling constants. The intent

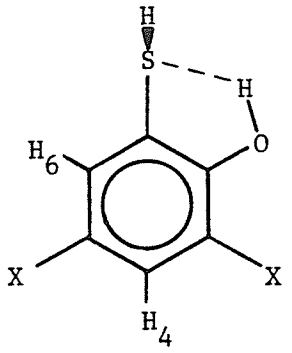

12

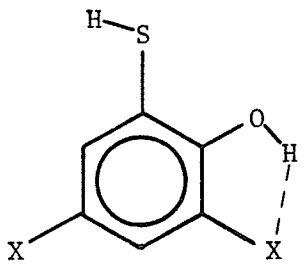

13

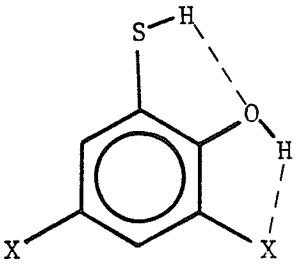

14

was to observe the competition between conformations with an O-H hydrogen bond to the ortho sulfur atom, and to the ortho chlorine atom, and thus to determine the relative strengths of the O-H···S and O-H···Cl hydrogen bonds.

The relative strength of the O-H···Cl hydrogen bond has been determined by Schaefer and Rowbotham from competition experiments in 2,4,6-trisubstituted phenols.[3b,c,d] They found the order of hydrogen bond strengths to O-H as Cl ≃ Br > F > I > CF_3.

B. Experimental Method

1. Materials

The 3,5-dichloro-2-hydroxythiophenol was prepared via the following reaction:

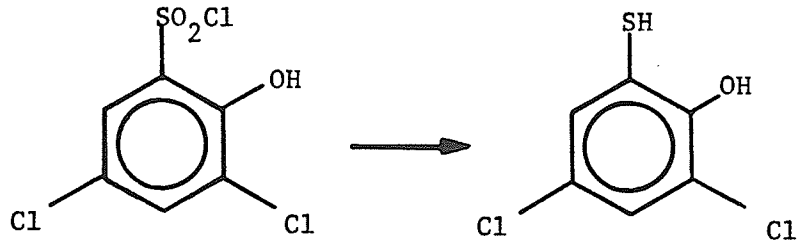

The details of the procedure, modified from that described by Adams and Marvel,[89] are given below.

To 2 grams of 3,5-dichloro-2-hydroxybenzenesulfonyl chloride (I, obtained from Aldrich Chemical) were added 40 mL of tetrahydrofuran, 2 mL of water, and 12 mL of concentrated hydrochloric acid. The solution was held at 0 °C, while 8 gm of powdered zinc was added with vigorous stirring over a half-hour period. When all evolution of gas had ceased, the mixture was warmed to room temperature, then boiled under reflux for 3 hours. The mixture was cooled, a further 5 mL of concentrated hydrochloric acid was added, and the mixture was boiled under reflux for two hours.

The mixture was filtered to remove zinc particles, and the tetrahydrofuran was removed on a rotary evaporator. The solid product was dissolved in ether, washed with dilute aqueous hydrochloric acid, and dried with magnesium sulfate. The ether was

then removed on a rotary evaporator to give approximately 0.8 gm of the product, 3,5-dichloro-2-hydroxythiophenol (II), a fine yellow powder.

The mass spectrum of the product contained peaks at 194 and 196, presumably due to the molecular ion, as well as peaks due to the loss of one chlorine atom.

The proton nmr spectrum in CCl_4 showed the expected AB doublets with a splitting of about 2.5 Hz, typical of the four-bond coupling between meta ring protons. The only impurity visible in the nmr spectrum was a weak AB doublet with a splitting of 2.5 Hz, which could not be identified with the starting material (I). Presumably, this AB doublet was due to approximately 2 mole % of a disulfide dimer of 3,5-dichloro-2-hydroxthiophenol (II). A similar dimer has been observed for 2-hydroxythiophenol.[3g]

Carbon tetrachloride was spectral grade from Fisher, and 99.5 atom % D benzene-d_6 was from Aldrich. Tetramethylsilane from Aldrich was used as an internal lock.

2. Sample Preparation

The drying procedure for retarding intermolecular exchange of the sulfhydryl and phenolic protons has been described by Rowbotham and Schaefer,[3b] and follows below.

Alfa-Ventron sieve (1/16 inch pellets with 3 Å pore size), Davison molecular sieve from Fisher (4-8 mesh beads with 3 Å pore size), precision-bore 5 mm nmr sample tubes fitted with ground glass joints, stopcocks fitted with ground glass joints, and Pasteur pipettes were dried in an oven at 200 ° C. Some of these pipettes contained wads of cotton wool to be used as a filter. The dried materials were transferred to a hot plate held at 150 ° C inside a dry box. All solvents used in the subsequent sample preparation had been previously dried by storing over dried sieve beads. The 3,5-dichloro-2-hydroxythiophenol was previously dried by pumping under vacuum for at least 8 hours. For some samples this was preceded by recrystallizing the 3,5-dichloro-2-hydroxythiophenol from benzene, before drying under vacuum.

A solution of 2 mole % of 3,5-dichloro-2-hydroxythiophenol and approximately 4 mole % of tetramethylsilane was prepared in the solvent of choice. The solution was left over dried sieve beads in a sealed vial, inside the antechamber of a dry box, for approximately five days. The vial was shaken periodically during this period. In the dry box, the sample solution was filtered through a cotton wad in a pipette, into an nmr tube containing two pellets of dried sieve. Before the tube was removed from the dry box, a stopcock was

attached to close off the sample. The sample was then degassed using the freeze-pump-thaw technique. At least seven of these cycles were performed before the nmr tube was flame-sealed. Note that the nature of this involved preparation suggests that the actual concentration of a sample will not be exactly that given.

Altogether seven samples were prepared in either carbon tetrachloride or benzene-d_6. In only a single sample was the intermolecular exchange of both the sulfhydryl and hydroxyl protons sufficiently retarded to observe all the sidechain-ring proton couplings. This sample was one of those prepared in carbon tetrachloride, and in which the 3,5-dichloro-2-hydroxythiophenol had been recrystallized from benzene before drying under vacuum. In this sample, as for 2-hydroxythiophenol,[3g] there was no doubt that the exchange was too slow to contribute to the nmr peak widths. The latter were $\leq$ 0.10 Hz at half-height, and were dominated by magnetic field inhomogeneity.

3. Spectroscopic Method

The proton magnetic resonance experiments were done on a Varian Associates HA-100-D continuous wave spectrometer, in the frequency sweep mode. A Hewlett-Packard HP 4204A oscillator was used as an external manual oscillator, except where noted, to provide a more stable lock frequency than that supplied by the spectrometer. The probe temperature was 305 ± 1 K.

Peak positions in the spectra were measured in intervals of less than 5 Hz. Each interval was recorded from low to high field four or five times. Calibration lines were placed at the beginning and at the end of each interval. The frequency of these lines was the difference between the manual and sweep oscillator frequencies, which were read from a Hewlett-Packard HP 5323A frequency counter. The average frequency and standard deviation of each peak were calculated by interpolation of the peak positions between the calibration lines on each interval. Typical standard deviations in frequency were 0.01 Hz.

Double resonance experiments[90,91] using strong (decoupling) and weak (tickling) irradiation were performed utilizing a second HP 4204A oscillator as the source of the irradiating field. The frequency and the amplitude of this field were adjusted to perturb the desired transitions.

Triple resonance experiments required both available HP 4204A oscillators to supply the irradiating fields, and thus used the

HA-100-D spectrometer manual oscillator as an internal manual oscillator to supply the lock frequency.

4. Computations

Spectral simulations were performed with the program LAME,[92] in iterative and non-iterative modes. The program was coupled to a plotting routine, which drew calculated spectra on a Versatec plotter.

INDO and CNDO/2 molecular orbital calculations were performed using standard geometries,[93] with some exceptions. The non-standard geometries used for conformations 12, 13 and 14 in 2-hydroxythiophenol (X=H), and in 3,5-dichloro-2-hydroxythiophenol (X=Cl) are given in Table 1. These geometries follow those for 2-hydroxythiophenol,[3g] which were based on a partial STO-3G optimization. For thiophenol with the S-H bond in plane, the C-S bond length was taken as 1.783 Å, the S-H bond length as 1.330 Å, and the C-S-H bond angle as 95.4°. For the perpendicular conformation these values were also used, with a C_2-C_1-S-H dihedral angle of 104.6°. For phenol with the O-H bond in the plane of the ring, the C-O bond length was taken as 1.367 Å, and the O-H bond length as 0.956 Å. The C-O-H bond angle was taken as 105°.

All computations were performed on an Amdahl 470/V7 system.

Table 1

Non-standard Geometries for INDO and CNDO/2 Calculations on 2-hydroxythiophenol and 3,5-dichloro-2-hydroxythiophenol

Conformer	Geometric Parameter[a]			
	Bond Length (Å)		Bond Angle (°)	
	O-H	S-H	C_2-O-H	C_1-S-H
12	0.990	1.334	105.0	95.5
13	0.987	1.330	105.2	95.1
14	0.987	1.330	105.4	95.4

a all angles and bond lengths from a partial STO-3G optimization of 2-hydroxythiophenol, reference 3g; C-O and C-S bond lengths of 1.390 Å and 1.783 Å respectively, were used for all conformations, with a C_2-C_1-S-H angle of 104.6°.

C. Experimental Results

1. LAME Spectral Analysis

The proton nmr spectral parameters for 2.0 mole % solutions of 3,5-dichloro-2-hydroxythiophenol in carbon tetrachloride and in benzene-d_6 at 305 K are tabulated in Table 2. Also tabulated are aromatic solvent induced shifts (ASIS), the resonance frequency relative to internal TMS in CCl_4 minus the resonance frequency relative to internal TMS in benzene-d_6.

For the sample in CCl_4, the spectral parameters are those calculated by the computer program LAME. The signs of the coupling constants are those found by multiple resonance experiments. The numbers in parentheses are the standard deviations in the last digit of the parameters, and were also calculated by LAME. These quoted errors are considered to be compatible with the calibration errors of the analysis.

Laatikainen has studied the error estimates of LAOCOON3-type analyses, and has found them reliable when the accuracy of the observed spectrum is known.[95] Schaefer and Sebastian[96] have recently shown that the measurement errors need not be an important source of error in spectral parameters, and accuracies of at least 0.01 Hz are obtainable with calibrations of the type used here.

For the 3,5-dichloro-2-hydroxythiophenol sample in CCl_4, the analysis was highly precise, as spectral linewidths were small, less than 0.10 Hz, and as all of the calculated transitions were assigned. In view of these considerations, the confidence limits for the spectral

Table 2

Proton NMR Spectral Parameters[a] for 3,5-dichloro-2-hydroxythiophenol at 305 K.

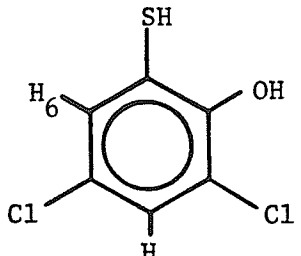

	2.0 mole % in CCl_4[b]	2.0 mole % in C_6D_6[c]	ASIS[d] (Hz)
ν_{SH}	373.302(2)	316.8	56.5
ν_{OH}	582.090(2)[e]	529.9	52.2
ν_4	711.726(3)	675.3	36.4
ν_6	714.867(3)	675.3	39.6
^4J_mH(4),H(6)	2.402(3)[f]	-	-
^5J_mOH,H(4)	0.084(4)	-	-
^5J_mOH,H(6)	0.550(4)	-	-
^4J_oSH,H(6)	-0.115(4)	-	-
^6J_pSH,H(4)	-0.271(4)	-	-
^5J_oSH,OH	-0.253(3)	-	-
rms deviation	0.0054		
largest deviation	0.011		
peaks observed	31		
transitions calculated	33		
transitions assigned	33		

Notes for Table 2

a at 305 ± 1 K; chemical shifts in Hz at 100 MHz to low-field of internal TMS; coupling constants in Hz; numbers in parentheses are standard deviations in last digit of parameters

b calculated from a LAME analysis

c chemical shifts measured directly from nmr spectrum; couplings not observed due to fast intermolecular exchange, and chemical shift degeneracy of ring protons

d aromatic solvent induced shift, the chemical shift relative to internal TMS in CCl_4 minus the chemical shift relative to internal TMS in C_6D_6

e A 1.9 mole % solution of 2,4,6-trichlorophenol has ν_{OH} as 561.8 Hz at 305 K and 100 MHz in CCl_4.

f The signs of all couplings were determined by multiple resonance experiments relative to $^4J_m^{H(4),H(6)}$.

parameters should lie within three times their standard deviations.

The experimental and calculated spectra of the ring protons are shown in Figure 5, and of the sulfhydryl and hydroxyl protons in Figure 6.

For the 3,5-dichloro-2-hydroxythiophenol sample in benzene-d_6, the spectral parameters were measured directly from the spectrum. Due to the degeneracy of the 4 and 6 ring protons, and the fast intermolecular exchange in this sample, no couplings were resolved. A more detailed analysis was not considered useful, and was not attempted.

Figure 5

the spectra of the ring protons of 3,5-dichloro-2-hydroxythiophenol

a calculated spectrum

b observed spectrum

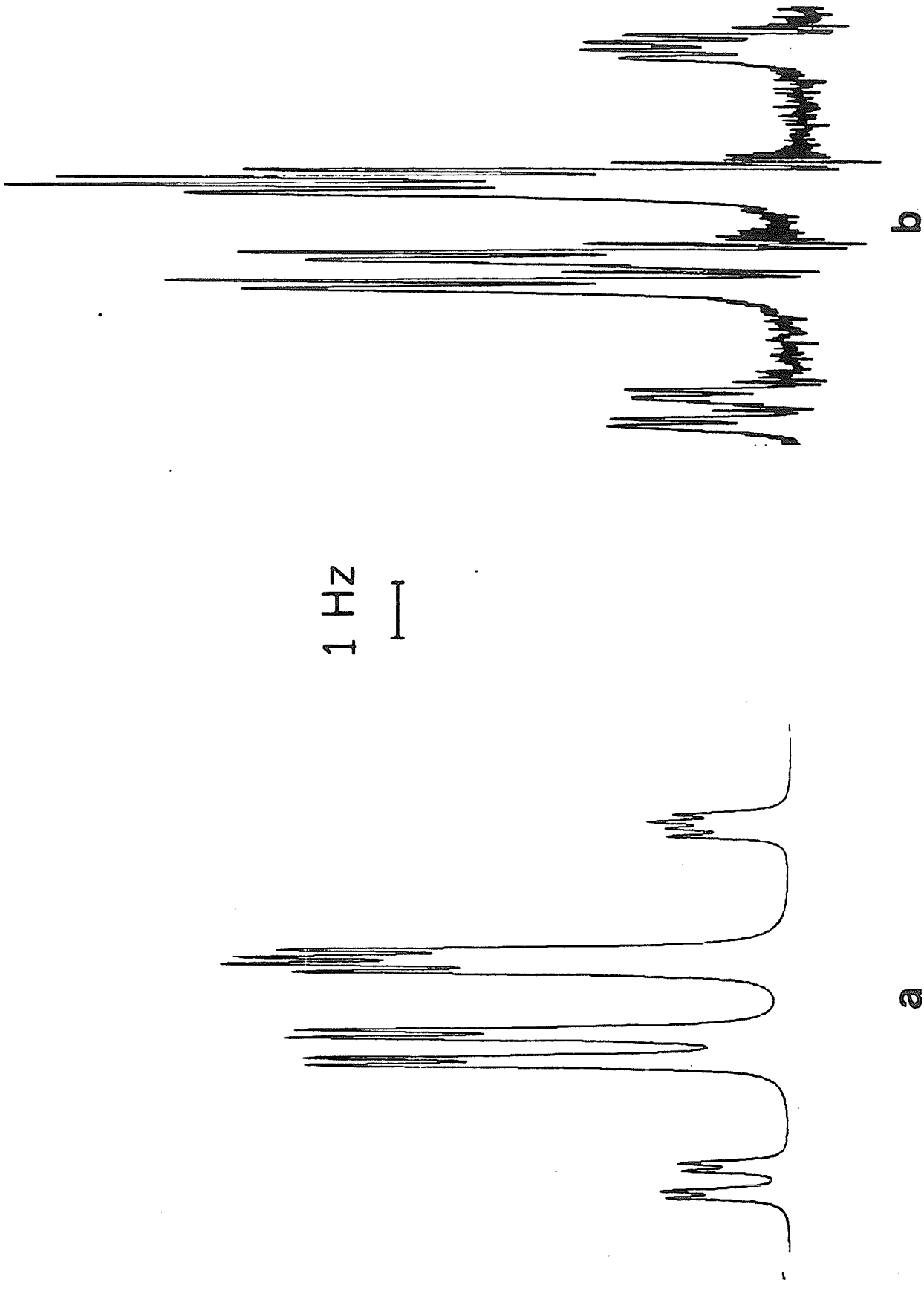
b
1 Hz
a

Figure 6

the spectra of the hydroxyl and sulfhydryl protons of 3,5-dichloro-2-hydroxythiophenol

a calculated spectrum of the hydroxyl proton resonance

b observed spectrum of the hydroxyl proton resonance

c calculated spectrum of the sulfhydryl proton resonance

d observed spectrum of the sulfhydryl proton resonance

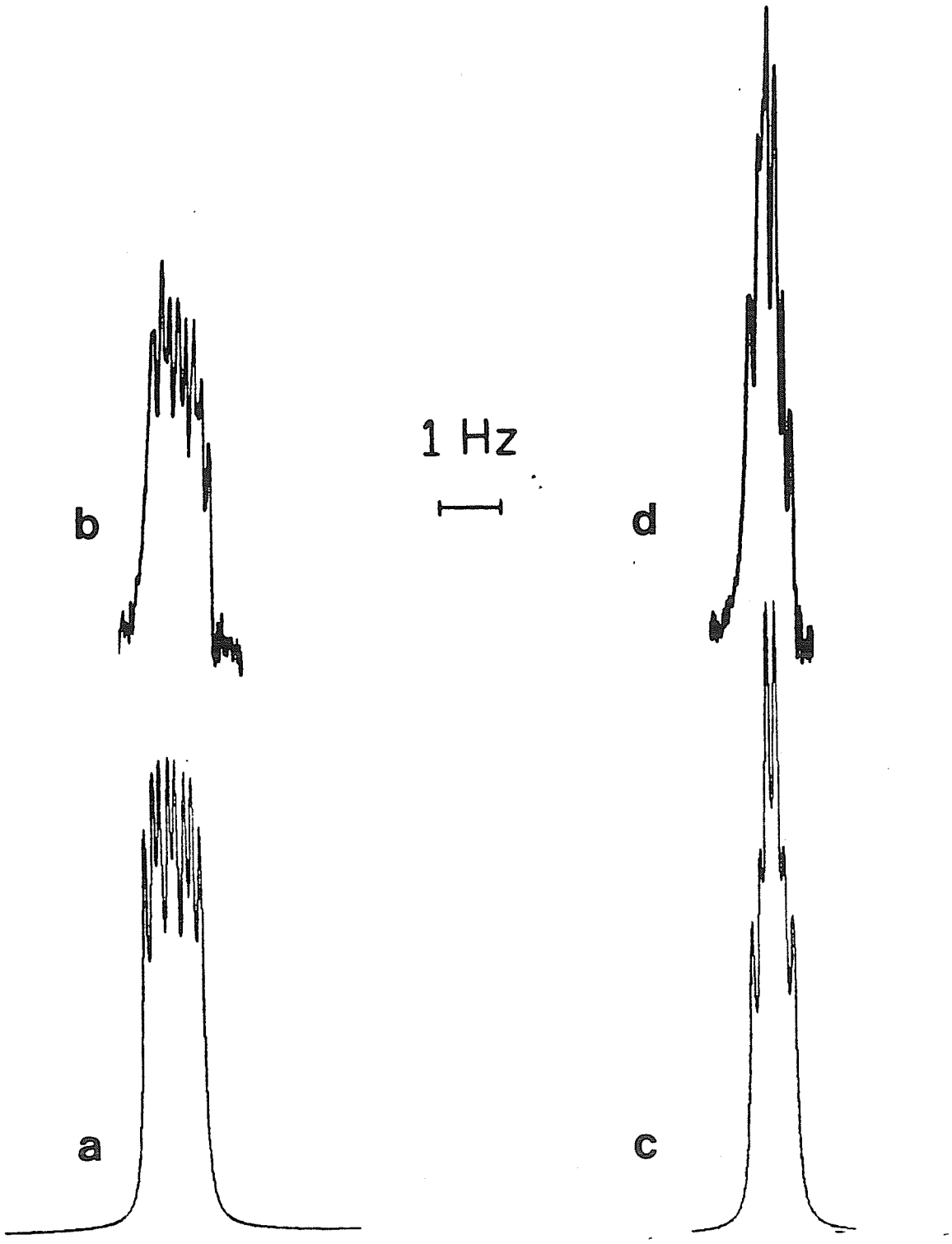
1 Hz
a
b
c
d

2. Assignment of the Ring Proton Resonances

For the spectral analysis of the ABMX spectrum of 3,5-dichloro-2-hydroxythiophenol given in Table 2, the low-field doublet in the AB region was assigned to the ring proton 6, and the high-field doublet to the ring proton 4 (see Figure 5). This assignment may be confirmed as follows.

The proton chemical shifts with respect to TMS in chlorobenzene are 7.265 ppm and 7.141 ppm, ortho and para to the chlorine substituent[97] respectively, and in 2-hydroxythiophenol are 7.382 and 7.156 ppm, ortho and para to the sulfhydryl substituent[3g] respectively. The former was measured as a 12 mole % solution in CCl_4, the latter as a 1.9 mole % solution in CCl_4. The chemical shift for a 3 mole % solution of benzene in CCl_4 is 7.253 ppm.[98] Using these values and assuming a simple additivity scheme for substituent effects, the chemical shifts of the ring protons in 3,5-dichloro-2-hydroxythiophenol can be calculated. Ring proton 6 is predicted to be 10 Hz to low-field of proton 4 according to this scheme, compared to the observed difference of 3.1 Hz for the assignment in Table 2. It should be noted that this calculation does not include the effect of conformational changes in the sidechain protons on the chemical shifts of the ring protons. Although the above agreement is only qualitative, this calculation does support the ring proton assignments.

Further support derives from the aromatic solvent induced shifts (ASIS). The change in proton chemical shifts for a solute in

a non-aromatic solvent, compared to that in an aromatic solvent, has been interpreted in terms of a preferential "packing" of the aromatic solvent about the solute, compared to the solvent packing about the approximately spherical TMS reference molecule. It has been observed that the π-electron rich area above the plane of the aromatic ring, on the average, avoids the electron-rich regions of the solute molecule.[100] Since the diamagnetic anisotropy of the aromatic ring produces a magnetic shielding above the plane of the ring, and a deshielding in the plane of the ring,[99] the electron rich areas of the solute will show the least shielding due to the aromatic solvent, and thus the lowest ASIS. According to this model, for 3,5-dichloro-2-hydroxythiophenol the S-H proton should be the most shielded and have the highest ASIS, followed by the O-H proton, H6, and H4, the latter being flanked by two electronegative chlorine atoms. The observed ASIS values follow this order, confirming the ring proton assignment.

3. Determination of the signs of $^{5}J_{m}^{H(4),OH}$ and $^{5}J_{m}^{H(6),OH}$

A first-order representation of the stick spectrum for the ring proton resonances 4 and 6, and of the hydroxyl proton resonance, is depicted in Figure 7. The coupling between these transitions and the sulfhydryl proton resonance has been ignored.

The position of a transition within a multiplet depends on the magnetic environment of the nucleus undergoing that transition. Thus each transition for a nucleus corresponds to a specific orientation of all the other coupled nuclei in the molecule. Suppose the proton spin states are assigned as + and −, where the low-field transition is designated as + for a positive coupling constant. Then Figure 7 can be constructed by extending this assignment, assuming all coupling constants have the signs given in Table 2. However, note that the high-resolution nmr Hamiltonian is symmetric with respect to the reversal of all the signs, and thus only the relative signs of the coupling constants can be deduced from the spectrum.

Irradiation of a particular transition or transitions in the resonance multiplet of a proton will only perturb those transitions, in the resonance multiplets of all other coupled magnetic nuclei, that share a common energy level. As the signs of the coupling constants determine which transitions have a common energy level, the relative signs can be determined from multiple resonance experiments.

The determination of the sign of $^{5}J_{m}^{H(4),OH}$ required a triple resonance experiment, in which two irradiating fields were applied. A strong irradiating field was applied to the sulfhydryl proton resonance,

Figure 7

a first-order representation of transitions in the ring proton resonances 4 and 6, and in the hydroxyl proton resonance of 3,5-dichloro-2-hydroxythiophenol

The coupling to the sulfhydryl proton resonance has been ignored. The table below the stick spectrum depicts the spin states of coupled protons not involved in the transitions, assuming the signs of the coupling constants are those given in Table 2.

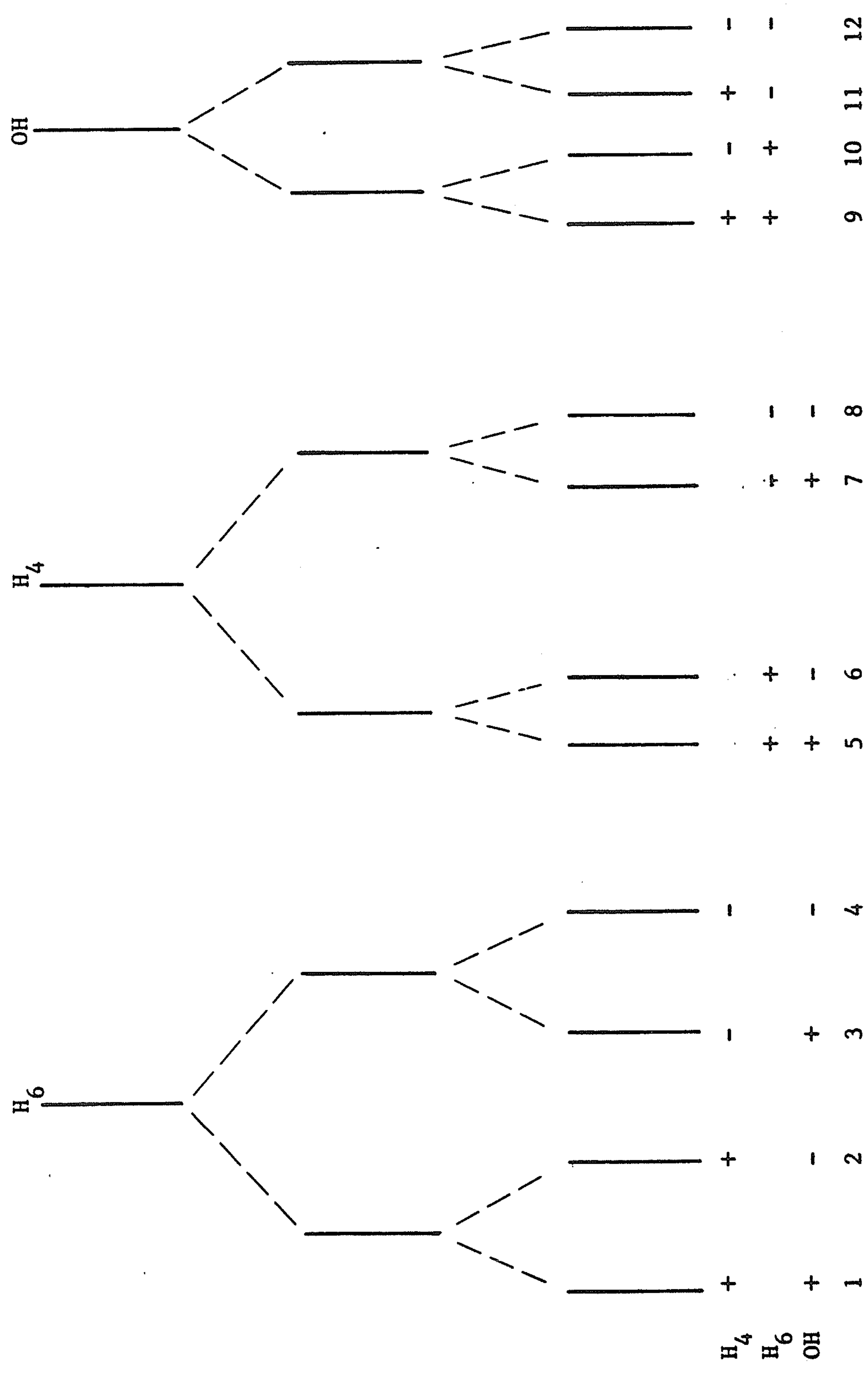
H6
H4
OH
H4
H6
OH
1
2
3
4
5
6
7
8
9
10
11
12

to decouple this resonance from all the other proton resonances. Simultaneously, a field of intermediate strength irradiated transitions 1 and 2 in the resonance multiplet of proton 6. This second field perturbs the transitions of proton 6 for the + spin state of proton 4, and both spin states of the O-H proton. This decouples transitions in the hydroxyl proton multiplet which have a + spin state for proton 4, from proton 6. These transitions should then collapse from a doublet to a singlet in this experiment. From Figure 7 it can be seen that only the signs of $^{4}J_{m}^{H(4),H(6)}$ and $^{5}J_{m}^{H(4),OH}$ determine which hydroxyl proton transitions collapse. The sign of $^{4}J_{m}^{H(4),H(6)}$ is known[101] to be positive in benzene, and is presumably unchanged in benzene derivatives. If $^{5}J_{m}^{H(4),OH}$ is positive, as was assumed in Figure 7, then irradiation of transitions 1 and 2 will collapse the doublet consisting of transitions 9 and 11 of the hydroxyl proton resonance, to a singlet. If $^{5}J_{m}^{H(4),OH}$ is negative, then the sign designations in Figure 7 for proton 4 in the hydroxyl resonance must be reversed, and transitions 10 and 12 are predicted to collapse to a singlet. Similarily, irradiation of transitions 3 and 4 will cause collapse of transitions 10 and 12 if the sign of $^{5}J_{m}^{H(4),OH}$ is positive, and 9 and 11 if the sign is negative.

In the same way, if $^{5}J_{m}^{H(6),OH}$ is positive, the irradiation of transitions 5 and 6, or 7 and 8 of proton 6 will cause the collapse of the hydroxyl proton resonance transitions 9 and 10, or 11 and 12 respectively.

The results of these four partial decoupling experiments, with simultaneous decoupling of the sulfhydryl resonance, are depicted in

Figure 8. As the predictions for the positive signs of these couplings were borne out, this was definite proof that the meta couplings from the ring protons to the hydroxyl proton are positive.

Figure 8

some observations of the hydroxyl proton resonance of 3,5-dichloro-2-hydroxythiophenol in the presence of irradiation of peaks in the ring proton resonances, while decoupling the sulfhydryl resonance

a the ring proton resonances with decoupling of the sulfhydryl resonance

Transitions are number according to Figure 7.

b the hydroxyl proton resonance decoupled from the sulfhydryl resonance

c the hydroxyl proton resonance decoupled from the sulfhydryl resonance with irradiation of transitions 1 and 2

d with irradiation of transitions 3 and 4

e with irradiation of transitions 5 and 6

f with irradiation of transitions 7 and 8

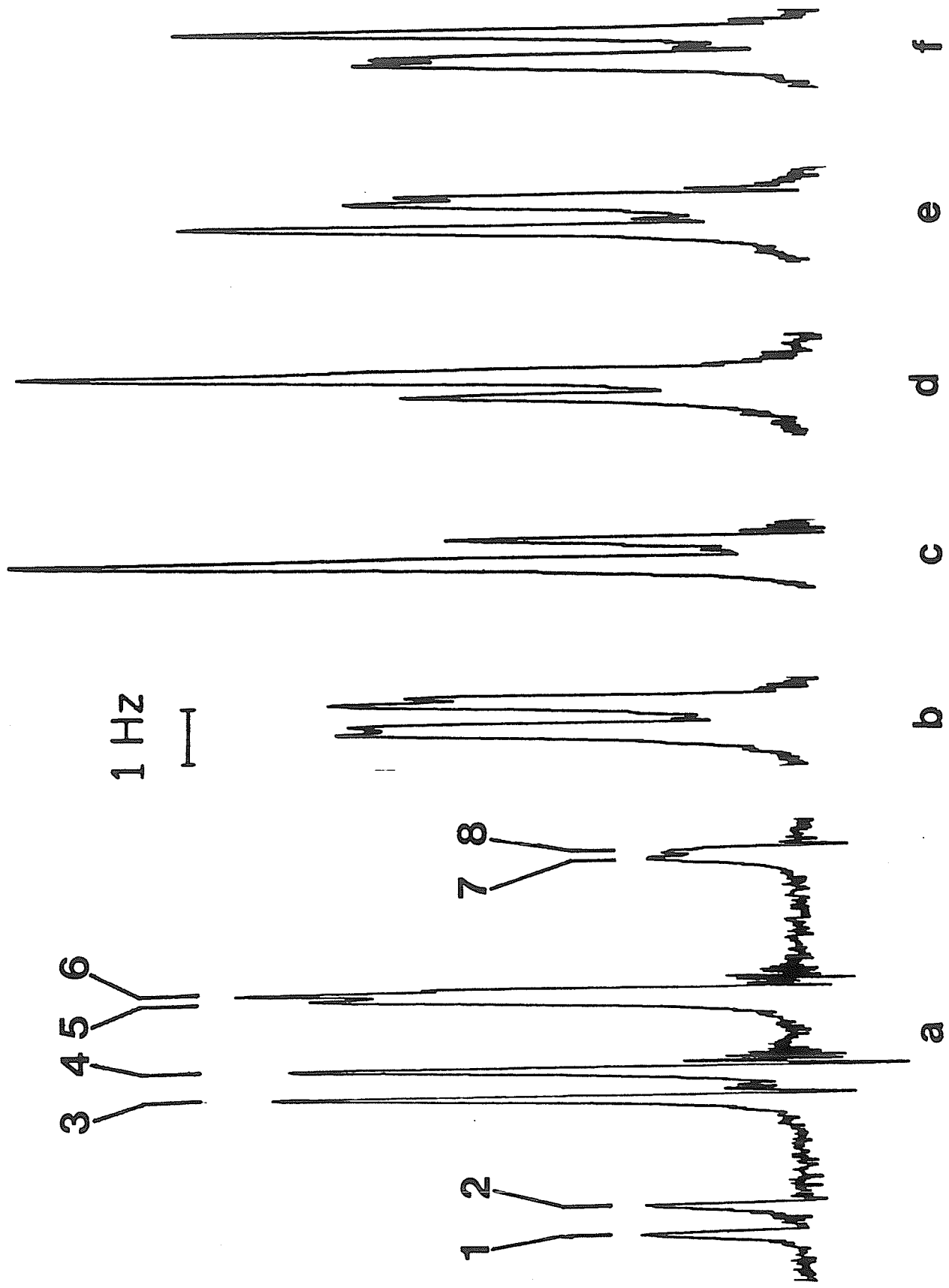
1 Hz
1
2
3
4
5
6
7
8
a
b
c
d
e
f

4. Determination of the Signs of $^{6}J_{p}^{SH,H(4)}$ and $^{4}J_{o}^{SH,H(6)}$

The signs of the couplings from the ring protons to the sulfhydryl protons were determined with the aid of Figure 9. The hydroxyl resonance was decoupled with a strong irradiating field, while simultaneously irradiating pairs of transitions in the ring proton resonances, and observing the sulfhydryl resonance. The pairs of transitions 1 and 2, 3 and 4, 5 and 6, 7 and 8 in the ring proton resonances were irradiated in turn, resulting in the collapse of the doublets 11 and 12, 9 and 10, 10 and 12, and 9 and 11, respectively, in the sulfhydryl proton resonance. These experiments are depicted in Figure 10, and are in agreement with the predictions of Figure 9 using the signs given in Table 2. Since $^{4}J_{m}^{H(4),H(6)}$ has been found to be positive, the couplings from the ring protons to the sulfhydryl protons were conclusively shown to be negative.

Figure 9

a first-order representation of the transitions in the ring proton resonances 4 and 6, and in the sulfhydryl proton resonance of 3,5-dichloro-2-hydroxythiophenol

Coupling to the hydroxyl proton has been ignored.

The signs of the coupling constants are assumed to be those given in Table 2.

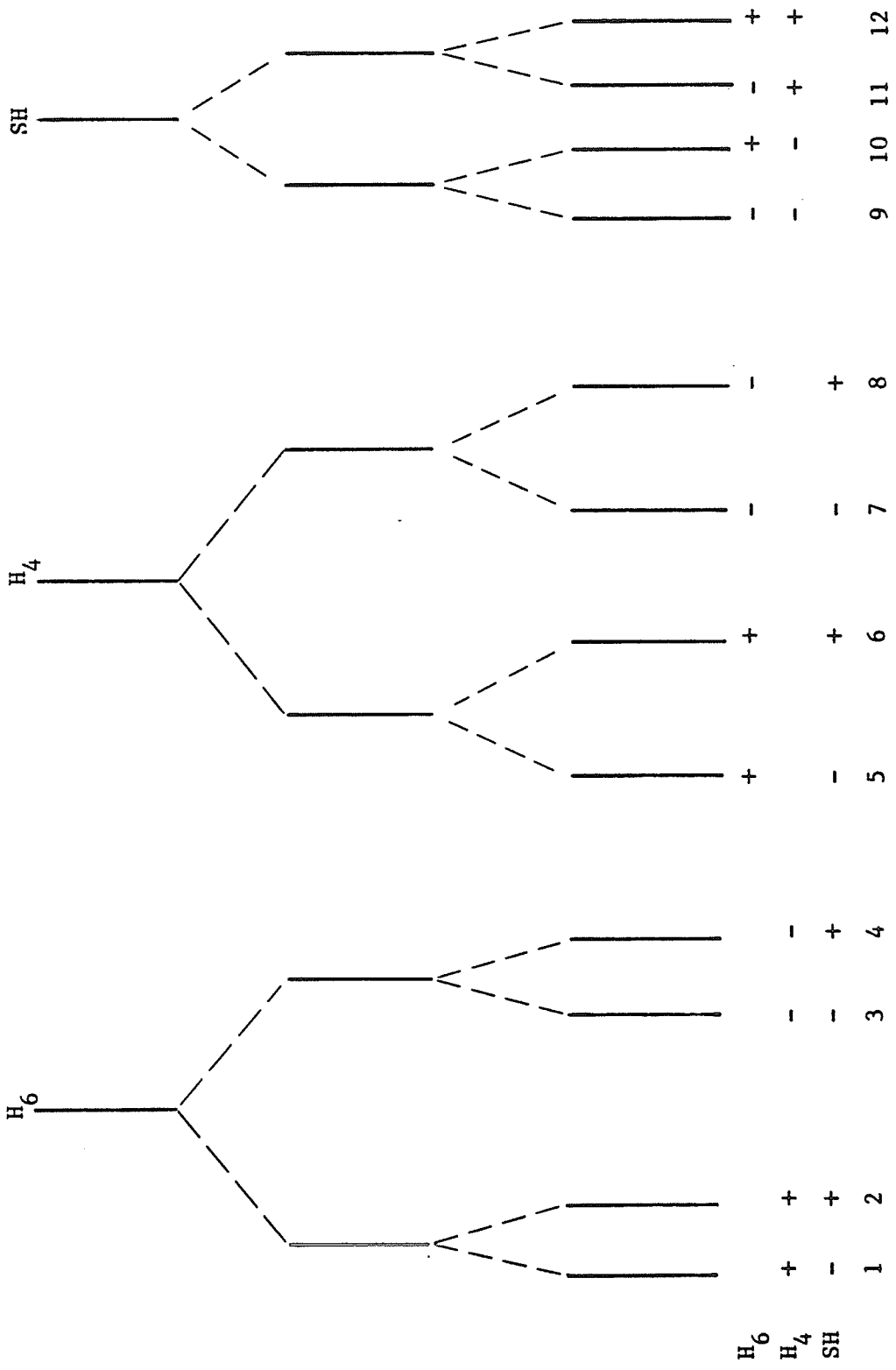
SH
H4
H6
H6 H4 SH
1 2 3 4 5 6 7 8 9 10 11 12

Figure 10

some observations of the sulfhydryl proton resonance of 3,5-dichloro-2-hydroxythiophenol in the presence of irradiation of peaks in the ring proton resonances, while decoupling the hydroxyl proton resonance

a the ring proton resonances decoupled from the hydroxyl proton resonance

Transitions are numbered according to Figure 9.

b sulfhydryl resonance decoupled from hydroxyl proton

c sulfhydryl resonance decoupled from hydroxyl proton with irradiation of transitions 1 and 2

d with irradiation of transitions 3 and 4

e with irradiation of transitions 5 and 6

f with irradiation of transitions 7 and 8

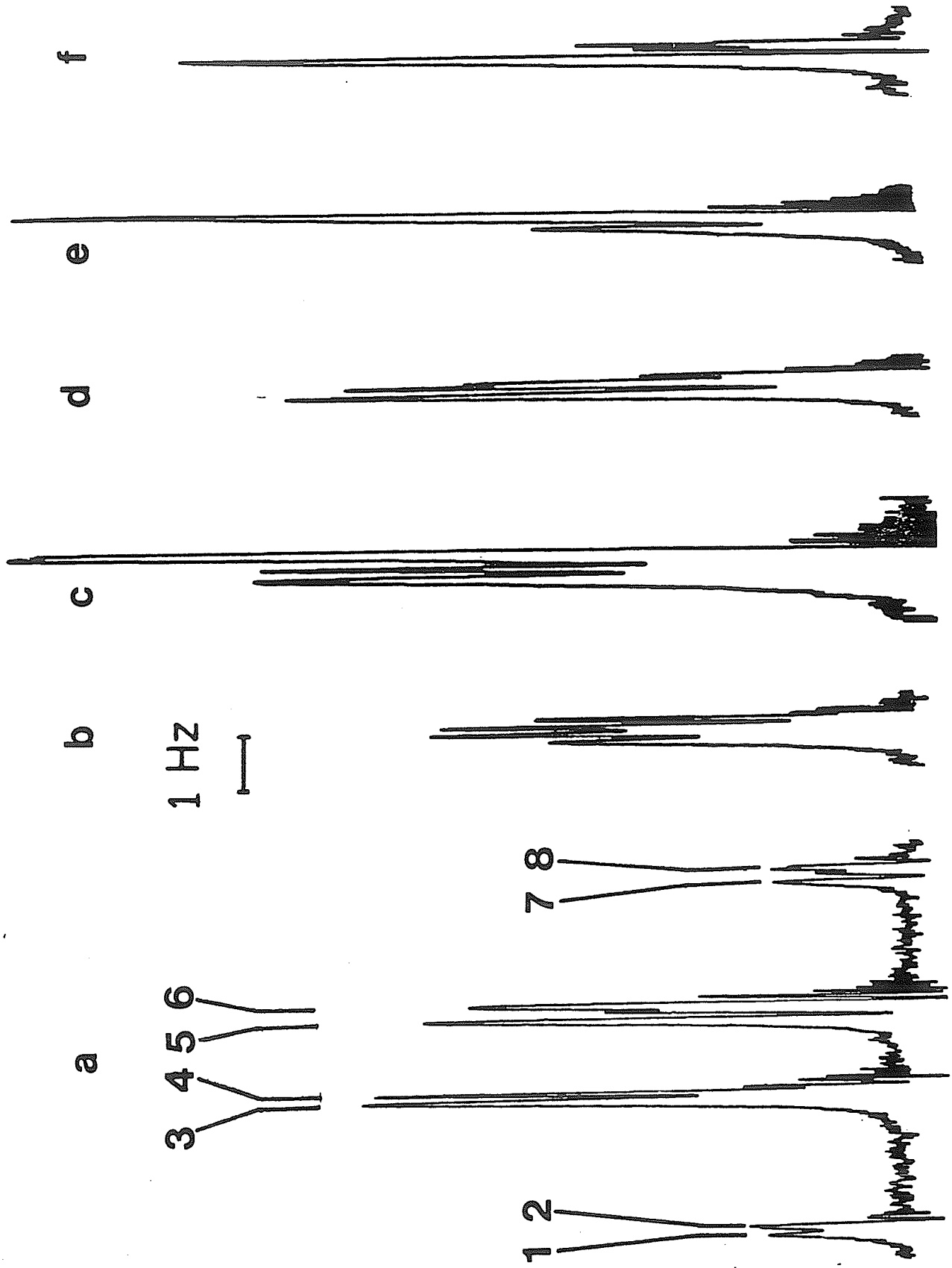
f
e
d
c
b
1 Hz
a
3
4
5
6
7
8
1
2

5. Determination of the Sign of $^{5}J_{o}^{SH,OH}$

The sign of the coupling between the hydroxyl and sulfhydryl protons was determined with the aid of Figure 11. Single transitions in the hydroxyl resonance were weakly irradiated, while observing the resonance of ring proton 6. In this type of experiment (a tickling experiment) transitions that share a common energy level with the irradiated transition will be split into doublets of reduced intensity.[90]

Weak irradiation of transition 9 in the hydroxyl proton resonance resulted in the reduction in intensity of transitions 1 and 3 in the sulfhydryl proton resonance. Weak irradiation of transition 16 of the hydroxyl proton resonance resulted in the splitting of both transitions 6 and 8 of the sulfhydryl proton resonance into doublets of reduced intensity. The results of these tickling experiments are depicted in Figure 12, and agree with the predictions of Figure 11 based on the signs given in table 2. Since the signs of all the other coupling constants are known, the sign of the coupling between the hydroxyl and sulfhydryl protons was proved to be negative.

Figure 11

a first-order representation of transitions in the ring proton resonance 6, and in the hydroxyl resonance of 3,5-dichloro-2-hydroxythiophenol

The signs of coupling constants were assumed to be those given in Table 2.

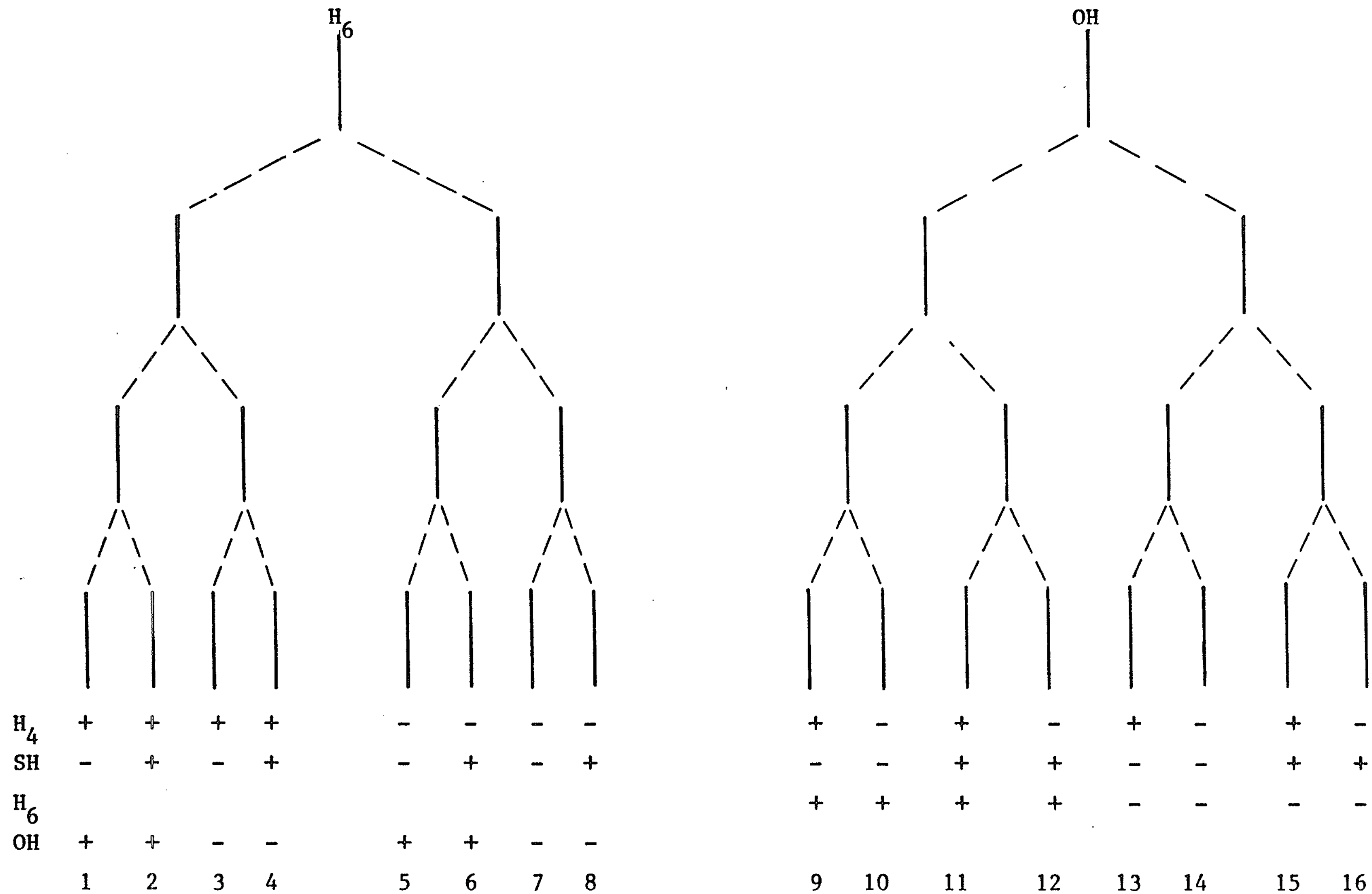
H6
OH
H4 + + + + − − − − + − + − + − + −
SH − + − + − + − + − − + + − − + +
H6 + + + + − − − −
OH + + − − + + − −
1 2 3 4 5 6 7 8 9 10 11 12 13 14 15 16

Figure 12

some observations of the resonance of ring proton 6 in the presence of weak irradiation of the hydroxyl proton resonance of 3,5-dichloro-2-hydroxythiophenol

a the hydroxyl proton resonance

b the resonance of ring proton 6

c the resonance of ring proton 6 in the presence of irradiation of transition 16

d in the presence of irradiation of transition 9

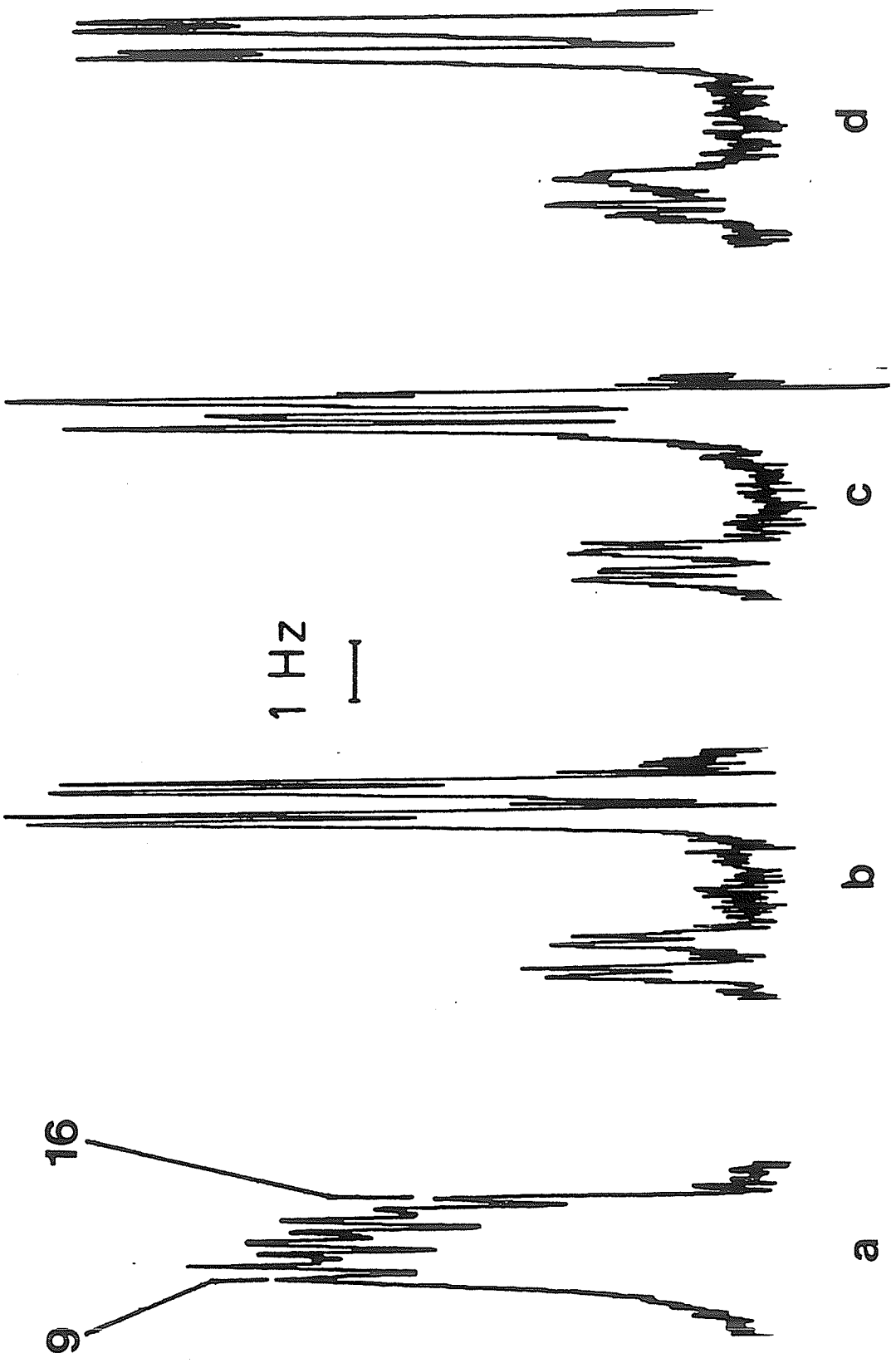
d
c
1 Hz
b
16
9
a

D. Discussion

1. Calculation of Free Energy Differences Using the Stereospecific Five-bond Coupling

The calculation of the free energy differences between conformers using the equation

$$\Delta G^{o} = -RT \ln \frac{{}^{5}J_{m}^{OH,H(5)}}{{}^{5}J_{m}^{OH,H(3)}} \qquad (30)$$

from (1) and (4) (see Figure 1), depends on two assumptions. Equation (30) is valid if the ratio of the conformers' activity coefficients is unity, and if the observed coupling constants are directly proportional to the conformer populations.[102]

As the activity coefficients of the conformers at infinite dilution are unity, and as the structures of the conformers are very similar, it is reasonable that the difference between the coefficients is small in the dilute solutions studied in this work.

The existence and uniqueness of the proportionality constant, J_t, between the conformer population and the observed coupling, has has been supported by experiment and by molecular orbital calculations. Forsen and Akermark observed that the five-bond couplings over the all-trans path to the aldehydic proton in 5-nitro-2-hydroxybenzaldehyde and in 3-nitro-2-hydroxybenzaldehyde were equal,[2] and thus J_t is independent of the nitro group substitution. Wasylishen and Schaefer have done INDO and CNDO FPT MO calculations on benzaldehyde, and on some monofluorobenzaldehyde derivatives. These calculations show that ${}^{5}J_{m}^{CHO,H}$ is essentially invariant to ring substitution.[5]

Suppose that a benzene derivative has only the two planar conformers a and b (see Figure 1) significantly populated, with populations p_a and p_b respectively. Then the sum of the two meta couplings is

$$ {}^{5}J_{m}^{OH,H(5)} + {}^{5}J_{m}^{OH,H(3)} = p_a J_{t,a} + p_b J_{t,b} \qquad (31) $$

where $J_{t,a}$ and $J_{t,b}$ are the proportionality constants, J_t, for the all-trans coupling in the conformers a and b respectively. If J_t is unique, $J_{t,a} = J_{t,b} = J_t$, and since $p_a + p_b = 1$, (31) can be written as

$$ {}^{5}J_{m}^{OH,H(5)} + {}^{5}J_{m}^{OH,H(3)} = J_t \qquad (32) $$

If J_t is unique for a series of related compounds, (32) predicts that the sum of the two five-bond couplings in each compound should be equal to a constant, J_t.

Wasylishen and Schaefer observed that the sum of the two five-bond couplings were 0.76, 0.85, and 0.88 Hz in benzaldehyde, 2-fluorobenzaldehyde, and 4-fluorobenzaldehyde respectively.[5]

In a number of 2,4,6-trisubstituted phenols, Schaefer and Rowbotham observed that the sum of the two five-bond couplings to the hydroxyl proton was approximately invariant, falling in the range of 0.534 to 0.614 Hz.[3b,d]

As discussed in the Introduction, Chapter I, Schaefer and coworkers have applied the stereospecific five-bond coupling to a large number of molecules with a variety of sidechains. Their results have

led to free energy differences that are internally consistent, and in agreement with results from other techniques. This experimental evidence supports the assumptions that J_t does exist, and is insensitive to substitution.

2. The Conformational Equilibrium in 3,5-dichloro-2-hydroxythiophenol

i) the long-range coupling constants

$^5J_m^{OH,H(6)}$ is 0.550 ± 0.012 Hz and $^5J_m^{OH,H(4)}$ is 0.084 ± 0.012 Hz in 3,5-dichloro-2-hydroxythiophenol. The quoted errors are three times the standard deviations from Table 2, presumably at the 99.7 % confidence level. The sum of the two couplings is 0.634 ± 0.024 Hz, in agreement with those observed for a series of trihalophenol derivatives.[3b] This agreement is expected if J_t is unique in these phenol derivatives.

Applying (30) one may write

$$\Delta G^o = -RT \ln (0.550/0.084) = -1140 \pm 100 \text{ cal/mole} \qquad (33)$$

(1 cal = 4.184 joule) for the free energy difference favouring the conformation with the hydroxyl proton cis to the chlorine substituent at the 3 position, relative to the conformation with the hydroxyl proton trans to the chlorine substituent. Anticipating the ensuing discussion, which shows that conformers 12 to 14 (X=Cl) exist in CCl_4 solution at 305 K, the cis conformer can be identified with 13 and 14 (X=Cl), and the trans conformer with 12 (X=Cl). Thus the population of conformers 13 + 14 is $p_{13} + p_{14} = 0.87$, and of conformer 12 is $p_{12} = 0.13$. Note that the error quoted in (33) is based on the uncertainty of 0.012 Hz in the two five-bond couplings.

Conformer 12 (X=Cl) is analogous to 12 (X=H) which is present almost exclusively in 2-hydroxythiophenol.[3g] Conformers 13 and 14 (X=Cl) are analogous to 15 and 16, respectively, present in almost equal

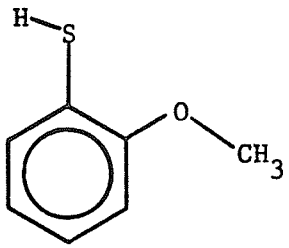

15

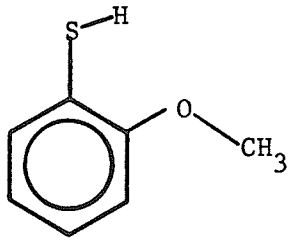

16

abundance in 2-methoxythiophenol.[3f] The exact relative abundance of 13 and 14 (X=Cl) is not important in the following discussion, but it must be very nearly the same as that of 57 % and 43 % for 15 and 16, respectively, in order to reach the ensuing good agreement between the calculated and observed parameters. It should be pointed out that conformations 13 + 14 (X=Cl), or 15 + 16, include contributions from non-planar orientations of the S-H group, including an orientation in which the S-H bond lies in a plane perpendicular to the molecular plane. This latter orientation is unfavorable energetically because the barrier to rotation about the C-S bond in 15 + 16, and thus in 13 + 14 (X=Cl), is substantial.[3f]

Using the values of the coupling constants for a 1.9 mole % solution of 2-hydroxythiophenol in CCl_4,[3g] and for a 4.6 mole % solution of 2-methoxythiophenol in CCl_4,[3f] as well as the populations of the conformers 12, 13 and 14 (X=Cl), the coupling constants in 3,5-dichloro-2-hydroxythiophenol can be calculated, and compared to the experimental values. One has $p_{12} = 0.13$ and $p_{13} + p_{14} = 0.87$. For 2-hydroxythiophenol $^6J_p^{SH,H}$ is -0.973 Hz,[3g] and is -0.136 Hz in 2-methoxythiophenol.[3f] Therefore $^6J_p^{SH,H}$ in 3,5-dichloro-2-hydroxythiophenol should be 0.13(-0.97) + 0.87(-0.14)

or -0.25 Hz. The observed coupling is -0.27 Hz. Similarily, $^{4}J_{o}^{SH,H}$ is calculated as -0.14 Hz, and the observed value is -0.115 Hz.

These calculations assume that the presence of the two chlorine substituents in 3,5-dichloro-2-hydroxythiophenol does not alter the values of $^{6}J_{p}^{SH,H}$ and $^{4}J_{o}^{SH,H}$ from those observed in 2-hydroxythiophenol and in 2-methoxythiophenol. If these substituents, placed meta to the S-H group, were to alter the rotational barrier about the C-S bond, the two couplings would also be altered.[3f,24,103] Unfortunately, the couplings in 3,5-dichlorothiophenol cannot be extracted due to chemical shift degeneracy.[24] In 3,4-dichlorothiophenol $^{4}J_{o}^{SH,H}$ is the same as in thiophenol,[24] suggesting minor perturbations by chlorine substituents placed meta or para to the S-H group. However, in 3,5-dichloro-4-hydroxythiophenol, $^{4}J_{o}^{SH,H}$ is -0.590 Hz,* and is -0.649 Hz in p-methoxythiophenol,[103] both in CCl_4. Here the coupling is reduced by roughly 0.59/0.65. If this reduction is applied in the calculation above, $^{4}J_{o}^{SH,H}$ becomes -0.12 Hz, in close agreement with the value observed in 3,5-dichloro-2-hydroxythiophenol.

$^{6}J_{p}^{SH,H}$ is a σ-π transmitted coupling. For another such coupling, $^{6}J_{p}^{CH,H}$ in toluene, no intrinsic perturbation by meta substituents has been observed.† For example, $^{6}J_{p}^{CH,H}$ is -0.62 Hz in toluene,[70] and is

---

* Unpublished results in this laboratory

† Note, however, that $^{6}J_{p}^{CH,H}$ in toluene is independent of the conformation of the methyl group, as a result of the symmetry of this sidechain.

-0.60 Hz in 3,5-dichlorotoluene.[104] Any perturbation of $^{6}J_{p}^{SH,H}$ should therefore be no larger than that observed for $^{4}J_{o}^{SH,H}$, due to conformational changes. Then the calculated $^{6}J_{p}^{SH,H}$ becomes -0.23 Hz, still within the cumulative experimental error of the observed value.

In 3,5-dichloro-2-hydroxythiophenol $^{5}J_{o}^{OH,SH}$ is -0.25 Hz, and is -0.14 Hz in 2-hydroxythiophenol. Proton couplings over five-bonds are usually positive. In 3,5-dichloro-2-hydroxythiophenol, as in 2-hydroxythiophenol,[3g] it is likely that direct or proximate interactions,[105] probably involving lone-pairs on sulfur and oxygen, are important; in a way similar to those observed and calculated for the hydroxyl and fluorine nuclei in the cis forms of 2-fluorophenol[3c] and 2-hydroxybenzotrifluoride.[3a]

INDO MO FPT calculations tend to exaggerate the magnitudes of five-bond couplings in benzene derivatives, compared to CNDO/2 calculations which are in better agreement with experiment.[3c] CNDO/2 calculations for the conformers of 2-hydroxythiophenol yield $^{5}J_{o}^{OH,SH}$ as -0.11, -0.11 and -1.38 Hz for 12, 13 and 14 (X=H) respectively, using partially optimized geometries (see Table 1). CNDO/2 calculations using the same geometries gives $^{5}J_{o}^{OH,SH}$ as -1.33 Hz for 14 (X=Cl) in 3,5-dichloro-2-hydroxythiophenol: the coupling is insensitive to the presence of the chlorine substituents in this conformer. Table 3 shows CNDO/2 calculations of $^{5}J_{o}^{OH,SH}$ in 3,5-dichloro-2-hydroxythiophenol for conformer 14 (X=Cl) as a function of the C-S-H angle. If this angle is increased by 5° to 100.4°, $^{5}J_{o}^{OH,SH}$ changes to -0.84 Hz, while the H···O distance increases by only 0.1 Å.

Table 3

CNDO/2 Calculations of $^{5}J_{o}^{OH,SH}$ in 3,5-dichloro-2-hydroxythiophenol for Conformer 14 (X=Cl)

∠ C-S-H (°)	O···H Distance (A)	$^{5}J_{o}^{OH,SH}$ (Hz)
95.4	2.203	-1.33
96.4	2.225	-1.21
97.4	2.246	-1.11
98.4	2.268	-1.01
99.4	2.290	-0.92
100.4	2.311	-0.84

Thus the coupling is very sensitive to the H···O distance in 14 (X=Cl), as expected for proximate interactions.[3a,c]

Note that 12 (X=H) has a calculated $^{5}J_{o}^{OH,SH}$ of -0.11 Hz, close to the observed value in 2-hydroxythiophenol, as expected. These present calculations cannot give the relative proportions of 13 and 14 (X=Cl), even though 14 has a large calculated magnitude for $^{5}J_{o}^{OH,SH}$ and 13 a small one. They do indicate that this coupling should be enhanced in magnitude relative to 2-hydroxythiophenol, due to the significant population of 14 (X=Cl), as is observed.

ii) the proton chemical shifts

In 2-hydroxythiophenol, the chemical shift of the SH proton, δ_{SH}, is 2.82 ppm,[3g] and is 3.66 ppm in 2-methoxythiophenol.[3f] Weighting these shifts according to the relative populations of 12, 13 and 14 (X=Cl) yields δ_{SH} as 3.55 ppm for 3,5-dichloro-2-hydroxythiophenol. δ_{SH} is 3.41 ppm for 3,5-dichlorothiophenol as a 1 mole % solution in CCl_4 at 305 K,* and is 3.23 ppm for thiophenol as a 5 mole % solution in CCl_4.[10b] Thus the correction for the chlorine substituents is 0.18 ppm. Since the dilution shifts are very small for thiophenol derivatives,* the observed shift of 3.73 ppm for 3,5-dichloro-2-hydroxythiophenol agrees well with the calculated shift of 3.73 ppm. This agreement is expected because the local environment of the SH proton is similar in 12, 13 and 14 (X=Cl) and in the reference compounds. The agreement implies that 13 and 14 (X=Cl) have the same relative populations as 15 and 16, respectively, in 2-methoxythiophenol.

In contrast, the reference compounds for the hydroxyl proton shifts are unavailable. For example, δ_{OH} in 2,4-dichlorophenol is 5.40 ppm,* is 5.66 ppm in 2,6-dichlorophenol,* and is 5.61 ppm in 2,4,6-trichlorophenol (all in CCl_4 at 305 K). In 2,4-dichlorophenol the O-H···Cl conformer is at least 96 % abundant in dilute solution,[3b] and the 4-chloro substituent causes only a small shift perturbation.

---

* Unpublished work in this laboratory

The latter follows as δ_{OH} is the same in 2-methylphenol and in 4-chloro-2-methylphenol, both as 2.5 mole % solutions in CCl_4.[3e]

These increased shifts to low field cannot be explained by electric fields from the second ortho substituent. This follows as replacement of the chlorine at the 6 position by F,or by Br and I in 2,4,6-trichlorophenol causes high and low field shifts,* respectively, in opposite directions to the change in the dipole moment of the carbon-halogen bond. These shifts are contrary to that expected from electric fields due to the ortho substituent.[106]

Probably the best explanation of these observations invokes a small repulsion between the lone-pairs on oxygen and the lone-pairs on the non-hydrogen-bonded ortho chlorine substituent. Steric crowding of this type by an ortho substituent has been observed in the proximated $^4J_o^{OH,F}$ values in 2-fluoro-4,6-dihalophenols.[3c] Anomolously large $^4J_o^{OH,F}$ values were seen, the deviations increasing with the "size" of the halogen, in the order I > Br > Cl. If this explanation is invoked, it becomes apparent that δ_{OH} in 12 and 13 (X=Cl) should be larger than δ_{OH} in 12 (X=H) and in 2,4-dichlorophenol. The perturbation of δ_{OH} by SH in 14 is also quantitatively unknown.

If the δ_{OH} values of 6.03 ppm in 12 (X=H) and of 5.40 ppm in 2,4-dichlorophenol are weighted by 13 and 87 %, respectively, then the calculated shift becomes 5.48 ppm for 3,5-dichloro-2-hydroxythiophenol. The observed shift is 5.82 ppm. The excess shift of 0.34 ppm may be

---

* Unpublished work done in this laboratory

reasonably attributed to steric or other perturbations of the type exemplified above. This discussion is only meant to ensure that the observed δ_{OH} in 3,5-dichloro-2-hydroxythiophenol is not taken as evidence against the conformational populations derived above.

The ring proton shifts in 3,5-dichlorothiophenol are both 7.12 ppm.† In 3,5-dichloro-2-hydroxythiophenol δ_6 is 7.15 ppm, and is 7.14 ppm in 2-methoxythiophenol.[3f] Thus the proton at position 6 does not display the substantial low-field shift of 7.36 ppm observed in 2-hydroxythiophenol.[3g] In the latter, existing predominantly in conformer 12 (X=H), the directional 3p orbital of sulfur lies approximately in the ring plane. The effect of this orientation on the paramagnetic shielding contribution[53] may well turn out to account for the large deshielding of the proton at position 6 in 2-hydroxythiophenol, as the $n\rightarrow\pi^*$ excitation energy will be lower in this orientaion. The absence of this low-field shift in 3,5-dichloro-2-hydroxythiophenol is consistent with the small population of conformer 12 (X=Cl).

---

† Unpublished work done in this laboratory

iii) the OH hydrogen bond to sulfur and to chlorine

With reference to (33), the free energy preference of conformations 13 + 14 (X=Cl) with an O-H···Cl hydrogen bond, over conformation 12 (X=Cl) with an O-H····S hydrogen bond is -1140 ± 100 cal/mole. Note, however, that while both the O-H···Cl and O-H···S bonds may well involve an O-H···3p interaction, the O-H···S bond is formed at the expense of 3p,π conjugation. The latter amounts to about 0.8 kcal/mole.[10a,103] Thus the intrinsic O-H···S bond strength appears to be nearly as large as the O-H···Cl interaction (relative to 13 and 14, there is not an entropy of R ln 2 favouring 12).

In previous competition experiments of this kind for 2,4,6-trisubstituted phenols,[3b-d] the free energy preferences were found as Cl ≈ Br > F > I > CF_3. Relative to iodine, they were -75 ± 20 for F, -460 ± 60 for Cl and Br, and +1230 ± 200 cal/mole for CF_3. Therefore SH appears to fall between I and CF_3, with an estimated free energy difference of +680 ± 160 cal/mole relative to iodine.

Of course, the order of hydrogen bond strengths in these compounds need not be the same as in monosubstituted phenols. One would expect that solvent and dimerization perturbations are probably lower for the 2,4,6-trisubstituted phenols. Nevertheless, for 2-iodophenol[3i] and 2-hydroxythiophenol,[3g] the couplings provide no evidence for other than an intramolecularly hydrogen bonded conformer in dilute CCl_4 solution at 305 K, suggesting a free energy preference of not less than 1.9 kcal/mole. Using this value for

2-hydroxythiophenol, the present competition experiment implies a free energy preference of about 3 kcal/mole for the O-H···Cl bond of 2-chlorophenol in CCl_4. However, this value must be treated with circumspection. CNDO/2 calculations overestimate the magnitude of the dipole moments in thiophenol, phenol and m-dichlorobenzene, predicting values of 1.7, 1.8 and 2.0 D, compared to the experimental values[107] of 1.2, 1.5 and 1.5 D respectively. CNDO/2 calculations give dipole moments of 1.2 D for each of 13 and 14, and 1.8 D for 12 (X=Cl). The electrostatic theory of solvent stabilization of polar conformers[108] then yields not more than 100 cal/mole for the increased stability of 12 relative to 13 or 14 (X=Cl) in CCl_4 solution. This correction is within the limits of error for the free energy difference in 3,5-dichloro-2-hydroxythiophenol.

E. Summary and Conclusions

The long-range spin-spin coupling constants to the sidechain protons in benzene derivatives have found wide application in the determination of the conformation of the sidechain.

In 3,5-dichloro-2-hydroxythiophenol these couplings show that the molecule exists as a mixture of three conformers in dilute CCl_4 at 305 K. All conformers have the O-H bond in the plane of the aromatic ring, as a result of the large barrier to internal rotation of the OH group. Two conformers, of approximately equal proportions, contain an O-H···Cl hydrogen bond. The orientation of the S-H bond in these conformers is analogous to that observed in 2-methoxythiophenol: one conformer has the S-H bond cis to the OH group, and the other has the S-H bond trans. The third conformer is analogous to that found almost exclusively in 2-hydroxythiophenol, and contains an O-H hydrogen bond to the directional 3p lone-pair orbital of sulfur, which holds the S-H bond perpendicular to the ring plane. The abundance of the latter conformer is 13 %. The chemical shifts of the SH proton and of the ring proton ortho to SH are in agreement with these conclusions. The chemical shift of the OH proton is not useful for conformational deductions in this molecule, but does not contradict the above results.

In previous competition experiments of this type in 2,4,6-trisubstituted phenols, Rowbotham, Smith and Schaefer have found the free energy preference of the hydrogen bond to the OH proton as $Cl \simeq Br > F > I > CF_3$. For 3,5-dichloro-2-hydroxythiophenol the free energy preference of the O-H···Cl bond over the O-H···S bond is

1140 ± 100 cal/mole at 305 K. The SH group falls somewhere between I and CF_3 in the above series, with a free energy estimated to be +680 ± 160 cal/mole relative to iodine. However, the formation of the hydrogen bond to the sulfur atom occurs at the expense of 3p,π conjugation, amounting to about 800 cal/mole. Thus the intrinsic O-H···S hydrogen bond strength appears to be nearly as large as the O-H···Cl bond strength. Based on the results for 3,5-dichloro-2-hydroxythiophenol, the free energy preference for the O-H···Cl hydrogen bond in 2-chlorophenol in dilute CCl_4 solution is estimated as 3 kcal/mole.

In 3,5-dichloro-2-hydroxythiophenol the five-bond coupling between the sidechain protons, $^5J_o^{OH,SH}$, is negative, and very likely involves "through-space" or proximate interactions via lone-pairs on either or both, sulfur and oxygen.

F. Suggestions for Future Research

A number of proposals for future research are suggested by the present work.

It would be very useful to determine the conformational preferences in a series of competition experiments for 3-substituted 2-hydroxythiophenols, where the substituent at position 3 is Br, I, F or CF_3. This would more firmly define the relative free energy of the O-H···S bond in the free energy sequence determined by Rowbotham, Smith and Schaefer for 2,4,6-trisustituted phenols.

A similar series of competition experiments in asymmetric 2,6-disubstituted thiophenols might evaluate the relative preference for a hydrogen bond between the SH proton and the various ortho substituents. These studies may be of special interest, as no strong intramolecular hydrogen bonds have been observed in a number of 2,4-dihalothiophenols.

Conformational studies of a series of 3-substituted 1,2-dimercaptobenzenes might prove to give some interesting insights into the nature of the S-H···S hydrogen bond. Similarly, conformational studies in 3-substituted catechols might determine the relative strength of the O-H···O hydrogen bond. However, in this laboratory to date, it has not proved possible to "stop" intermolecular exchange in catechols, although some sidechain couplings have been observed in 3,5-dichlorocatechol and 3-methoxycatechol.

Chapter IV

The Internal Rotational Barrier in 2,6-difluoroisopropylbenzene

A. Introduction to the Problem

In α,α,2,6-tetrasubstituted toluenes it has been shown that the conformation of minimum energy, 1, has the benzalic proton in the ring plane, while that of maximum energy, 3, has the benzalic C-H bond in a plane perpendicular to the ring plane (see Chapter II.F). Thus the rotational barrier is predominantly two-fold. In the minimum energy conformation shown in Figure 3, the two ortho substituents are not chemically equivalent. Thus for slow rates of internal rotation, if the ortho substituents are magnetic nuclei, the nuclei will give rise to two nmr resonances of different chemical shift. A similar argument holds for nuclei at the meta position. At higher temperatures these resonances will broaden as the rotation of the sidechain interchanges the two ortho sites. The barrier to rotation can then be measured by dynamic nmr methods.

Using this method Peeling and coworkers measured the free energy barriers to internal rotation in a series of 2,6-dihalobenzal halides.[6,7,8,31] Peeling showed that these barriers are due predominantly to the steric interaction between the α and ortho halogen substituents.[32] Based on an empirical relationship taking account of only steric factors, he predicted a free energy barrier of approximately 8 kcal/mole (1 cal = 4.184 joule) in 2,6-difluorobenzal chloride. As the steric hindrance of the methyl and chlorine substituents are approximately equal (see Chapter I.C), the barrier to internal rotation in 2,6-difluoroisopropylbenzene is predicted to be about 8 kcal/mole at 345 K.

However, the two-fold barrier, V_2, to internal rotation in 3,5-dibromoisopropylbenzene has been measured as 2.0 ± 0.2 kcal/mole.[17] As the bromine substituents are assumed not to affect the rotational barrier,

and as the van der Waals volume of a ring fluorine is only 60 % larger than a ring proton,[29] the predicted barrier of 8 kcal/mole in 2,6-difluoroisopropylbenzene appears rather large.

The intent of the present work was to determine the free energy, enthalpy, and entropy of activation, as well as the two-fold potential energy barrier for the internal rotation of the isopropyl group in 2,6-difluoroisopropylbenzene. The latter was to be determined from the long-range coupling between the sidechain and the <u>para</u> ring proton, using the J method. The other parameters were to be determined from the temperature dependence of the fluorine nmr spectrum on the rate of internal rotation, using the dnmr method. The steric origin of the barrier to internal rotation was to be established. Comparison of the barriers determined by the two methods was intended to verify the J method, with respect to the established dnmr method.

It was also the intent of this work to contribute to the knowledge of the conformational dependence of the long-range couplings between the sidechain protons and the ring fluorine nuclei.

B. Experimental Method

1. Preparation of 2,6-difluoroisopropylbenzene

The 2,6-difluoroisopropylbenzene was synthesized* via the reaction scheme shown below. The procedure was as follows.

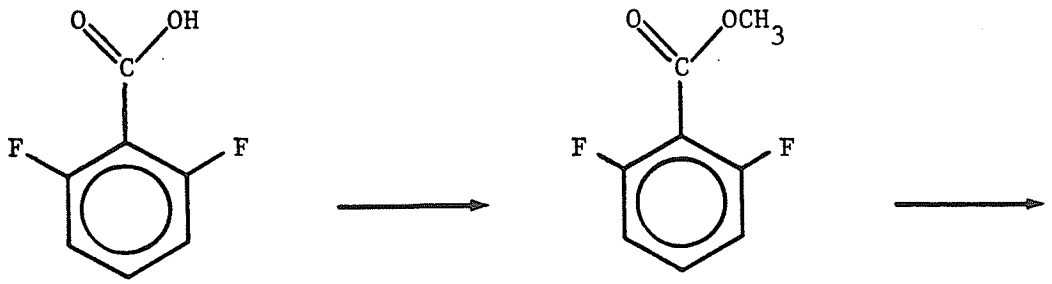

III IV

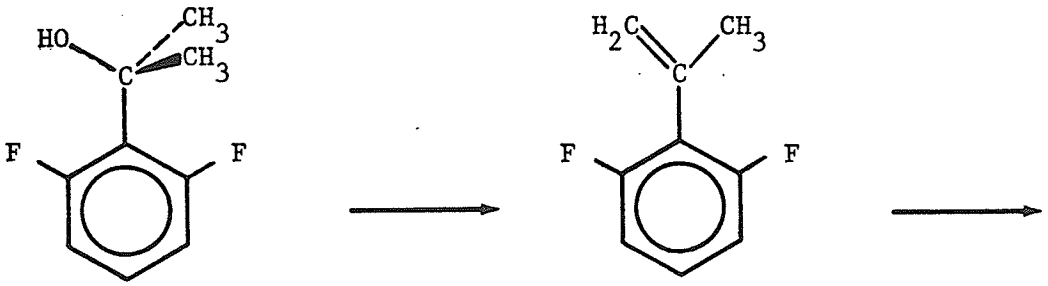

V VI

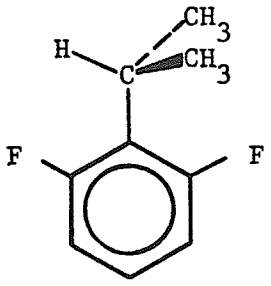

VII

---

* This synthesis was done in Dr. J. Charlton's laboratory, the University of Manitoba, in 1980.

2.1 gm of 2,6-difluorobenzoic acid (III) was dissolved in a solution of 3 mL of acetyl chloride and 60 mL of methanol. This solution was stirred at room temperature overnight, then refluxed for 7 hours. After evaporation of the solvent, the remaining residue was dissolved in chloroform, washed with sodium bicarbonate, and dried with magnesium sulfate. The solvent was removed under vacuum to give about 1.4 gm of a colourless oil. The proton nmr spectrum was consistent with that expected for the methyl benzoate (IV), and the acid (III) was not detected.

A methyl magnesium iodide Grignard reagent was prepared by addition of 12 gm of methyl iodide to 2 gm of magnesium in ether (previously dried with sodium). This mixture was heated until all the magnesium had reacted. A solution of 1.3 gm of (IV) in 20 mL of ether was slowly added to this Grignard reagent. The mixture was refluxed for 20 minutes, poured into a mixture of ice and dilute hydrochloric acid, extracted with ether, and dried with magnesium sulfate. The solvent was evaporated to yield 1.2 gm of a clear yellow oil. The proton nmr spectrum was consistent with that expected for the alcohol (V).

A few crystals of toluene-p-sulfonic acid and 0.6 gm of the alcohol (V) were added to 13 mL of benzene. This solution was left at room temperature overnight, washed with dilute hydrochloric acid, and dried with magnesium sulfate. The solvent was removed with a steam bath on a Vigreaux column. The proton nmr spectrum of the product was that expected of the alkene (VI), with no trace of the alcohol detected.

The alkene (VI) was dissolved in ethanol (distilled before use) and hydrogenated at room temperature and atmospheric pressure with 0.2 gm of Pd/C catalyst in a low-pressure hydrogenator. The carbon was filtered off with water (three times the solution volume), and the product was extracted from the solution with pentane. The pentane was then backwashed with water to remove the ethanol, dried with magnesium sulfate, filtered, and then distilled through a Vigreaux column. The residue was distilled on a microdistillation apparatus, yielding a clear liquid. The product showed the proton and fluorine spectra expected of 2,6-difluoroisopropylbenzene (VII).

2. NMR Samples

NMR samples of 2,6-difluoroisopropylbenzene were prepared by weighing appropriate amounts of the compound and the solvent of choice. The solutions were transferred to precision-bore 5 mm nmr sample tubes, filtering the solution through a small wad of cotton wool in a Pasteur pipette. 5 mole % solutions were prepared in carbon disulfide (Fisher Scientific) and in acetone-d_6 (99.5 atom % D from Aldrich Chemical). The sample in carbon disulfide contained 4 mole % tetramethylsilane (Aldrich Chemical) as an internal locking material, while that in acetone-d_6 contained a drop of hexafluorobenzene (Pierce Chemical). The samples were then degassed using the freeze-pump-thaw technique, completing at least seven cycles. The nmr tubes were then flame-sealed.*

In addition, two nmr samples were prepared as approximately 5 mole % solutions in 1:1 volume/volume solvent mixtures. One sample was prepared in a mixture of acetone-d_6 and isopentane (Eastman Kodak), the other in a mixture of methylene chloride-d_2 (99 atom % D from Aldrich Chemical) and isopentane. These samples were not degassed or sealed.

---

* This sample preparation was done by Rudy Sebastian, University of Manitoba, in this laboratory in 1981.

3. Spectroscopic Method*

i) proton nmr experiments

The proton magnetic resonance experiments were done on a Varian Associates HA-100-D continuous wave spectrometer in the frequency sweep mode, and on a Bruker WH-90 acquiring a free induction decay and obtaining the spectrum in the frequency domain via a Fourier transform. The single and multiple resonance experiments on the HA-100-D were performed on the sample prepared in carbon disulfide. The procedure followed that described in Chapter III.B.3, except that the line positions were not calibrated. The experiments on the WH-90 made use of a dedicated Nicolet 1180 computer system, and utilized an internal deuterium lock on the deuterated solvent. The proton nmr spectra of the sample in acetone-d_6 were acquired at 90.02 MHz using a sweep width of 760 Hz. Line frequencies to be used in the ensuing spectral analysis were measured directly from computer-stored spectra, and were averaged from three different spectra. The average deviation of the final line frequencies was about 0.015 Hz. All proton nmr experiments were done at a probe temperature of 305 ± 1 K.

---

* Fluorine and proton single resonance experiments were done by Rudy Sebastian in this laboratory, in 1981. Some of the variable temperature experiments were done by Kirk Marat, University of Manitoba, in 1981.

ii) fluorine nmr experiments

All fluorine nmr spectra were obtained on a Bruker WH-90, operating in the mode described previously. The fluorine nmr spectrum of 2,6-difluoroisopropylbenzene in acetone-d_6 was acquired three times at 84.67 MHz, with a probe temperature of 305 ± 1 K. Due to the complexity of the fully-coupled spectrum, these spectra were acquired with modulated decoupling (1 watt) of the methyl protons. A sweep width of 200 Hz was used for 300 acquisitions. The calibration of line frequencies was as described previously, the average deviation of the line frequencies from the three spectra being approximately 0.020 Hz.

Fluorine spectra were also acquired at temperatures varying from 305 K to 140 K, with broadband proton decoupling, for the samples prepared in acetone-d_6, acetone-d_6/isopentane, and methylene chloride-d_2/isopentane. Typical sweep widths were 500 Hz or 1000 Hz. The broadening due to chemical exchange in these spectra was characterized by measuring points on the spectral lineshape at 1/4, 1/2, and 3/4 of the maximum peak heights, the measurements being taken from spectra plotted by the WH-90.

The Bruker WH-90 was equipped with a standard variable temperature accessory (B-VT-1000). This temperature controller had been previously calibrated by inserting a thermocouple into a dummy nmr tube. Any time the temperature has been measured in this way, the controller temperature has been within ± 1 K. This temperature controller utilizes a stream of nitrogen gas, which is passed through a heat-exchange coil immersed in liquid nitrogen, before passing through the nmr probe. To reach the low temperatures required in these variable temperature experiments, the nitrogen gas stream was pre-cooled before it reached the heat-exchanger, by passing it through a copper coil immersed in liquid nitrogen.

4. Analysis of 305 K Fluorine and Proton Spectra

Spectral simulations of the fluorine nmr spectra at 305 K, with decoupling of the methyl resonance, were performed by the computer program LAME.[92] However, the fully-coupled proton spectrum at 305 K is an $AA'XX'BMR_6$ 12-spin system, which is too large to be handled by LAME. Thus simulations of the fully-coupled proton spectrum were performed by the computer program NUMARIT,[4] which can handle large spin systems with both magnetic and chemical equivalence.*

Simulation of multiple resonance experiments was performed by the computer program DOR,[113] which can simulate double resonance experiments for systems with up to 6 spins. Thus for all DOR simulations, it was necessary to ignore the coupling to the methyl protons.†

All three simulation programs were coupled to a plotting routine, which drew calculated spectra on a Versatec plotter.

---

* The original program was written by J. Martin, University of Alberta. It was modified by W. J. E. Parr, University of Manitoba, in 1976.

† A modified version, DOR8 was available, but could handle only as many as 8 spins.

5. Determination of $\langle \sin^2\theta \rangle$

The observed value of ^6J_p, the coupling between an α-proton of a sidechain and a para ring proton, can be related to the expectation value of $\sin^2\theta$, $\langle \sin^2\theta \rangle$ by (5). In turn, $\langle \sin^2\theta \rangle$ is related to the potential energy barrier to internal rotation, and thus a measurement of ^6J_p can be used to determine the rotational barrier.

Ayscough, Brice and McClung have outlined a quantum mechanical solution to this hindered rotor problem for a two-fold barrier to internal rotation.[112] Based on this solution, the computer program EXPECT has been written in this laboratory. The major input parameters for this program consist of the temperature, the reduced moment of inertia about the bond between the sidechain and the aromatic ring, the magnitude of the two-fold barrier V_2, and the number of free rotor states to be used as basis functions for the quantum mechanical treatment. The output consists of $\langle \sin^2\theta \rangle$ and V_2.

The program EXPECT was used to calculate $\langle \sin^2\theta \rangle$ as a function of V_2, for the moment of inertia about the exocyclic bond in 2,6-difluoroisopropylbenzene.

6. Determination of Preexchange Lifetimes

Preexchange lifetimes were extracted from the exchange-broadened variable temperature fluorine spectra by matching the experimental spectra with simulated spectra, which were calculated by the computer program EXCH. EXCH is modified from a program described by Krieger,[110] and is based on a matrix formulation[76] (see Chapter II.E.1). It was coupled to a plotting routine that drew calculated spectra on a Versatec plotter. The input parameters for the program consisted of the preexchange lifetime τ, the linewidth in the absence of exchange $1/\pi T_2$, and the chemical shift difference between the exchanged sites, as well as some scaling factors for the plot. The output consists of a simulated exchange-broadened nmr spectrum drawn by the Versatec plotter.

If preexchange lifetimes are to be determined by matching the experimental and calculated spectra, the program requires values for $1/\pi T_2$ and the chemical shift difference for the magnetic nucleus in the exchanged sites. Unfortunately, these could not be determined directly from the exchange-broadened spectra. Alternately, the temperature dependence of $1/\pi T_2$, and the chemical shift difference could be determined at temperatures below which exchange-broadening occurs, then extrapolated to the temperature region in which exchange-broadening occurs. However, due to the extremely low temperatures required, this measurement could not be made. Values of $1/\pi T_2$ were estimated by measuring the linewidths of the signals due to internal hexafluorobenzene added to the samples, and the linewidths of a number of intense sharp lines due to impurities. Below the coalescence temperature, the nmr lineshape consisted of two

peaks. In this temperature region the exchange-broadened spectra contained enough information to match the experimental spectra to the spectra calculated by EXCH for two independent parameters, the preexchange lifetime and the chemical shift difference. Above the coalescence temperature, the spectral lineshape consisted of only a single peak, which contained too little information to determine two independent parameters. In this temperature region, the chemical shift difference was assumed to be temperature independent. By varying the preexchange lifetime, the experimental and calculated spectra were then matched to give a best fit.

The matching of experimental and calculated spectra followed the procedure outlined below. Calculated spectra were produced by EXCH for varying values of the preexchange lifetime (and chemical shift difference, below the coalescence temperature) for the measured value of $1/\pi T_2$ at a particular temperature. Since the Versatec plotter does not produce plots on an <u>exactly</u> uniform scale, the scale of each calculated spectrum was measured. Points on the calculated spectral lineshape at 1/4, 1/2, and 3/4 of the maximum peak heights were measured, as was done for the experimental spectra. The best fit of the calculated and experimental spectra was then determined by matching the positions of these measured points on both spectra. As a final check, the total lineshapes from the calculated and experimental spectra were compared by eye.

7. Determination of the Activation Parameters

From the temperature dependence of the rate constant, $k = 1/\tau$, obtained from the previously described lineshape analysis, the computer program ACTPAR[111] was used to determine values of the activation parameters $\Delta H^{\dagger}$, $\Delta S^{\dagger}$, E_A and log A for the exchange. The input for the program consists of the temperatures and the associated rate constants, as well as the standard deviation of these values. The program calculates the activation parameters on the basis of the Eyring equation

$$k_r = \frac{\kappa kT}{h} \exp\ (-\Delta H^{\dagger}/RT)\ \exp\ (\Delta S^{\dagger}/R) \qquad (34)$$

and the Arrhenius equation

$$k_r = A \exp\ (-E_A/RT) \qquad (35)$$

where the symbols have their usual meanings. The output from the program consists of the activation parameters and their corresponding standard errors. Values of $\Delta G^{\dagger}$ at a specific temperature were calculated from $\Delta H^{\dagger}$ and $\Delta S^{\dagger}$ using equation (3).

C. Experimental Results

1. Spectral Parameters at 305 K

i) LAME and NUMARIT spectral analyses

The fluorine and proton nmr spectral parameters for a 5 mole % solution of 2,6-difluoroisopropylbenzene in acetone-d_6 are tabulated in Table 4.

The spectral parameters for fluorine are those calculated by the computer program LAME, from the fluorine spectrum with the methyl groups decoupled. The numbers in parentheses are the standard deviations in the last digit(s) of the parameters, also calculated by LAME. Blank entries represent parameters not iterated upon in the LAME analysis. These parameters were treated as constants, with their values taken from the analysis of the proton spectrum.

The proton spectral parameters are those calculated by the computer program NUMARIT from the fully coupled proton spectrum, except where noted. The numbers in parentheses are the standard deviations in the last digit(s) of the parameters, also calculated by NUMARIT. Blank entries represent parameters not iterated on in the NUMARIT analysis. The fluorine nucleus was treated by the X approximation in the NUMARIT calculations, and thus the calculated proton spectrum was insensitive to the fluorine chemical shift. The calculated proton spectrum was also insensitive to $^4J_m^{F,F}$. It was thus not possible to iterate on this coupling: the value of the coupling was held constant, and was taken from the fluorine spectral analysis. The value of $^6J_p^{CH,H}$ and its estimated error was calculated from an analysis of the <u>para</u> ring proton

Table 4

Spectral Parameters for a 5.0 mole % solution of

2,6-difluoroisopropylbenzene in acetone-d_6 [a]

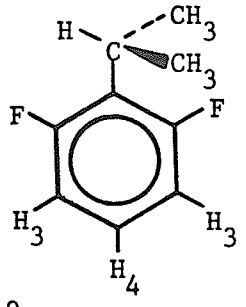

	^{19}F Spectral Analysis[b]	^{1}H Spectral Analysis[c]
ν_{CH_3}	-	119.064(2)
ν_{CH}	-	303.319(3)
$\nu_{H(3)}$	-	622.041(2)
$\nu_{H(4)}$	-	650.281(2)
ν_{F}	4133.9	-
$^{3}J_{CH_3,CH}$	-	7.098(2)
$^{3}J_{o\,H(3),H(4)}$	-	8.380(2)
$^{3}J_{o\,H(3),F}$	10.348(14)	10.416(4)
$^{4}J_{o\,CH,F}$	-0.599(13)[d]	-0.603(4)[d]
$^{4}J_{m\,H(3),H(3)}$	-	1.147(6)
$^{4}J_{m\,H(4),F}$	6.386(13)	6.383(3)
$^{4}J_{m\,F,F}$	6.339(17)	-
$^{5}J_{CH_3,F}$	-	0.956(3)[d]
$^{5}J_{p\,H(3),F}$	-1.295(14)	-1.311(4)
$^{5}J_{m\,CH,H(3)}$	-	0.292(3)
$^{6}J_{p\,CH,H}$	-	-0.080(20)[e]

Notes for Table 4

a at 305 ± 1 K; signs of coupling constants are taken from related compounds, except where noted; numbers in parentheses are errors in last digit of parameters.

b measured with decoupling of the methyl proton resonance; chemical shifts in Hz at 84.67 MHz to low-field of internal C_6F_6; coupling constants in Hz; blanks are parameters not iterated upon in the analysis, and were taken from ^1H analysis; all parameters determined by a LAME analysis with an rms deviation of 0.034 Hz, a largest deviation of 0.068 Hz, 24 observed peaks, and 48 calculated transitions, 36 of them assigned.

c fully coupled proton spectrum at 305 ± 1 K; coupling constants in Hz; chemical shifts in Hz to low-field of internal TMS at 90.02 MHz; blanks indicate parameters not iterated upon in the analysis, and were taken from ^{19}F analysis; all parameters, except where noted, determined by a NUMARIT analysis with an rms deviation of 0.033 Hz, a largest deviation of 0.078 Hz, 100 observed peaks, and 1777 calculated transitions, 1089 of them assigned.

d sign determined by multiple resonance experiments

e estimated from fit of two Lorentzian peaks to some peaks in the <u>para</u> ring proton resonance

resonance. The signs of coupling constants were taken from those in related compounds. However, the signs of $^{4}J^{CH,F}_{o}$ and $^{5}J^{CH_3,F}$ were determined by double resonance experiments.

The quoted errors in the parameters, as calculated by LAME and NUMARIT, are considered to be compatible with calibration errors in the analysis (see Chapter III.C.1). The error limits for these parameters are presumably three times their standard deviations, to the 99.7 % confidence level.

The experimental and calculated spectra of the fluorine nuclei are shown in Figure 13, of the ring protons in Figure 14, and of the methyl and methine protons in Figure 15. The fluorine spectrum was measured at 84.67 MHz, and the proton spectra at 90.02 MHz. Note that at 305 K the exchange produced by the rotation of the isopropyl group was too fast to contribute significantly to the peak widths. The latter were about 0.18 Hz and 0.30 Hz at half-height in the proton and fluorine spectra, respectively, and were dominated by magnetic field inhomogeneity (and, in the fluorine spectrum, by residual couplings due to incomplete proton decoupling).

Figure 13

the spectra of the fluorine nuclei of 2,6-difluoroisopropylbenzene with decoupling of the methyl proton resonance

a observed spectrum

b calculated spectrum

The scale beneath the calculated spectrum has units of Hz.

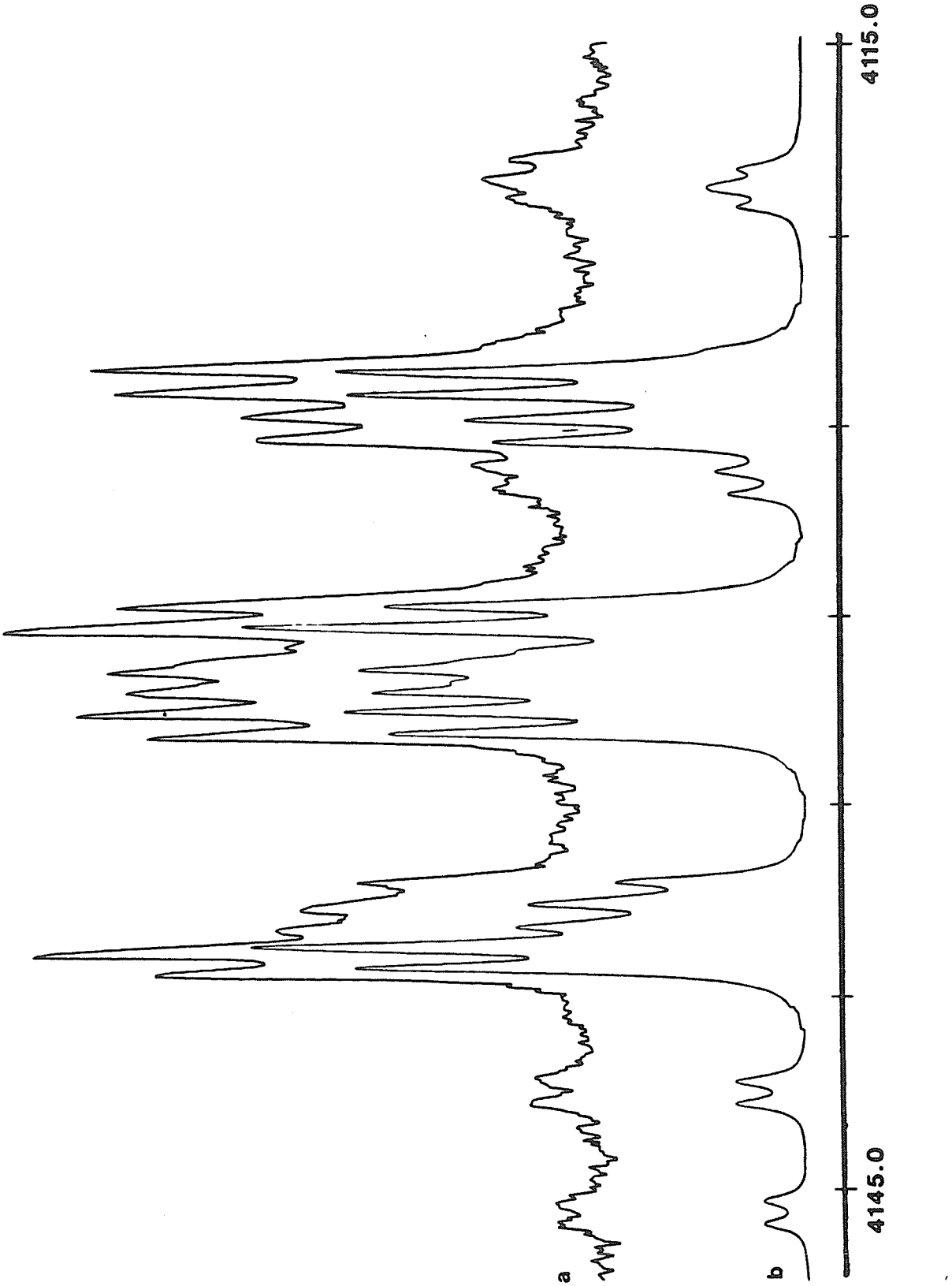
4115.0
4145.0
a
b

Figure 14

the spectra of the ring proton resonances of

2,6-difluoroisopropylbenzene

a observed spectrum

b calculated spectrum

The scale beneath the calculated spectrum has units of Hz. Peaks marked with an asterisk are due to impurities.

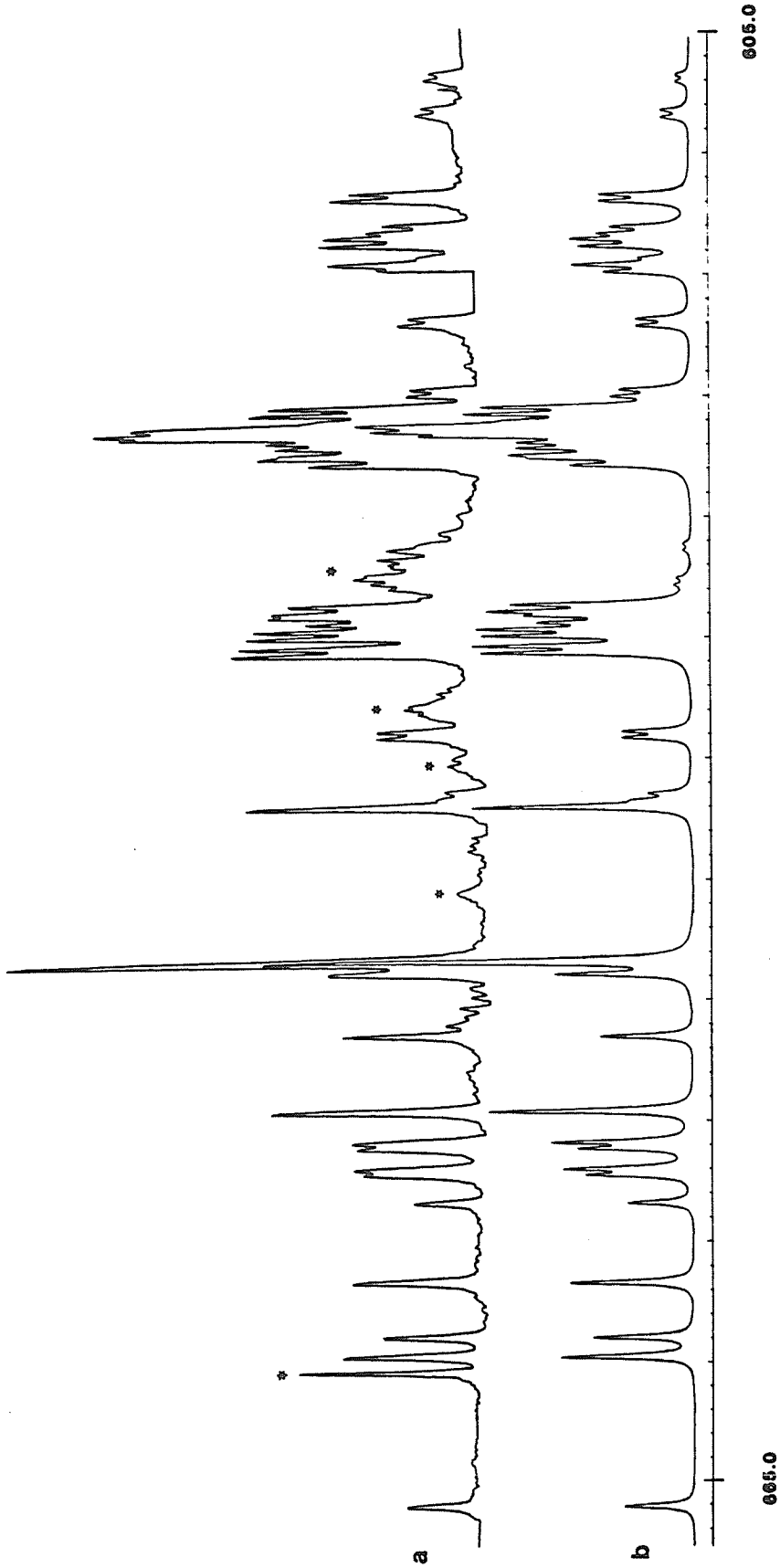
a
b
605.0
665.0

Figure 15

the spectra of the methine and methyl proton resonances of 2,6-difluoroisopropylbenzene

a observed methine proton resonance spectrum

b calculated spectrum

c observed methyl proton resonance spectrum

d calculated spectrum

The scale beneath the calculated spectra has units of Hz.

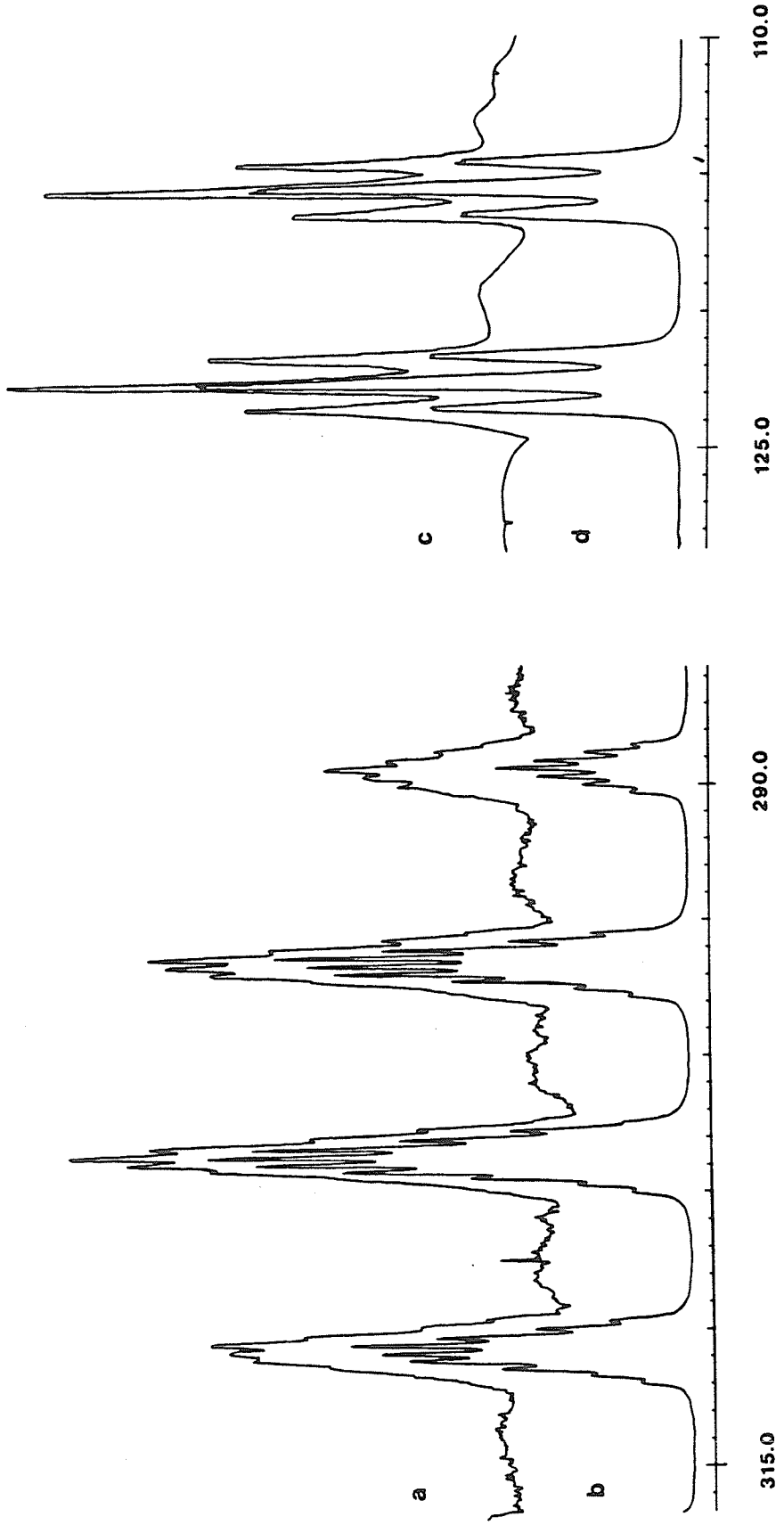
a
b
c
d
315.0
290.0
125.0
110.0

ii) estimation of $^{6}J^{CH,H}_{p}$

The spectrum of the para ring proton (see Figure 14) shows no resolvable splitting into a doublet, due to coupling to the methine proton, and thus the value of the coupling could not be determined from the NUMARIT analysis. However, peaks due to the para ring proton were clearly broadened compared to those due to the meta ring protons.

The absence of quadrupolar nuclei in this molecule suggests that quadrupolar broadening does not contribute to the linewidths of the ring protons. Presumably, other relaxation mechanisms do not contribute significantly to the linewidth of proton resonances in compounds of this type in solution. Thus the broadening of the para proton linewidths can be interpreted to be due to an unresolved coupling between the para ring proton and the methine proton. Note that the complexity of the methine resonance (Figure 15) prevents observation of a similar broadening in the methine proton resonance.

The best resolution attained for the ring proton resonances is illustrated in Figure 16, for a portion of the para and meta resonances. The spectra were obtained on a Varian HA-100-D spectrometer at 100 MHz. The linewidths of single transitions in the para resonance are about 0.18 Hz, and in the meta resonance 0.13 Hz. The coupling to the para resonance does appear to be partially resolved in this spectrum, with a clear hesitation on the side of these peaks opposite to the direction from which the plotter on the spectrometer sweeps. As experience in this laboratory has shown, this is indicative of an unresolved coupling. The computer program LAME was used to simulate the overlap of a doublet of Lorentzian peaks, each of linewidth 0.13 Hz, and with separations of 0.02

to 0.10 Hz. These simulations are depicted in Figure 16. Comparison of the observed <u>para</u> peak lineshapes with those from the computer simulation suggests a value of 0.06 to 0.10 Hz for the unresolved coupling. Thus the value of $^{6}J_{p}^{CH,H(4)}$ was estimated as 0.08 ± 0.02 Hz.

Figure 16

the spectra of the para ring proton resonance of

2,6-difluoroisopropylbenzene

a a portion of the meta proton resonance

b a portion of the para proton resonance, with a frequency sweep from left to right

c with a frequency sweep from right to left

d a LAME simulation of the overlap of two Loerentzian peaks of 0.13 Hz width at half-height, with a separation of 0.10 Hz

e with a separation of 0.08 Hz

f with a separation of 0.06 Hz

g with a separation of 0.04 Hz

h with a separation of 0.02 Hz

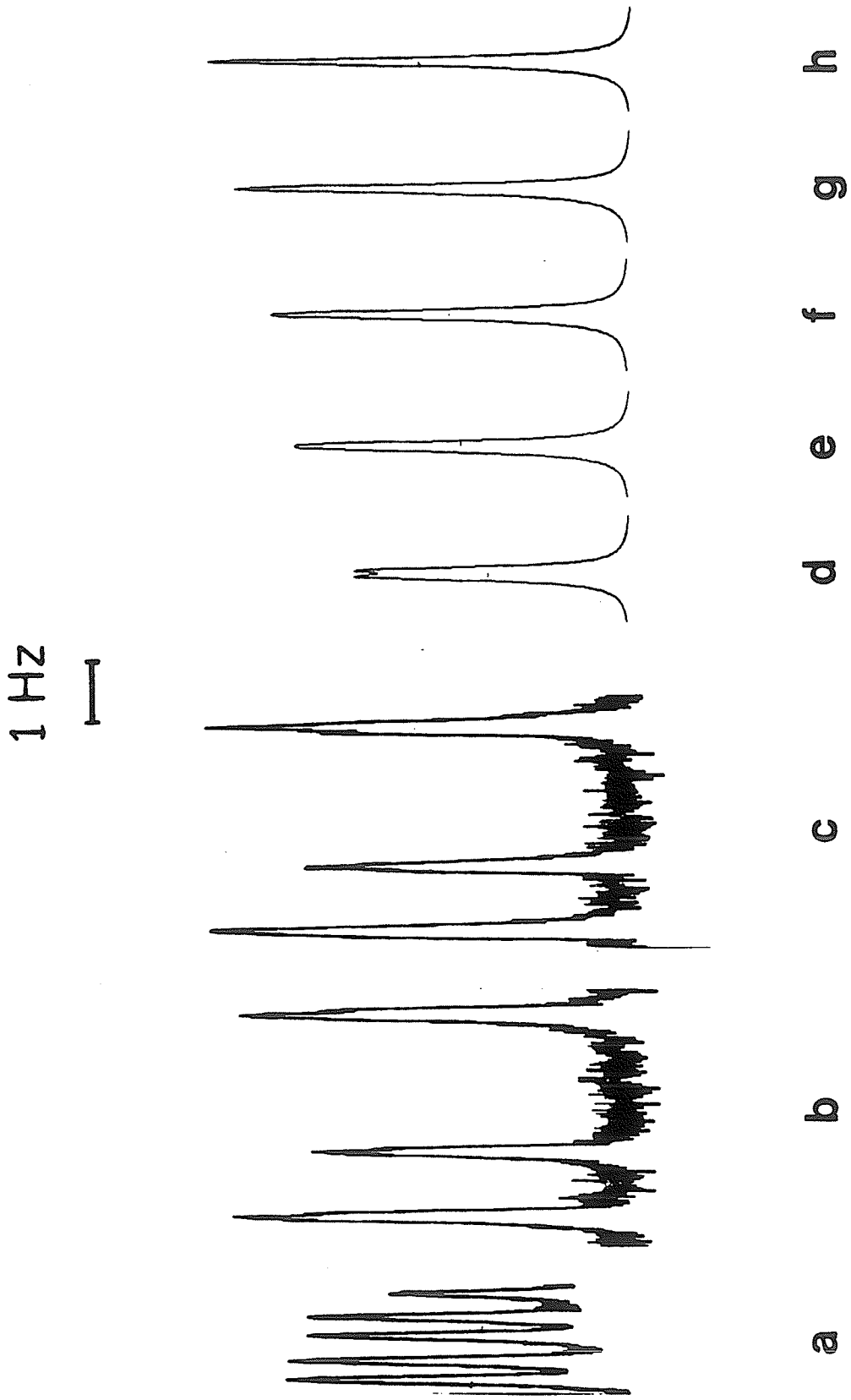
a
b
c
d
e
f
g
h
1 Hz

iii) determination of the sign of $^4J_o^{CH,F}$

The sign of the coupling from the methine proton to the ortho fluorine nuclei was determined with the aid of Figure 17. The figure shows a first order representation of the doublet that was second from low-field in the meta proton resonance, and one of the septets of the methine resonance. The figure was constructed as described in Chapter III.C.3. However, for a symmetric pair of nuclei, the designation +2 represents both nuclei in a + spin state, 0 represents one nucleus of the pair in a + spin state and one in a - spin state, and -2 represents both nuclei in a - spin state. The spin states shown in the methine multiplet are based on the signs in Table 4. The spin state of the fluorine nucleus in the meta proton doublet depends on the sign of the meta proton-fluorine coupling constant, $^3J_o^{H(3),F} + {}^5J_p^{H(3),F}$. As $^3J_o^{H(3),F}$ has a positive sign, and is larger than $^5J_p^{H(3),F}$, the sign of the sum is positive. Based on the low-field position of this doublet, the fluorine spin state is then presumed to be + for the doublet.

The meta proton doublet was irradiated with a field of intermediate strength, while observing the methine septets that were second from low-field and second from high-field in this resonance. Simultaneous irradiation of the transitions 1 and 2 resulted in the collapse of transitions 8 and 9 to a singlet (with 7 also slightly affected). These experiments, for the two methine septets, are depicted in Figure 18, and are in agreement with the above predictions. Thus $^4J_o^{CH,F}$ is shown to be negative.

However, these experiments must be treated with circumspection, as second-order effects are significant in the proton spectrum of

Figure 17

a first-order representation of some transitions in the meta ring proton resonance H_3 and the methine proton resonance H_2 of 2,6-difluoroisopropylbenzene.

Only the second from the lowest field doublet of the H_3 resonance, and one of the septets of the methine resonance are depicted. Signs of the coupling constants were taken to be those given in Table 4.

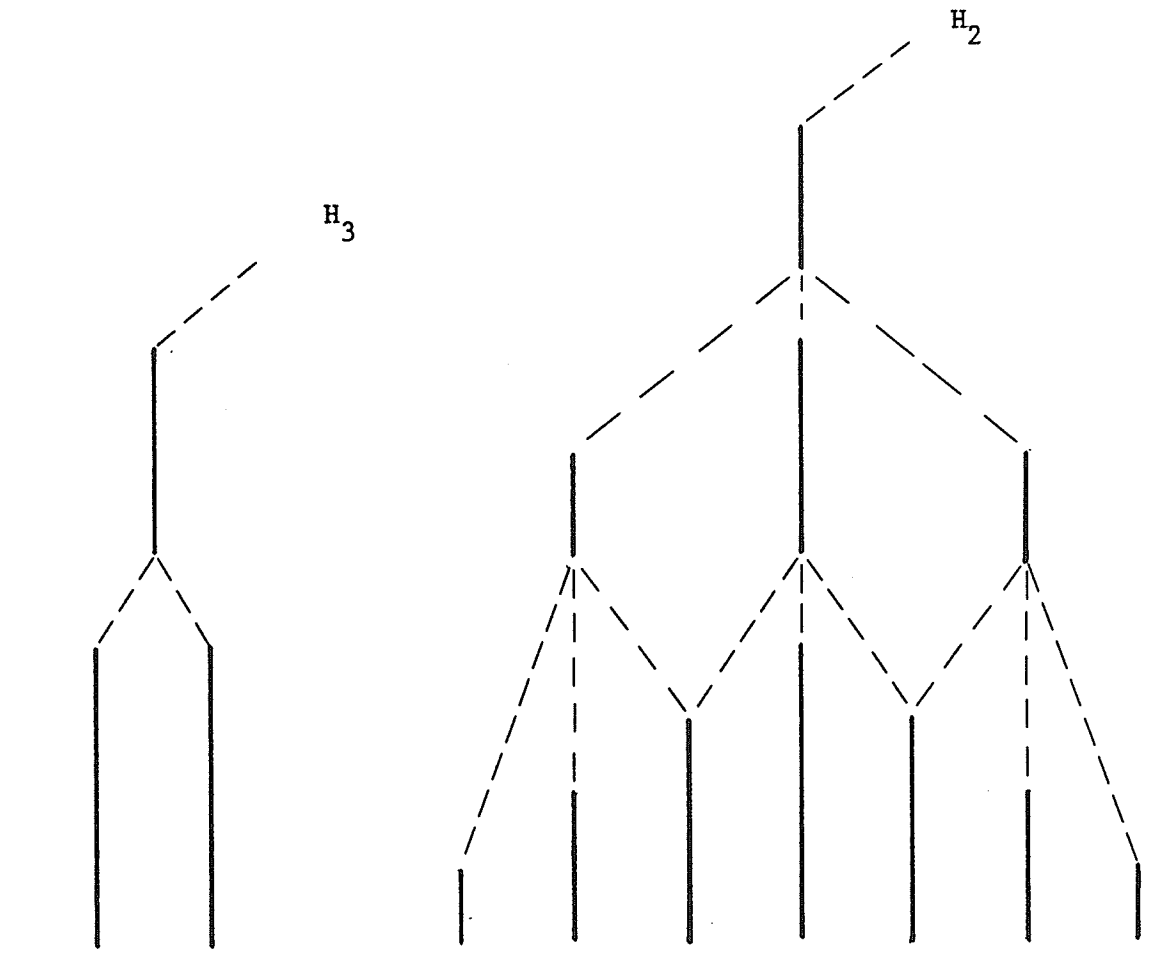

F	+2	+2	-2	-2	-2,0	0	0,+2	+2	+2
H_3			+2	0	-2,+2	0	-2,+2	0	-2
H_2	+	-							
	1	2	3	4	5	6	7	8	9

Figure 18

some observations of the methine proton resonance of 2,6-difluoroisopropylbenzene with irradiation of some peaks in the meta ring proton resonance

a a portion of the meta proton resonance

Transitions are numbered according to Figure 17.

b methine proton resonance septet second from high field

c methine proton resonance septet second from high field with irradiation of transitions 1 and 2

d methine proton resonance septet second from low field

e methine proton resonance septet second from low field with irradiation of transitions 1 and 2

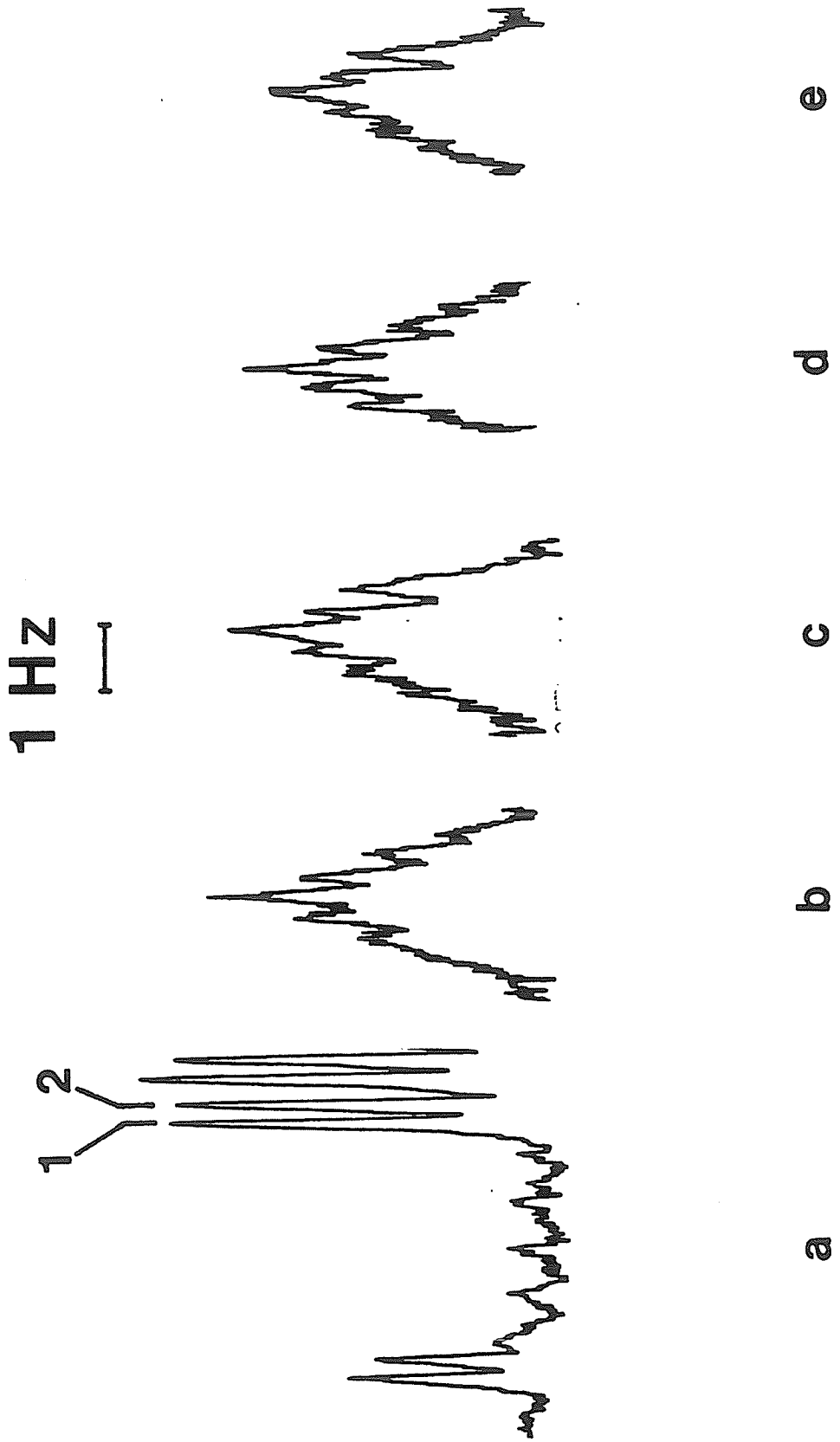
1 Hz
1
2
a
b
c
d
e

2,6-difluoroisopropylbenzene. The above assignment of the fluorine spin state for the meta proton doublet is based on a first-order interpretation of the ring proton spectrum. Figure 19 shows a DOR simulation of a methine multiplet (ignoring coupling to the methyl protons) in the absence of irradiation of the meta proton doublet, and in the presence of a 0.5 Hz irradiating field. The signs of the coupling constants were taken from Table 4, with a positive and with a negative sign for $^4J^{CH,F}_o$. This DOR simulation shows that $^4J^{CH,F}_o$ is negative, in agreement with the above results based on the assignment of the fluorine spin state.

However, the effect of the methyl group on these experiments has not been ascertained. Second-order effects due to coupling between the methyl and ring protons are presumably unimportant. However, the effect of the second-order coupling between the methyl and methine protons is illustrated in Figure 20. This figure depicts the LAME simulation of the methine resonance, decoupled from the ring resonances, for the CH_3CH fragment in 2,6-difluoroisopropylbenzene. The first order spectrum would be a 1:6:15:20:15:6:1 septet. The simulated spectrum shows a number of second-order transitions, increasing in number and intensity toward the center of the resonance. In the double resonance experiments described above, the methine proton multiplets second from low-field, and second from high-field, were observed. As the simulation in Figure 20 illustrates, the second-order lines for these multiplets are relatively weak, and to the low-field side of these multiplets. As the effects observed in these experiments involved the high-field side of the multiplets, the second-order coupling to the methyl protons does not affect the interpretation of the double resonance experiments.

Figure 19

a DOR simulation of double resonance experiments for the methine proton resonance shown in Figure 18

a a septet of the methine proton resonance with $^{4}J_{o}^{CH,F}$ negative

b a septet of the methine proton resonance in the presence of irradiation of the meta proton transitions 1 and 2 with $^{4}J_{o}^{CH,F}$ positive

c with $^{4}J_{o}^{CH,F}$ negative

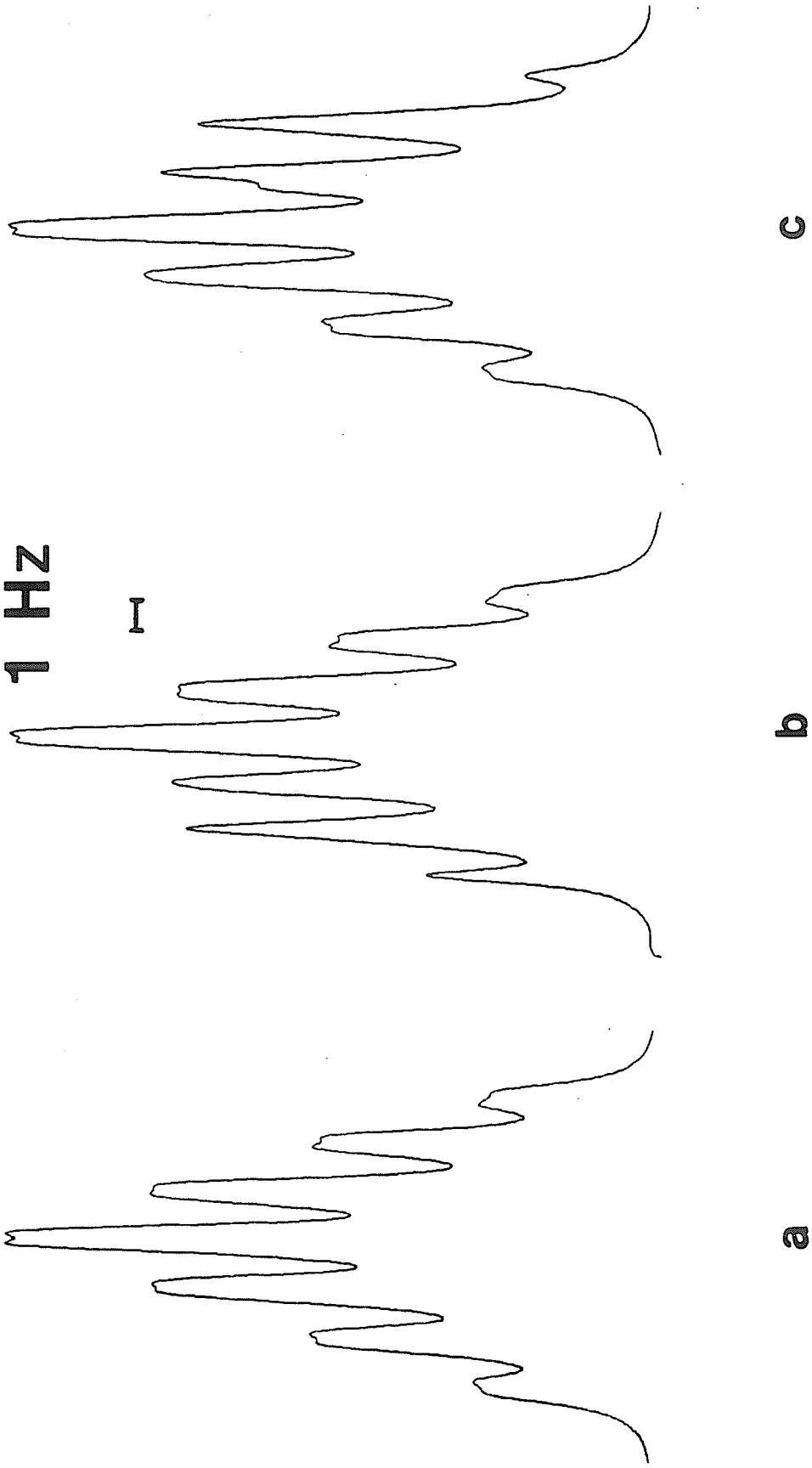
1 Hz
a
b
c

Figure 20

the LAME calculated spectrum of the isopropyl fragment of 2,6-difluoroisopropylbenzene, ignoring coupling to the ring nuclei

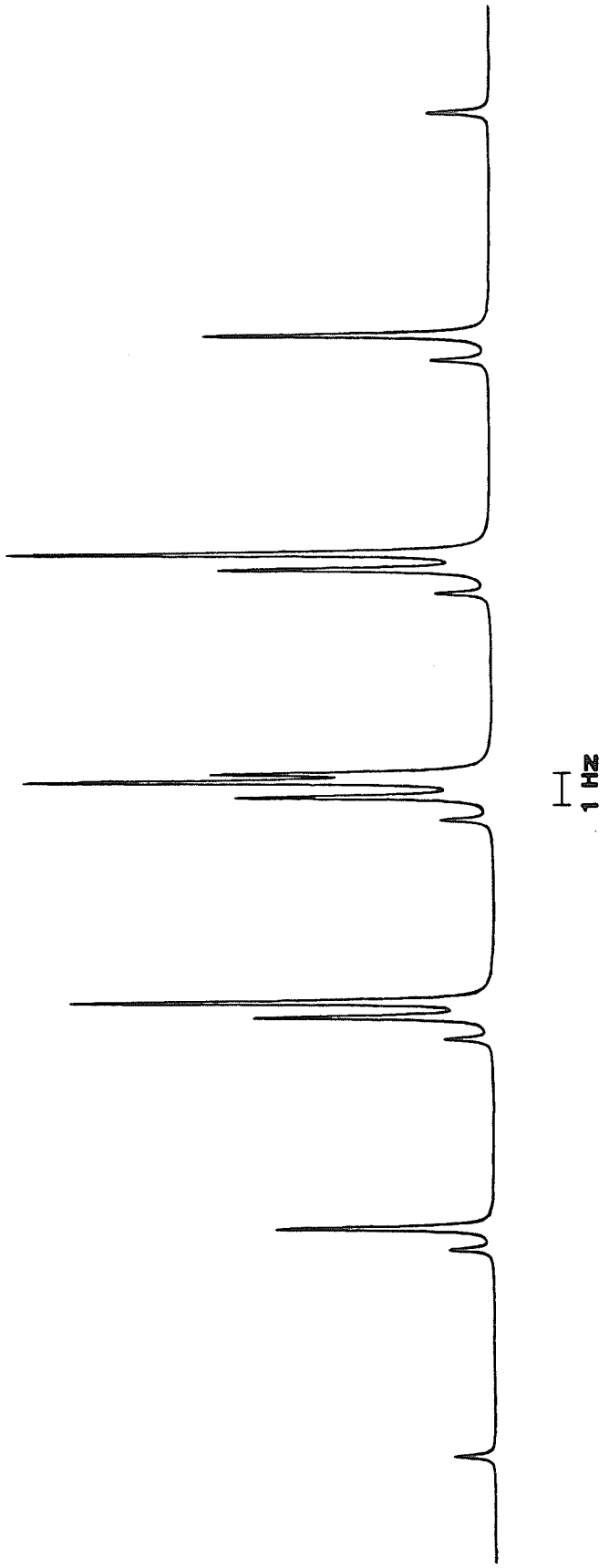
1 Hz

iv) determination of the sign of $^{5}J_{CH_3,F}$

The sign of the coupling from the methyl protons to the fluorine nucleus was determined with the aid of Figure 21. A transition in the methyl resonance was very weakly irradiated, while observing the second multiplet from low-field, and the second multiplet from high-field in the methine resonance. Irradiation of transitions 8 and 10 of the methyl resonance in turn resulted in the collapse of transitions 5,6 and 7, and of transitions 1,2 and 3, respectively, in the methine multiplets. These experiments are depicted in Figure 22. Note that due to the intensity of the irradiated transitions, the methine multiplets are very strongly perturbed, despite the use of a very weak irradiating field.

The results in Figure 22 are in agreement with the predictions of Figure 21. Since $^{4}J_{o}^{CH,F}$ has been determined to be negative, the value of $^{5}J_{CH_3,F}$ is conclusively shown to be positive. This conclusion is not affected by second-order coupling between the methyl and methine protons, as discussed in the preceding section.

Figure 21

a first-order representation of some transitions in the methine proton resonance H_2 and the methyl proton resonance H_1 of 2,6-difluoroisopropylbenzene

Only one multiplet for each of the resonances is depicted. Signs of the coupling constants were taken to be those given in Table 4.

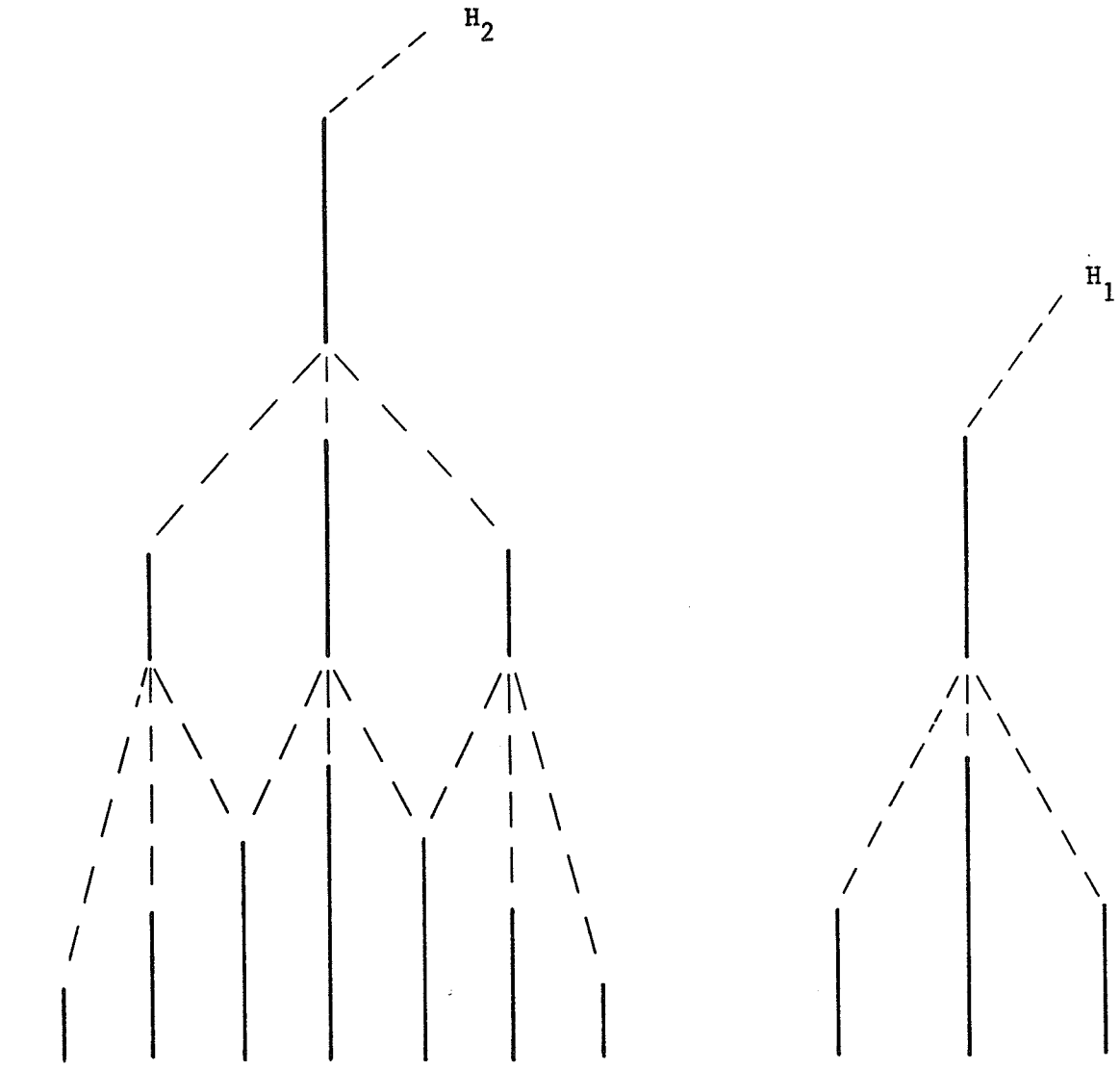
H_2
H_1
F -2 -2 -2,0 0 0,+2 +2 +2
H_3 +2 0 -2,+2 0 -2,+2 0 -2
1 2 3 4 5 6 7
+2 0 -2
8 9 10

Figure 22

some observations of the methine proton resonance of 2,6-difluoroisopropylbenzene with weak irradiation of peaks in the methyl proton resonance

The numbering of the peaks follows Figure 21.

a the low-field triplet of the methyl proton resonance

b the second from low-field septet of the methine proton resonance

c the second from low-field septet of the methine proton resonance with irradiation of transition 10

d with irradiation of transition 8

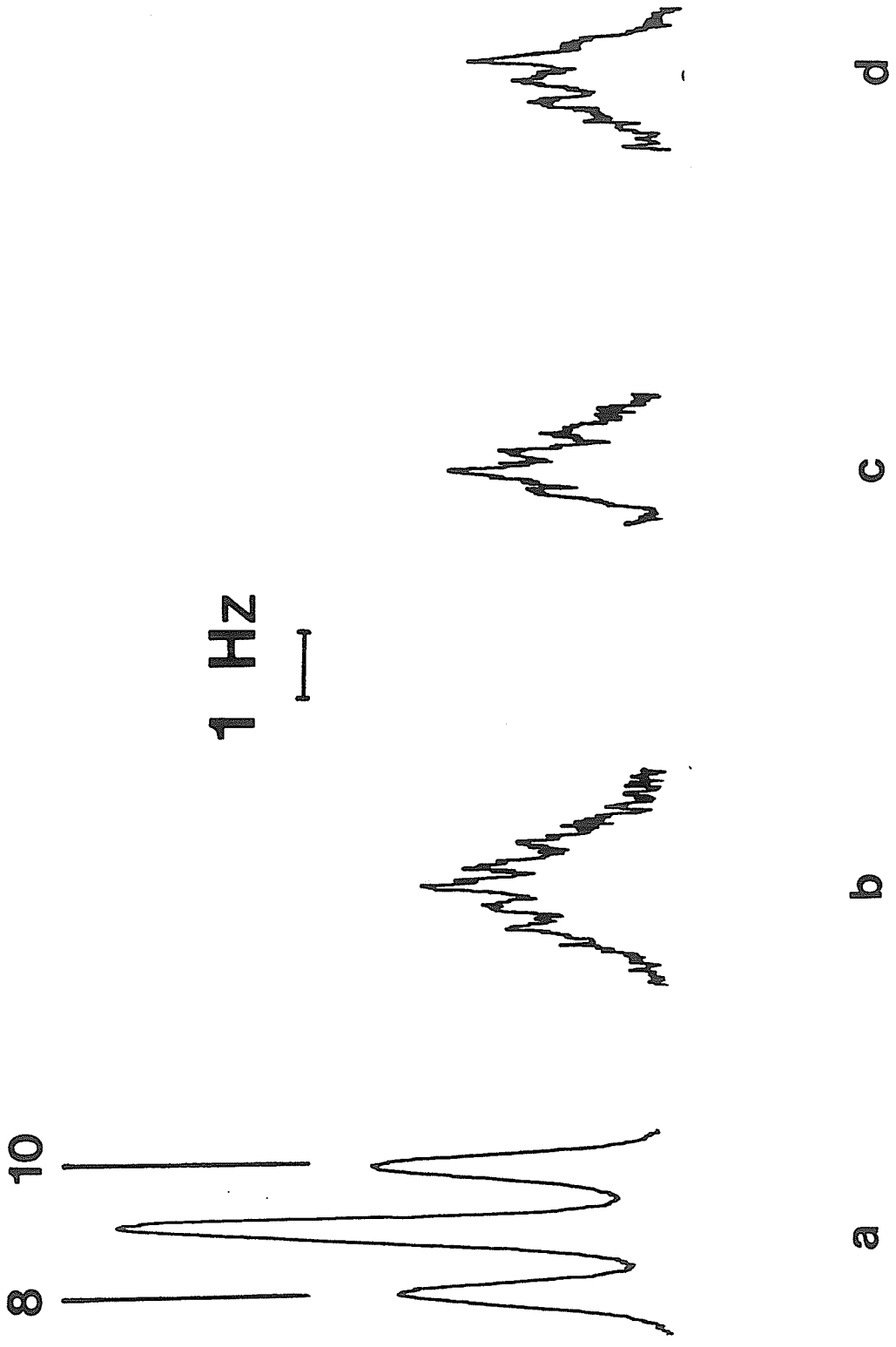
10
8
a
1 Hz
b
c
d

2. Fluorine Spectra under Conditions of Exchange

Fluorine nmr spectra in the presence of exchange were measured over a temperature range of 140 K to 200 K, in three different solvent mixtures. The coalescence of the two ortho fluorine signals occured at approximately 157 K. Preexchange lifetimes were determined by comparison of experimental spectra and spectra calculated by EXCH, and are tabulated in Table 5. Below the coalescence temperature, T_c, values of the chemical shift difference between the two fluorine nuclei in the ground state conformation 17 were also calculated, and tabulated. Above T_c the chemical shift difference could not be calculated, and was assumed to be constant, with a value of 295 Hz (the average of the values at 140 K and 150 K). Also tabulated are the linewidths of the peaks in the absence of

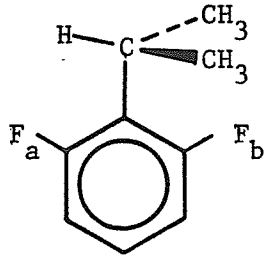

17

exchange, at one-half maximum peak height.

The quoted standard errors for preexchange lifetimes and chemical shift differences were determined as illustrated by the following example. The experimental fluorine spectrum at 150 K could be adequately matched by all spectra calculated with τ values in the range of 2.62×10^{-3} to 2.80×10^{-3} sec, and Δ values in the range of 299 to 301 Hz. Thus τ and Δ were taken as 2.71×10^{-3} sec and 300 Hz, with standard deviations of 9.0×10^{-5} sec and 1 Hz respectively.

Table 5

Preexchange Lifetimes in 2,6-difluoroisopropylbenzene as a Function of Temperature[a]

Temperature[b] (K)	Preexchange Lifetime[c] (sec)	Δ[d] (Hz)	$\nu_{1/2}$[e] (Hz)	Solvent[f]
200	$1.25(10) \times 10^{-5}$	295	0.95	A
190	$4.1(3) \times 10^{-5}$	295	1.2	M/I
180	$9.1(5) \times 10^{-5}$	295	1.5	A/I
180	$9.9(9) \times 10^{-5}$	295	1.5	A
170	$2.8(1) \times 10^{-4}$	295	2.3	A/I
165	$5.6(3) \times 10^{-4}$	295	1.8	A
160	$8.1(6) \times 10^{-4}$	295	4.2	M/I
160	$9.7(4) \times 10^{-4}$	295	4.2	A/I
155	$1.8(2) \times 10^{-3}$	305(5)	7.0	M/I
150	$2.71(9) \times 10^{-3}$	300(1)	5.4	M/I
145	$8.1(4) \times 10^{-3}$	292(2)	12.0	M/I
140	$1.46(4) \times 10^{-2}$	290(1)	7.5	M/I

Notes for Table 5

a determined from total lineshape fitted fluorine spectra at 84.67 MHz; bracketed numbers are standard errors in last digit(s) of parameters.

b Standard deviations in temperatures are ± 1 K.

c calculated from comparison of simulated and observed lineshapes

d calculated chemical shift difference between the fluorine nuclei in 17; Values were calculated from comparison of simulated and observed lineshapes below the coalescence temperature, T_c (between 155 and 160 K). Above T_c, Δ was assumed to be constant at 295 Hz.

e linewidth in the absence of exchange measured at one-half maximum peak height; estimated from linewidths of some sharp intense impurity peaks, and from internal hexafluorobenzene peak

f A, acetone-d_6; M/I, methylene chloride-d_2/isopentane (1:1 v/v); A/I, acetone-d_6/isopentane (1:1 v/v)

Some representative experimental and calculated fluorine nmr spectra are illustrated in Figure 23, for various temperatures and preexchange lifetimes.

Figure 23

some representative experimental and calculated fluorine resonance spectra of 2,6-difluoroisopropylbenzene in the presence of exchange between 140 and 200 K

Peaks marked with an asterisk are due to impurities.

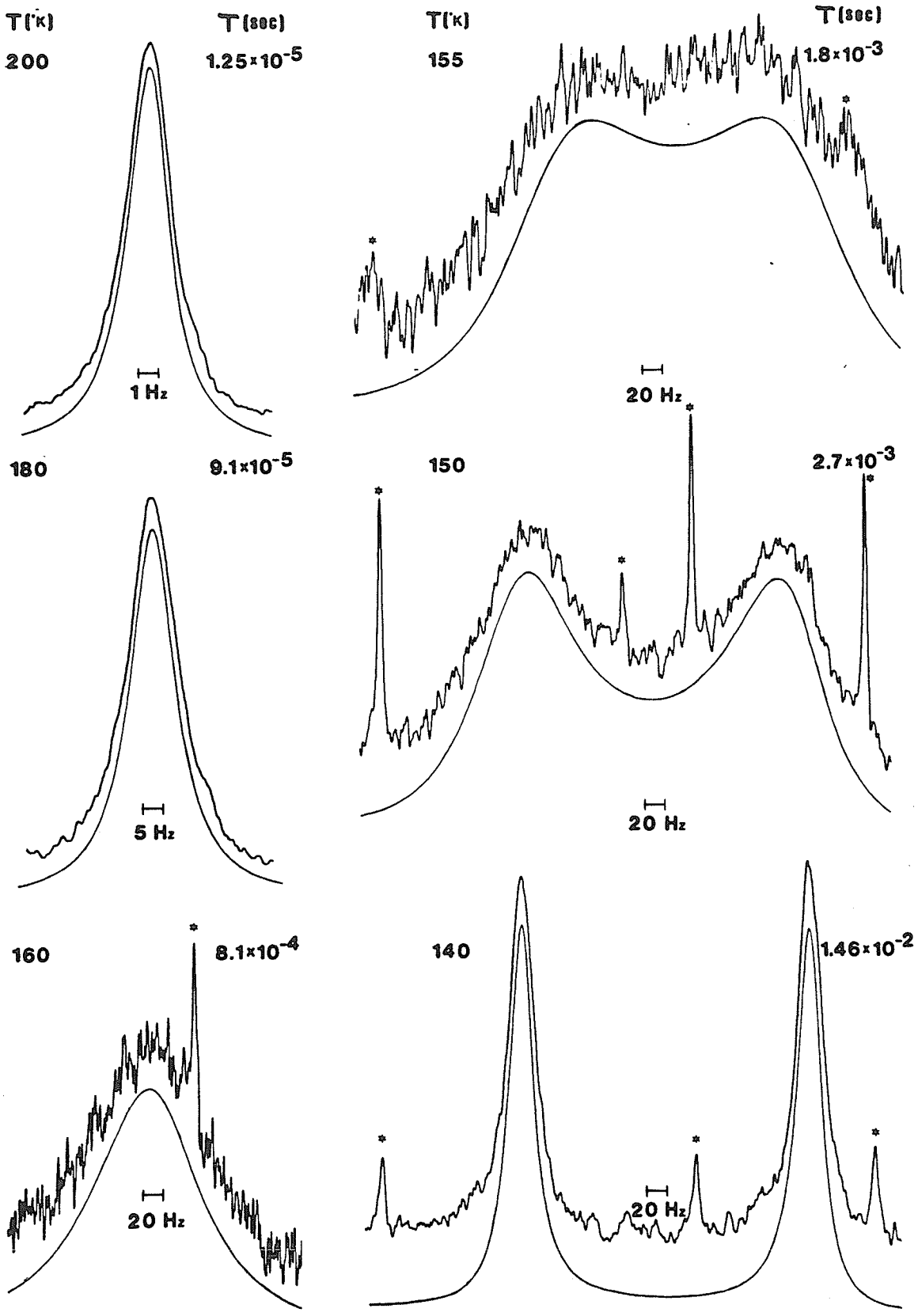
T(°K)
T(sec)
200
1.25×10⁻⁵
1 Hz
T(°K)
T(sec)
155
1.8×10⁻³
20 Hz
180
9.1×10⁻⁵
5 Hz
150
2.7×10⁻³
20 Hz
160
8.1×10⁻⁴
20 Hz
140
1.46×10⁻²
20 Hz

3. Experimental Activation Parameters

Using the rate data in Table 5, plots of ln k and ln k/T were prepared. Figure 24 displays the former, based on the Arrhenius equation (35), and Figure 25 displays the latter, based on the Eyring equation (34). The activation parameters E_A, log A, $\Delta H^{\dagger}$ and $\Delta S^{\dagger}$ were calculated from this data using the program ACTPAR. The value of $\Delta G^{\dagger}$ was calculated at 345 K from $\Delta H^{\dagger}$ and $\Delta S^{\dagger}$ using equation (3). These activation parameters are tabulated in Table 6. The bracketed errors for parameters calculated by ACTPAR, are the standard deviations in the last digit(s) of the parameters, and were also calculated by ACTPAR. The error in $\Delta G^{\dagger}_{345}$ was calculated from these errors using the procedure described by Binsch and Kessler.[1h] The correlation coefficients, from a linear regression analysis of the data plotted in Figure 24 and Figure 25, are also tabulated.

Figure 24

a plot of the Arrhenius equation of ln k versus 1/T for 2,6-difluoroisopropylbenzene in various solvents between 140 and 200 K

The correlation coefficient is -0.9982.

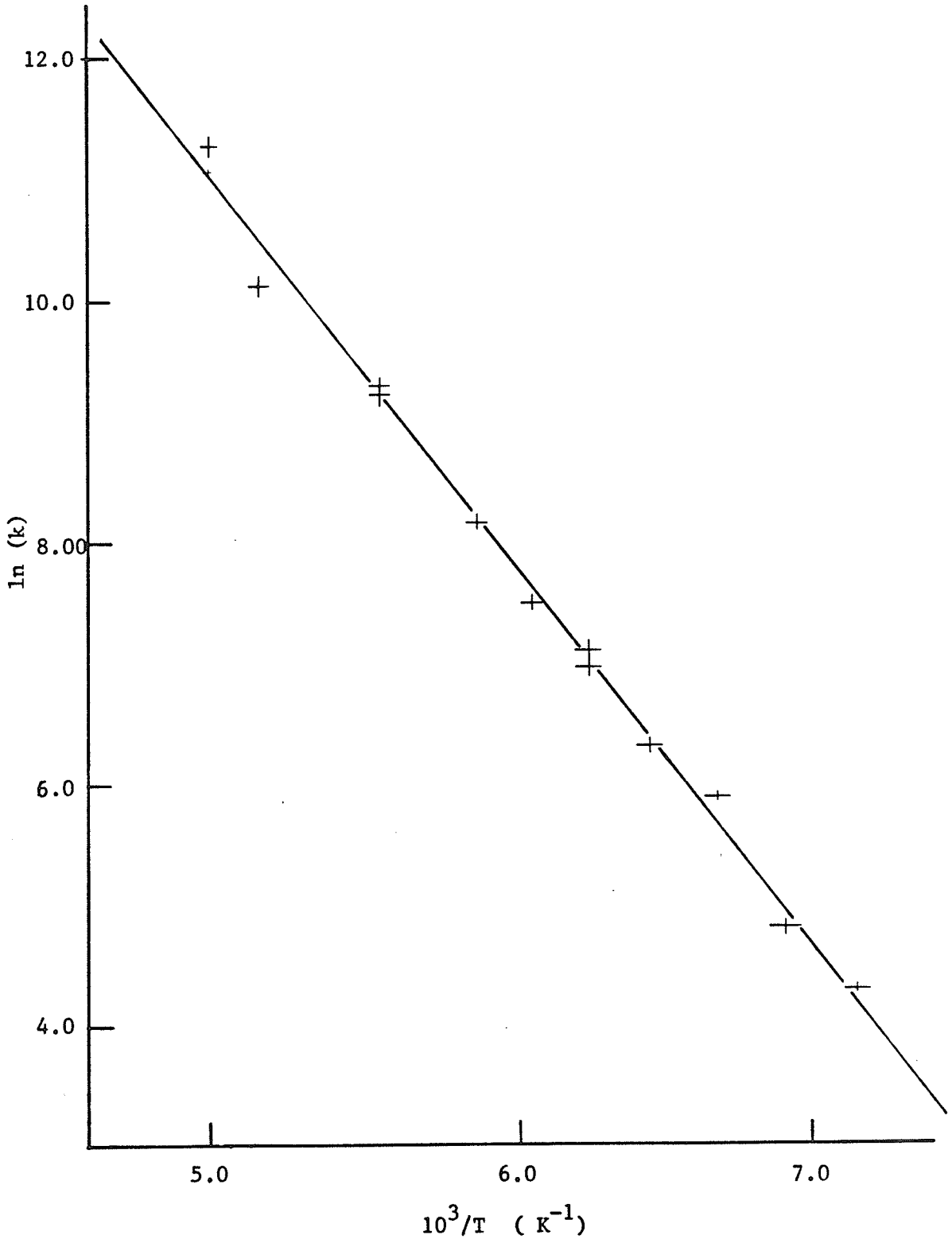
12.0
10.0
8.00
6.0
4.0
ln (k)
5.0
6.0
7.0
$10^3/T$ (K^{-1})

Figure 25

a plot of the Eyring equation of ln (k/T) versus 1/T for 2,6-difluoroisopropylbenzene in various solvents between 140 and 200 K

The correlation coefficient is -0.9980.

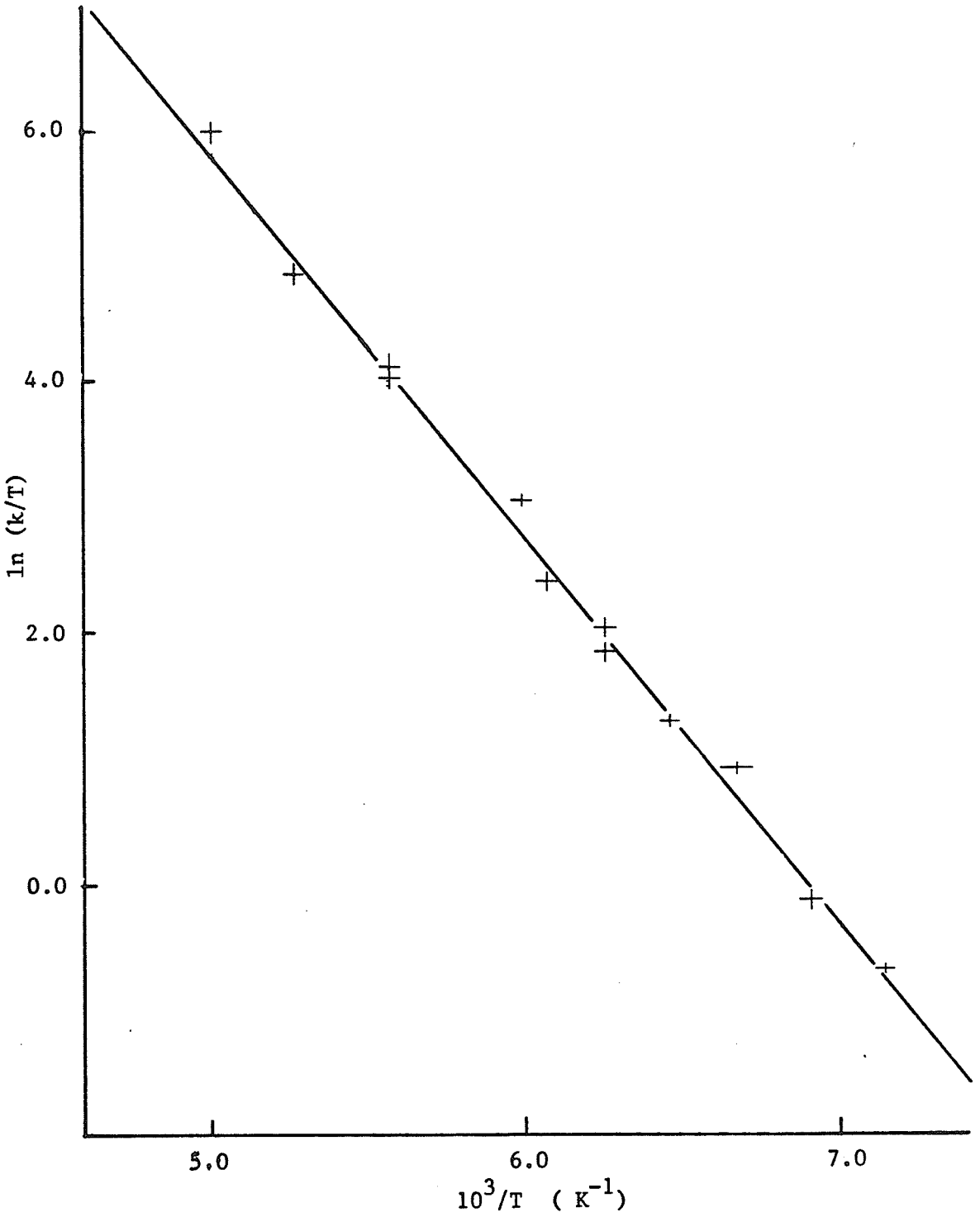
6.0
4.0
2.0
0.0
ln (k/T)
5.0
6.0
7.0
$10^3/T$ (K^{-1})

Table 6

Activation Parameters[a] for Internal Rotation of the Isopropyl Group in 2,6-difluoroisopropylbenzene

Eyring Activation Parameters[b]				Arrhenius Activation Parameters		
$\Delta H^{\dagger}$	$\Delta S^{\dagger}$	$\Delta G^{\dagger}_{345}$ [c]	r [d]	E_A	log A	r[e]
6.1(1)	-5.0(8)	7.8(1)	-0.9980	6.5(1)	11.9(2)	-0.9982

a $\Delta H^{\dagger}$, $\Delta G^{\dagger}_{345}$ and E_A have units of kcal/mole, $\Delta S^{\dagger}$ has units of cal $mole^{-1}$ K^{-1}; parameters calculated from temperature dependence of preexchange lifetimes by ACTPAR,[111] assuming a standard deviation of ± 1 K in temperature; assuming a standard deviation of ± 2 K in temperature does not change the calculated parameters significantly.

b Using only the 4 data points below the coalescence temperature gives values of 6.2(8) kcal/mole and -4.8(54) cal $mole^{-1}$ K^{-1} for $\Delta H^{\dagger}$ and $\Delta S^{\dagger}$ respectively.

c free energy of activation at 345 K calculated using equation (3); error calculated as described in reference 1h

d correlation coefficient calculated from a linear regression analysis of ln (k/T) versus 1/T

e correlation coefficient calculated from a linear regression analysis of ln k versus 1/T

D. Discussion

1. The Barrier to Internal Rotation

i) the activation parameters

The activation parameters for the internal rotation of the isopropyl group of 2,6-difluoroisopropylbenzene are listed in Table 6. In the absence of undetected systematic errors, the errors quoted for these parameters are the true errors in the activation parameters. However, systematic errors caused by ignoring changes in the relative chemical shifts, or changes in the linewidths in the absence of exchange, with temperature, or by improper temperature calibration can have a large effect on the accuracy of these activation parameters, particularily when the rate data are obtained over a narrow temperature range.

For the rate study described here, the measurements of temperatures are believed to be accurate to ±1 K, with perhaps ±2 K at the lowest temperatures. The temperature range over which the rate data were obtained is 60 K (over this range the rate constants change by a factor of 1000). When combined with the accuracy of the temperature measurements, this should ensure that systematic errors of this type will be small.

Similarily, changes in the linewidth in the absence of exchange, W, as a function of temperature were taken into account. It was assumed that the linewidth of all signals in the absence of exchange is the same, dominated by the magnetic field inhomogeneity and by the drift of the magnetic field during acquisition. Broadening due to relaxation effects, as well as the broadening of the 2,6-difluoroisopropylbenzene resonance due to incomplete proton decoupling, was ignored. The former will be insignificant in the absence of special relaxation effects; the latter follows as the linewidths of hexafluorobenzene and

2,6-difluoroisopropylbenzene are equal at 305 K. These values of W were then taken into account when calculating the rate constants. Further, the observed lineshapes for 2,6-difluoroisopropylbenzene are fairly insensitive to W, as the exchange-broadened linewidths are at least five times W for most measurements. In the worst case, the rate data at 200 K, increasing W by as much as 25 % results in a 14 % decrease in the calculated preexchange lifetime. For the remaining rate data, possible errors in W introduce errors in the preexchange lifetimes that are probably within the limits of error quoted in Table 5. It has been noted that this type of error has its least effect on activation parameters in molecules such as 2,6-difluoroisopropylbenzene, where the chemical shift difference is large.[1h,79d]

One source of systematic error that may be significant, results from ignoring possible temperature dependence of the relative chemical shifts of the two fluorine nuclei in 17. In the temperature region below coalescence, the observed lineshapes were fitted to both the preexchange lifetime, τ, and the chemical shift difference, Δ. Δ was found to be temperature dependent in this region, increasing by 15 Hz for a temperature increase of 15 K. However, above coalescence Δ could not be determined, and was assumed constant. As previously noted, this assumption could seriously affect the values determined for the activation parameters. Yet in this study, the effect of this assumption does not seem to be significant. This follows as the values of the activation parameters determined from the rate data below the coalescence temperature only (the data fitted to both τ and Δ) are virtually identical to those calculated over the full temperature range, as shown in Table 6.

Of course, other sources of systematic error cannot be ruled out.

Solvent effects apparently have a negligible effect on the rate data, although the fluorine nmr spectra were measured in three solvents. Measurements of preexchange lifetimes made in different solvents at the same temperature were in good agreement, and the rate data plotted in Figures 24 and 25 appear consistent for all three of the solvents.

Due to the logarithmic relationships which define $\Delta G^{\ddagger}$, and E_A, the determination of these parameters is fairly insensitive to the above errors, as well as to random errors, and can be determined to high accuracy. However, the determination of $\Delta H^{\ddagger}$, and $\Delta S^{\ddagger}$ is very sensitive to these errors, with the latter parameter being particularly sensitive.[1h,79d,e] Thus values of $\Delta H^{\ddagger}$, and especially $\Delta S^{\ddagger}$, should be treated with circumspection. A more realistic error for $\Delta H^{\ddagger}$ and $\Delta S^{\ddagger}$ would be three times the errors quoted in Table 6.

The Arrhenius activation energy, E_A, for α,α,2,6-tetrasubstituted toluenes represents the energy the molecule needs to acquire to undergo internal rotation. In accord with the relationship discussed in the Appendix, the value of E_A in 2,6-difluoroisopropylbenzene differs from the value of $\Delta H^{\ddagger}$ by RT, over the temperature range studied. Comparison of this value of E_A with those measured in α,α-diX-2,6-diY halotoluenes shows that the successive increase in the van der Waals volume of the <u>α</u> and <u>ortho</u> substituents[29] is paralleled by a concomitant increase in E_A. These activation energies are tabulated in Table 7, and indicate the dominant steric nature of the barrier in these molecules.

The Arrhenius frequency factor, A, has been interpreted to be the rate at which reactants move along the reaction coordinate toward the

Table 7

Activation Parameters in some α,α-diX-2,6-diY toluenes[a]

X	Y	E_A (kcal/mole)	log A	$\Delta H^{\dagger}$ (kcal/mole)	$\Delta S^{\dagger}$ cal $mole^{-1}$ K^{-1}	$\Delta G^{\dagger}_{345}$[b] (kcal/mole)	Reference
Cl	Cl	14.56(50)	12.19(88)	13.97(50)	-4.7(17)	15.4(1)	114
Br	Cl	-	-	-	-	18.39(5)	7,32
I	Cl	-	-	-	-	21.0(2)	8,32
Cl	Br	16.33(42)	11.76(2')	15.68(42)	-6.9(13)	18.14(5)	6,32
Br	Br	19.85(22)	13.23(13)	19.13(22)	-0.4(6)	19.3(1)	32
CH_3	F	6.5(1)	11.9(2)	6.1(1)	-5.0(8)	7.8(1)	c

a numbers in parentheses are standard deviations in last digit(s) of parameters

b calculated value of $\Delta G^{\dagger}$ at 345 K

c this work

transition state. Bimolecular collisions with energy greater than E_A will then result in the formation of the product. A similar interpretation for hindered internal rotation suggests that A is twice the libration frequency of the rotor in the potential well, E_A. Thus A can be written as [115,116,117]

$$A = \frac{1}{\pi}\sqrt{\frac{2E_A}{I_r}} \qquad (36)$$

where I_r is the reduced moment of inertia about the internal rotational axis. Using a moment of 0.9×10^{-38} gm cm^2, equation (36) yields a value of 12.5 for log A in 2,6-difluoroisopropylbenzene, in fair agreement with the experimental value.

According to absolute reaction rate theory, the entropy of activation, $\Delta S^{\dagger}$, for internal rotation is the increase in the entropy of the molecule in the rotation from the ground to the transition state conformation. Assuming a realistic error, the value of $\Delta S^{\dagger}$ in 2,6-difluoroisopropylbenzene is -5.0 ± 2.4 cal mol^{-1} K^{-1}. This may be rationalized in terms of the change in the vibrational and rotational contributions to the entropy between the ground and transition state conformers. Of the various contributions to the entropy, only these are expected to be significantly different for the two conformers. The transition state, 3 (X=CH_3,R=F) suffers larger steric interactions than the ground state, 1 (X=CH_3,R=F), and thus the former conformer is expected to be somewhat more rigid than the latter. In the transition state this results in a decrease in the rotational freedom of the methyl groups, as well as a decrease in the vibrational freedom, especially in bending modes, of bonds proximate to the α and ortho substituents.

The result is a small negative entropy of activation.

The entropy of a freely rotating rigid rotor, with a moment of inertia I_r, and a symmetry number n is[122]

$$S = R\left[\ln Q - \frac{1}{QT}\frac{\partial Q}{\partial(1/T)}\right] \qquad (37)$$

where Q is the partition function for the rotor, equal to $(8\pi^3 I_r kT)^{\frac{1}{2}}/nh$. Complete loss of the rotational freedom of the two methyl groups in the isopropyl sidechain of 2,6-difluoroisopropylbenzene may be estimated to contribute -6.0 cal mol^{-1} K^{-1} to the entropy of activation at 170 K. This calculation assumes that the methyl groups are free rotors in the ground state, an unlikely situation, but the calculation illustrates the importance of the effect.

However, in 2,6-difluoroisopropylbenzene the rotational contribution to $\Delta S^{\dagger}$ may not be important. In a series of 1,3,5-trineopentylbenzenes, Nilsson and coworkers have found that $\Delta S^{\dagger}$ is 0 ± 3 cal mol^{-1} K^{-1}, for the rotation of a neopentyl group past an ortho substituent; while in 1,2,3,4-tetramethyl-5,6-dineopentylbenzene $\Delta S^{\dagger}$ is -11.5 ± 2.1 cal mol^{-1} K^{-1}, for the rotation of one neopentyl group past the neopentyl group ortho to it.[28] They suggested that the transition state in the latter was much more sterically crowded than in the former, resulting in the loss of the $-CH_2-C(CH_3)_2$ rotation.* In the former series of molecules, apparently, this contribution, and the vibrational

---

* The contribution to the entropy of activation from the complete loss of this rotation was calculated as -7.0 cal mol^{-1} K^{-1} at 298 K, using equation (37).[28]

contribution, are not important. Furthermore, in the series of 2,6-dihalobenzenes shown in Table 7, the average entropy of activation is in the range of -3.5 ± 3 cal mol^{-1} K^{-1}, for the rotation of the dihalomethyl group, and is -5.4 ± 1.5 cal mol^{-1} K^{-1} in $\alpha,\alpha,\alpha',\alpha'$2,4,5,6-octachloro-m-xylene for rotation of the dichloromethyl group.[121] These values are very similar to that observed for 2,6-difluoroisopropylbenzene, despite the fact that only vibrational contributions are expected to be important in the former compounds. Thus it appears that the vibrational contribution dominates the entropy of activation in 2,6-difluoroisopropylbenzene, although a rotational contribution may also be present.

Brot, however, has argued that the entropy of activation has no intrinsic significance in reorientational processes such as hindered internal rotation.[116]

The value of the enthalpy of activation, $\Delta H^{\dagger}$, in 2,6-difluoroisopropylbenzene is given in Table 6, and is compared to $\Delta H^{\dagger}$ in some 2,6-dihalobenzal halides in Table 7. As with E_A, the value of $\Delta H^{\dagger}$ increases as the van der Waals volumes of the α and ortho substituents increase. As $\Delta H^{\dagger}$ is approximately equal to the potential energy barrier (see Appendix), this relationship is expected for barriers that originate in steric interactions. Peeling has reasoned, for the 2,6-dihalobenzal halides, that the barrier heights depend on the steric interactions between the α and ortho substituents, in both the ground and excited state conformations.[32] In both conformations in these compounds, the internuclear separation of the α and ortho substituents is less than

the sum of their van der Waals radii, and thus there is a significant amount of non-bonded repulsion. The energy of these steric interactions depends on the effective sizes of the substituents, and on their separation. Following the work of Peeling,[32] the internuclear separation of the α and ortho substituents was calculated using standard bond lengths and angles,[118] for both the ground state, 1, and the transition state, 3, for the compounds in Table 8. The difference between these two internuclear separations was multiplied by the sum of the van der Waals volumes[29] of the α and ortho substituents. This product, S, was found to be inversely proportional to $\Delta H^{\dagger}$. The values of S^{-1} and $\Delta H^{\dagger}$ for 2,6-difluoroisopropylbenzene studied in this work, some 2,6-dihalobenzal halides studied by Peeling,[32] and 3,5-dibromoisopropylbenzene studied by Schaefer and coworkers,[17] are given in Table 8, A plot of $\Delta H^{\dagger}$ versus S^{-1} is shown in Figure 27, and gave the equation

$$\Delta H^{\dagger} = -201.19\ S^{-1} + 28.71 \text{ kcal/mole} \qquad (38)$$

with a value of -0.993 for the correlation coefficient. Table 8 gives the barrier heights calculated from (38), as well as the experimental values. It should be noted that the experimental barrier tabulated for 3,5-dibromoisopropylbenzene is the two-fold potential energy barrier, V_2, measured by the J method.[17] V_2 is equal to $\Delta H^{\dagger}$ provided that the temperature dependence of the rate of exchange of the rotating group can be adequately described by the Eyring equation (34) (see Appendix). The temperature dependence of the exchange rate is not known in 3,5-dibromoisopropylbenzene, but in the other α,α,2,6-tetrasubstituted toluenes tabulated, plots of the Eyring equation are linear. Thus for

Figure 26

a plot of $\langle \sin^2 \theta \rangle$ as a function of V_2 for 2,6-difluoroisopropylbenzene, calculated by the computer program EXPECT

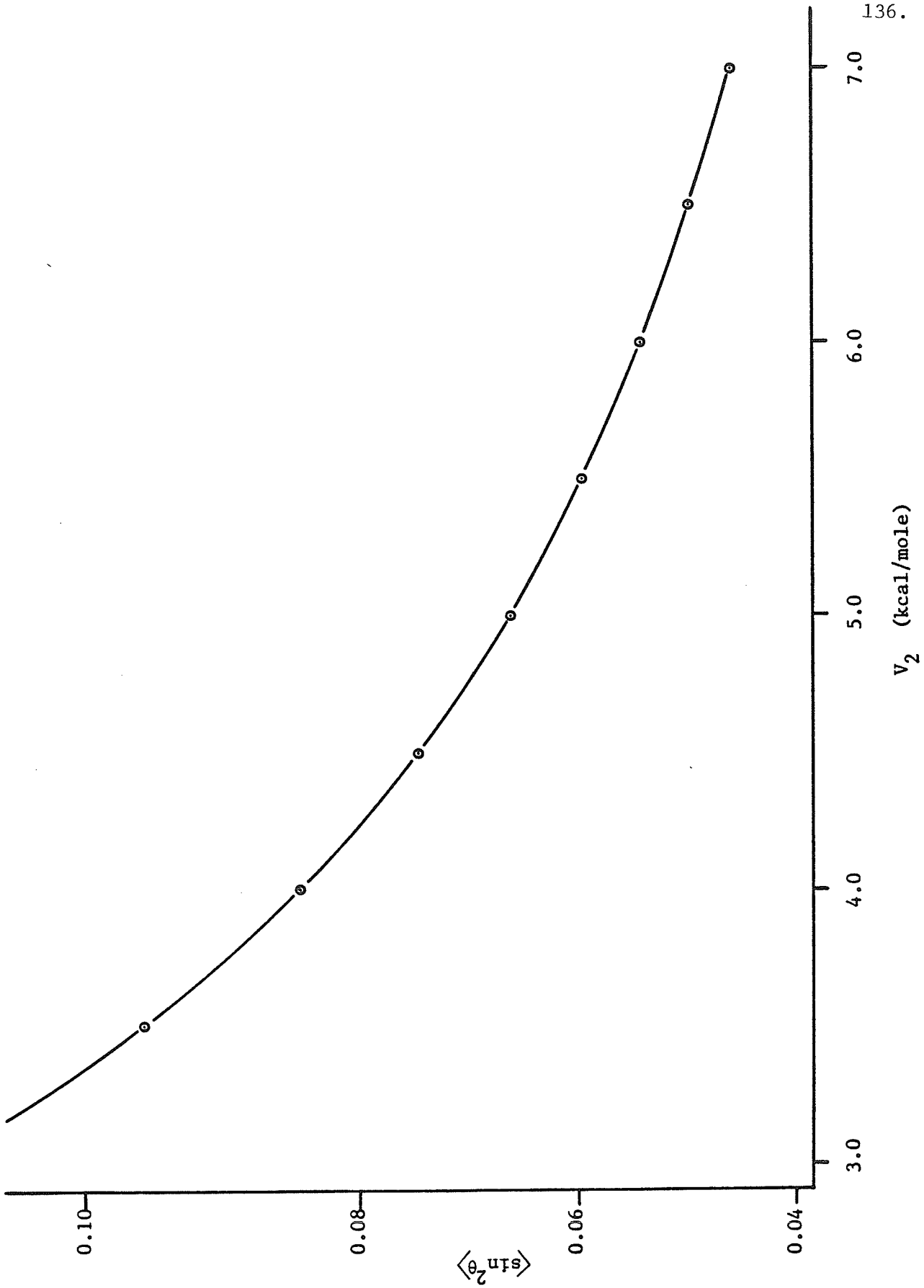
0.10
0.08
0.06
0.04
$\langle \sin^2\theta \rangle$
3.0
4.0
5.0
6.0
7.0
V_2 (kcal/mole)

Table 8

Empirical Correlation of Barriers to Internal Rotation in α,α-diX-2,6-diY toluene Derivatives with Steric Factors[a]

X	Y	S^{-1} [b]	$\Delta H^{\dagger}$ (kcal/mole)		$\Delta G^{\dagger}_{345}$ [c] (kcal/mole)		Reference[d]
			Experimental	Predicted[e]	Experimental	Predicted[f]	
CH_3	H	0.1366	2.0(2)[g]	1.23	-	2.36	17
CH_3	F	0.1092	6.1(1)	6.74	7.8(1)	7.85	h
Cl	Cl	0.0702	13.97(50)	14.59	15.3(1)	15.67	114
Cl	Br	0.0596	15.68(42)	16.72	18.14(5)	17.79	6,32
Br	Cl	0.0585	-	16.94	18.39(5)	18.01	7,32
Br	Br	0.0502	19.13(22)	18.61	19.3(1)	19.68	32
I	Cl	0.0433	21.0	20.00	21.0(2)	21.06	8,32

a numbers in parentheses are the standard errors in the last digit(s) of parameters

b calculated from steric factors as discussed in text

c the value of $\Delta G^{\dagger}$ calculated at 345 K

d reference for experimental values

e calculated from equation (38)

f calculated from equation (39)

g V_2 determined by the J method

h this work

Figure 27

a plot of the empirical correlation of $\Delta H^{\dagger}$ versus S^{-1} for $\alpha,\alpha,2,6$-tetrasubstituted toluenes

The correlation coefficient is -0.993.

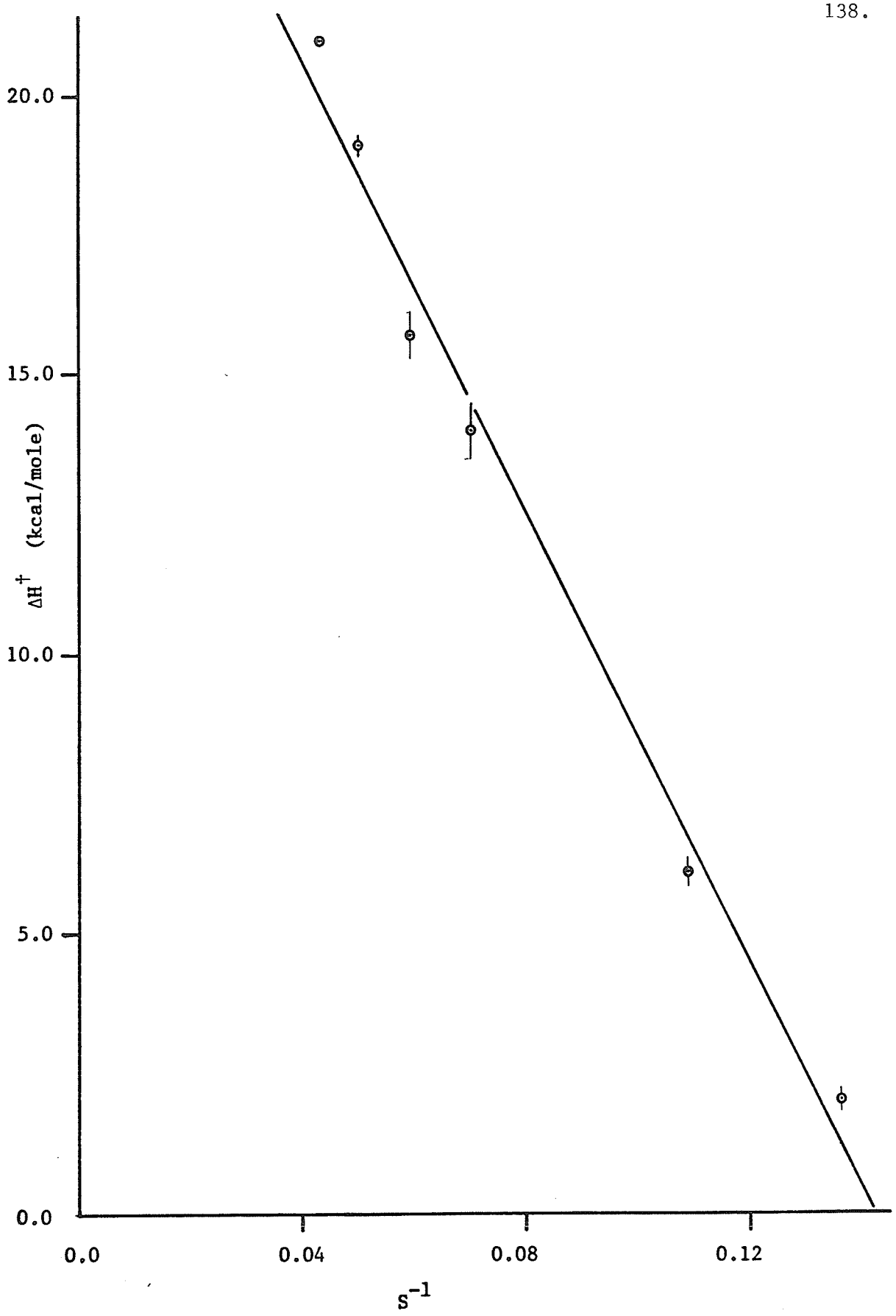
20.0
15.0
10.0
5.0
0.0
ΔH^{+} (kcal/mole)
0.0
0.04
0.08
0.12
s^{-1}

this type of molecule, it appears $\Delta H^{\dagger}$ is approximately equal to V_2.

As discussed previously, the values of the entropy of activation in the α,α,2,6-tetrasubstituted toluenes are approximately equal within experimental error. For these compounds, the values of $\Delta G^{\dagger}$ should thus parallel those of $\Delta H^{\dagger}$. The former have the advantage that their values are known much more accurately than those of the latter.[79e] The parameter S was found to be inversely proportional to $\Delta G^{\dagger}_{345}$, the value of $\Delta G^{\dagger}$ at 345 K, for the compounds in Table 8. A plot of $\Delta G^{\dagger}_{345}$ versus S^{-1} is shown in Figure 28, and gave the equation

$$\Delta G^{\dagger}_{345} = -200.35\ S^{-1} + 29.73 \text{ kcal/mole} \qquad (39)$$

with a correlation coefficient of -0.9978. Values of $\Delta G^{\dagger}_{345}$ calculated from (39), as well as experimental values, are tabulated in Table 8. Table 9 gives calculated and experimental barriers to internal rotation in some α,α,2,6-tetrasubstituted toluenes that were not included in the determination of the empirical relations (38) or (39).

The purely empirical correlations in (38) and (39) are surprisingly good, although the correlation with $\Delta G^{\dagger}_{345}$ is clearly superior. In most cases the observed barriers are in qualitative and quantitative agreement with experiment. The calculated values of $\Delta G^{\dagger}_{345}$ are all within 3 % of the experimental values for the compounds in Table 8. However, the barrier in benzal fluoride is predicted to be negative by (38). This arises because the internuclear separation between the α and ortho substituents in this compound is greater than the sum of the van der Waals radii, even in the transition state. Thus the barrier in this compound is suggested to be not primarily due to steric interactions.

Figure 28

a plot of the empirical correlation of $\Delta G^{\dagger}_{345}$ versus S^{-1} for $\alpha,\alpha,2,6$-tetrasubstituted toluenes

The correlation coefficient is -0.9978.

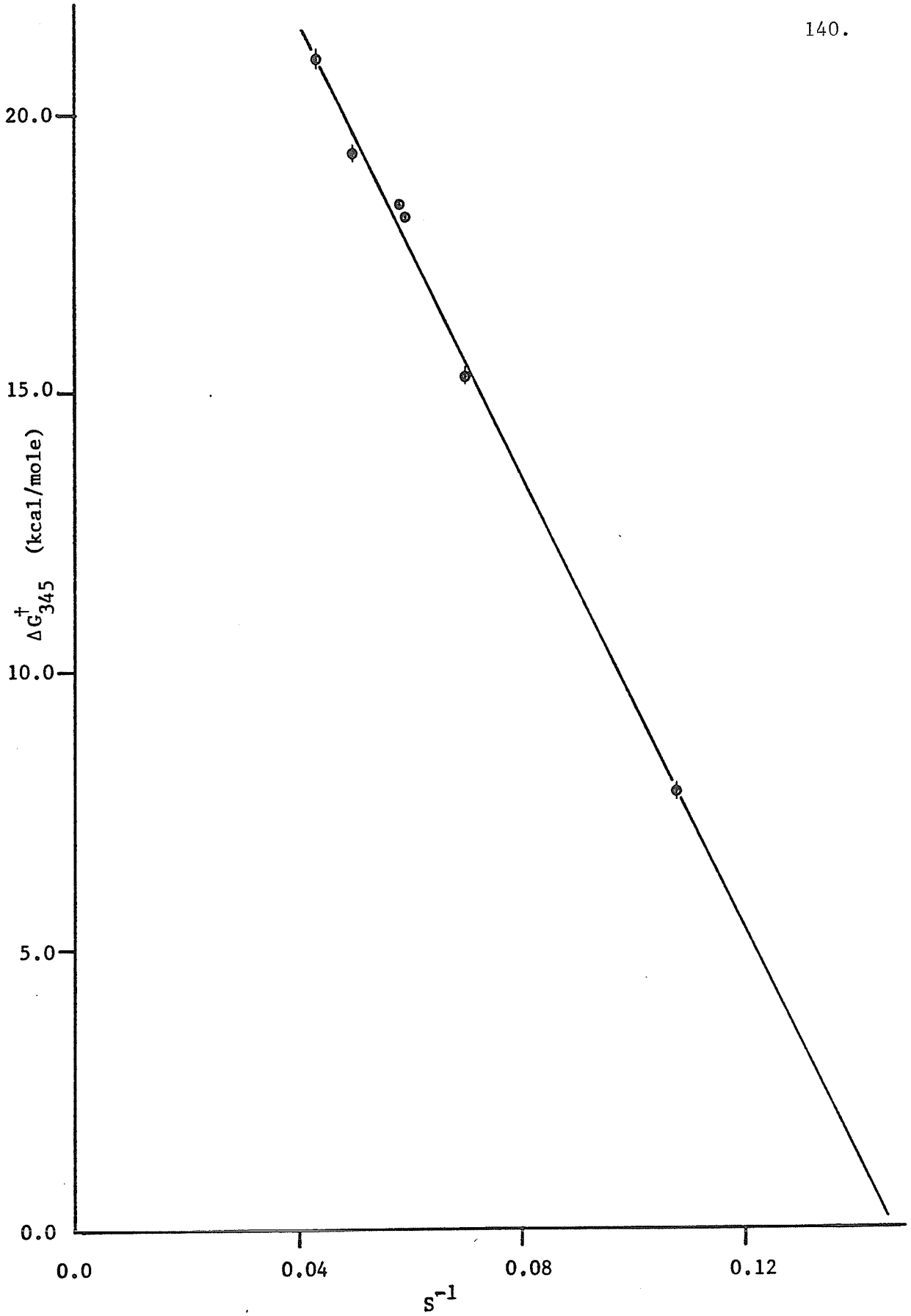
20.0
15.0
10.0
5.0
0.0
$\Delta G^{\dagger}_{345}$ (kcal/mole)
0.0
0.04
0.08
0.12
s^{-1}

Table 9

Experimental and Predicted Barriers in some α,α-diX-2,6-diY toluene Derivatives[a]

X	Y	S^{-1} [b]	Barrier to Internal Rotation (kcal/mole)		Reference[c]
			Predicted	Experimental	
F	H	0.2891	-29.5[d]	1.1(2)[f]	21
Cl	H	0.1357	1.41[d]	2.2(3)[f]	21
Br	H	0.1085	6.88[d]	3.5(6)[f]	21
I	H	0.0752	14.66[e]	-	-
CH_3	Cl	0.0742	13.79[d]	-	-
CH_3	CH_3	0.0732	15.07[e]	12.8(2)[g]	27b
Cl	CH_3	0.0692	15.87[e]	13.9(3)[h]	27b,27c
CH_3	Br	0.0638	15.88[d]	-	-
CH_3	I	0.0529	18.06[d]	-	-

a numbers in parentheses are standard errors in last digit of parameters

b parameter calculated from steric factors as described in text

c reference for experimental values

d $\Delta H^{\dagger}$ calculated from equation (38)

e $\Delta G^{\dagger}$ calculated at 345 K from equation (39)

f V_2 estimated by the J method

g $\Delta G^{\dagger}$ determined from coalescence at 238 K

h $\Delta G^{\dagger}$ determined from coalescence at 261 K

It is also of interest to note that the barriers in 2,6-dimethylisopropylbenzene and 2,6-dimethylbenzal chloride are both approximately 2 kcal/mole lower in energy than those predicted by (39). This lower energy might well be ascribed to a "gear effect" of the methyl groups involved, although the effect is not apparent in 2,6-difluoroisopropylbenzene.

The empirical correlations in (38) and (39) suggest very strongly that the barriers to internal rotation in compounds of this type are predominantly steric in nature. This conclusion is supported by classical molecular mechanics calculations. The experimental barrier heights in α,α,2,6-tetrasubstituted toluenes are well reproduced by Ernst's semiempirical potential energy calculations, which consider only non-bonded repulsions and the effects of bond bending and stretching due to these repulsions.[27b,32]

Equations (38) and (39) predict the barrier to internal rotation due to the steric hindrance of the substituents. As the hindrance of the α and ortho substituents increases, the value of the parameter S^{-1} approaches a limiting value of zero. Thus (38) and (39) suggest that the maximum barrier due to steric effects in these compounds is approximately 30 kcal/mole, no matter how large the steric hindrance of the substituents. Of course the validity of these equations for such large barriers is unknown.

ii) the potential energy barrier by the J method

The value of $^{6}J_{p}^{CH,H}$ in 2,6-difluoroisopropylbenzene was estimated as -0.080 ± 0.020 Hz at 305 K. The value of $^{6}J_{90}^{CH,H}$ in equation (5) is -1.24 Hz in toluene (see Chapter II.D), and has been shown to be insensitive to ring substitution:[64,65,70,87,104] in toluene $^{6}J_{p}^{CH,H}$ is -0.62 ± 0.02 Hz,[70] in 2-bromo-5-chlorotoluene -0.58 ± 0.03 Hz,[64] and in 2,6-dichlorotoluene -0.63 ± 0.02 Hz.[104] Thus the two ortho fluorine substituents will not affect the value of $^{6}J_{90}^{CH,H}$ in 2,6-difluoroisopropylbenzene. Furthermore, there is evidence that $^{6}J_{90}^{CH,H}$ is insensitive to the replacement of the α-protons in toluene with one or two methyl groups. In 2,6-dichloroethylbenzene, conformation 10 ($X=CH_3$) is preferred by at least 3 kcal/mole. Assuming $^{6}J_{90}^{CH,H}$ is -1.24 Hz predicts a value of -0.31 Hz for $^{6}J_{p}^{CH,H}$ from (5), as θ is approximately constant at 30°, and thus $\langle \sin^2\theta \rangle = 1/4$. The observed value is -0.29 ± 0.02 Hz,[14] in agreement with the calculated value. A value of -1.24 Hz for $^{6}J_{90}^{CH,H}$ was also used to determine a barrier in 3,5-dibromoisopropylbenzene that was in good agreement with ESR measurements of some similar radicals.[20] However, Janzen and Schaefer[87] have found a linear decrease in the magnitude of $^{6}J_{90}^{CH,H}$ with the electronegativity of the α-substituent in some benzyl compounds. The electron-withdrawing α-substituent polarizes the C-H bonds of the halomethyl group, decreasing the hyperconjugative overlap to the adjacent carbon π-orbital of the ring. This reduction in the value of $^{6}J_{90}^{CH,H}$ has been confirmed by other studies.[21,104,119] Using this linear relationship[87] predicts a value of -1.20 for $^{6}J_{90}^{CH,H}$ in ethylbenzene, and suggests a value no larger than -1.16 Hz in isopropylbenzene. However,

there is evidence that $^{6}J_{90}$ is -0.87 Hz in benzal fluoride.[21] Assuming a linear relationship between $^{6}J_{90}$ and the electronegativity of the two α-substituents in benzal compounds exists, then $^{6}J_{90}$ is predicted to be -1.20 Hz in isopropylbenzene. Taking $^{6}J_{90}$ to lie between -1.24 and -1.16 Hz gives $\langle \sin^2\theta \rangle$ = -0.08 ± 0.02/-1.20 ± 0.04 = 0.067 ± 0.019 using equation (5).

Recent work in this laboratory* has applied the computer program DAVINS[120] to calculate the spectral parameters, from a digitized spectrum stored on a disc memory, of a 5 mole % solution of 2,6-difluoroisopropylbenzene in acetone-d_6 at 305 K. This program does an automated analysis of the nmr spectrum, including a total lineshape analysis. This latter feature makes it possible to estimate the magnitudes of unresolved couplings. The spectral parameters for 2,6-difluoroisopropylbenzene, calculated by DAVINS only from the ring proton spectrum, are tabulated in Table 10. The values of the parameters are in general good agreement , with some exceptions, with those calculated previously, and tabulated in Table 4. Note, however, that the sign predicted for $^{6}J_{p}^{CH,H(4)}$ by DAVINS is incorrect. The value of $^{6}J_{p}^{CH,H(4)}$ from DAVINS was taken as -0.098 ± 0.020, assuming an error of three times the standard deviation. This value agrees, within the limits of error, with the value observed above. Using the value of -0.098 ± 0.020 in (5) gives $\langle \sin^2\theta \rangle$ = 0.082 ± 0.020, with $^{6}J_{90}$ as -1.20 Hz. The average value of $\langle \sin^2\theta \rangle$ from the two measurement techniques is then 0.075 ± 0.027.

---

* This work was done by Rudy Sebastian in 1982.

Table 10

DAVINS Spectral Parameters for the Ring Protons of 2,6-difluoroisopropylbenzene[a]

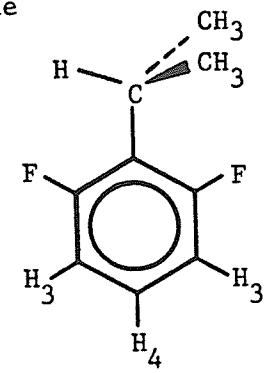

$\nu_{H(3)}$	621.946(2)
$\nu_{H(4)}$	650.194(3)
$^{3}J^{o}_{H(3),H(4)}$	8.386(3)
$^{3}J^{o}_{H(3),F}$	10.480(4)
$^{4}J^{m}_{H(3),H(3)}$	1.209(8)
$^{4}J^{m}_{H(4),F}$	6.389(4)
$^{5}J^{m}_{CH,H(3)}$	-0.289(3)
$^{5}J^{p}_{H(3),F}$	-1.367(4)
$^{6}J^{p}_{CH,H(4)}$	0.098(7)
linewidth	0.181(4)

a at 305 ± 1 K for a 5.0 mole % solution in acetone-d_6 at 90.02 MHz; analysis done by Rudy Sebastian, in this laboratory, in 1982; bracketed values are standard deviations in the last digit of parameters, calculated by DAVINS.

Figure 26 depicts a plot of $\langle \sin^2\theta \rangle$ versus V_2, the two-fold barrier to internal rotation in 2,6-difluoroisopropylbenzene at 305 K. These values were calculated by the computer program EXPECT, using a value of 0.9×10^{-38} gm cm^2 for the reduced moment of inertia about the exocyclic bond. Calculations with a reduced moment of 0.5×10^{-38} gm cm^2 gave identical results, illustrating that $\langle \sin^2\theta \rangle$ is insensitive to the reduced moment of inertia. From the graph, using a value of 0.075 ± 0.027 for $\langle \sin^2\theta \rangle$, the two-fold barrier to internal rotation was estimated to be 5.1 ± 1.6 kcal/mole in 2,6-difluoroisopropylbenzene. Note that the large uncertainty in the barrier is a result of the insensitivity of $\langle \sin^2\theta \rangle$ to V_2 for barriers over 3 kcal/mole.

iii) comparison of V_2 and $\Delta H^{\dagger}$ for internal rotation

The temperature dependence of the rate data for the internal rotation of the isopropyl group in 2,6-difluoroisopropylbenzene is adequately represented by the Eyring equation (34). The plot depicted in Figure 25 is linear, with no evidence of curvature. Within the limits of this approximation we can write

$$\Delta H^{\dagger} = V_2 + \Delta ZP \qquad (40)$$

where ΔZP is the zero-point energy of the activated state minus the zero-point energy of the ground state (see Appendix).

For 2,6-difluoroisopropylbenzene with a V_2 of 5.0 kcal/mole, the EXPECT calculations discussed above give a rotational zero-point energy of 0.066 kcal/mole for the hindered rotor. The magnitudes of other contributions to the zero-point energies of the ground and activated states are not known. However, the above calculation does suggest that these contributions will be negligible compared with the errors in the values of $\Delta H^{\dagger}$ and V_2. Thus $\Delta H^{\dagger}$ and V_2 are approximately equivalent.

From the dynamic nmr analysis, $\Delta H^{\dagger}$ was determined to be 6.1 ± 0.3 kcal/mole, assuming an error of three times the standard deviation. This barrier agrees, within the limits of error, with the value of 5.1 ± 1.6 kcal/mole for V_2 estimated by the J method. It is clear that the dnmr method yields greater precision than the J method for barriers as large as that in 2,6-difluoroisopropylbenzene. On the other hand, dnmr methods are difficult, if not impossible to apply to barriers that are substantially smaller.

iv) the sidechain and fluorine chemical shifts and the sidechain proton-fluorine coupling constants

The chemical shift of the α-proton in 2,6-difluoroisopropylbenzene is 3.37 ppm (as a 5 mole % solution in acetone-d_6), and is 2.86 ppm in isopropylbenzene[3h] (as a 2 mole % solution in CS_2). Ignoring possible solvent and concentration shifts, the substantial downfield shift of 0.51 ppm on substitution of the ortho protons by fluorine can be attributed to the electron-withdrawal and steric hindrance[67] of the fluorine atom, as well as to conformational changes. In 2,6-difluoroisopropylbenzene conformations with the α C-H bond out of the plane of the benzene ring are not significantly populated, because of the large barrier to internal rotation. In isopropylbenzene the barrier is only 2 kcal/mole,[17] and thus conformers with the α C-H bond out of plane will be more highly populated. The magnetic anisotropy of the benzene ring then leads to a deshielding of the C-H proton in 2,6-difluoroisopropylbenzene relative to isopropylbenzene. A similar downfield shift of 0.87 ppm between benzal fluoride and 2,6-dichlorobenzal fluoride (both 15 mole % in hexafluorobenzene) has been observed,[31] and can be attributed to these mechanisms.* However, the relative contributions of each of these mechanisms in 2,6-difluoroisopropylbenzene could not be established.

The chemical shift of the α methyl protons in 2,6-difluoroisopropylbenzene is 1.32 ppm, and is 1.21 ppm in

---

* While the former is approximately a free rotor, the latter has a rotational barrier greater than 2 kcal/mole.[31]

3,5-dibromoisopropylbenzene (10 mole % in CS_2).[17] As the α methyl protons are significantly out of the benzene ring plane in the ground state conformer, the conformational changes that were discussed above should not affect the chemical shift of the methyl protons. Ignoring the effect of the solvents and the meta substituents, the downfield shift can again be interpreted in terms of the electron-withdrawal and steric hindrance of the ortho fluorine atoms.

The chemical shift difference in 2,6-difluoroisopropylbenzene between the two fluorine nuclei in the ground state conformation 17 was 3.43 ppm at 140 K. In the analogous ground state conformation of 2,4,6-trimethylisopropylbenzene at 213 K, the chemical shift of the ortho methyl protons trans to the α C-H bond is 0.07 ppm to lowfield of the ortho methyl protons cis to the α C-H bond.[27b] Similarly, the chemical shift of the ortho methyl carbon trans to the α C-H bond is 0.16 ppm to low-field of the ortho methyl carbon cis to the α C-H bond, at 234 K, and has been attributed to steric interactions between the ortho and α methyl groups.[27d] A similar interpretation of the fluorine chemical shifts in 2,6-difluoroisopropylbenzene assigns the low-field fluorine resonance to F_b, the fluorine nucleus proximate to the two α methyl groups, in 17.

The conformational dependence of $^4J^{CH,F}_o$ and $^5J^{CH_3,F}$ in 2-fluoroisopropylbenzene derivatives can be estimated from the spectral analysis of 2,6-difluoroisopropylbenzene (see Table 4), and of 2,6-diisopropylfluorobenzene and 3,5-dibromo-2-fluoroisopropylbenzene, tabulated in Table 11.* In the following discussion, this estimation

---

* The latter two analyses are unpublished work, done in this laboratory by Rudy Sebastian.

Table 11

Spectral Parameters for some Isopropylbenzene Derivatives[a]

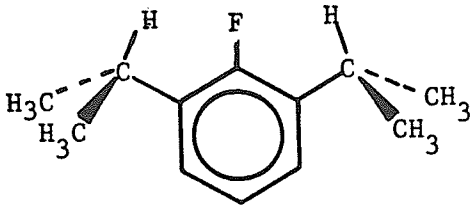

2,6-diisopropylfluorobenzene

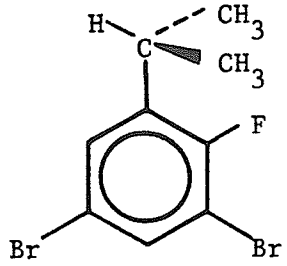

3,5-dibromo-2-fluoroisopropylbenzene

	LAME[b]	DAVINS[c]	LAME8[d]
$^{4}J^{CH,F}_{o}$	e	0.403(9)	0.592(12)
$^{4}J^{CH,H}_{o}$	-0.629(34)	-0.63[f]	-0.593(15)
$^{5}J^{CH_3,F}$	0.492[g]	-	0.510(14)
$^{5}J^{CH,H}_{m}$	0.420(7)	0.42[f]	-
$^{6}J^{CH,H}_{p}$	-0.218(34)	-0.22[f]	-0.233(5)

a all analyses done by Rudy Sebastian in this laboratory; at 305 ± 1 K; numbers in parentheses are standard errors in last digit of parameters

b as a 5 mole % solution in CCl_4, with decoupling of the methyl resonance; analysis from the proton spectrum at 100 MHz

c as a 5 mole % solution in CCl_4/C_6D_{12}; analysis of fluorine spectrum at 84.67 MHz with decoupling of the methyl resonance

d analysis of ^{1}H spectrum at 90.02 MHz and of ^{19}F spectrum at 84.67 MHz for a 5 mole % solution in acetone-d_6; signs of $^{4}J^{CH,F}_{o}$ and $^{5}J^{CH_3,F}$ were determined from double resonance experiments.

e could not be determined

f values taken from LAME analysis

g measured directly from spectrum

depends on the assumption that conformations with the α C-H bond out of the plane of the benzene ring are not significantly populated. The large barrier in 2,6-difluoroisopropylbenzene assures that this will be a good assumption. In the other two isopropylbenzenes, the barrier to internal rotation must be at least as large as that of 2 kcal/mole in 3,5-dibromoisopropylbenzene.[17] Thus it might be expected that the out of plane conformations of the α C-H bond may have a small population in these compounds. Nevertheless, the following treatment should be qualitatively correct.

In a 2-fluoroisopropylbenzene derivative the coupling between the α-proton, or the α methyl protons, and the fluorine nucleus can be written as

$$J^{H,F} = p_c J_c + p_t J_t \qquad (41)$$

For the coupling between the α methyl protons and the fluorine nuclei, $^5J^{CH_3,F}$, p_c is the population of 19, with a proton-fluorine coupling J_c, and p_t is the population of 18, with a coupling J_t. For the coupling between the α-proton and the fluorine nuclei, $^4J_o^{CH,F}$, p_c and J_c refer to 18, while p_t and J_t refer to 19.

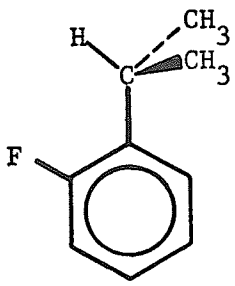

18

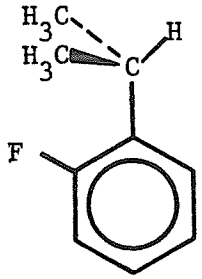

19

In 2,6-difluoroisopropylbenzene the symmetry of the molecule assures that p_c and p_t are equal in conformer 17, and in its mirror image. Thus $p_c = p_t = 0.5$ in this molecule, and from (41) we can write

$$^4J^{CH,F}_o = 0.5\ ^4J^{CH,F}_c + 0.5\ ^4J^{CH,F}_t = -0.601 \pm 0.002 \text{ Hz} \quad (42)$$

and,

$$^5J^{CH_3,F} = 0.5\ ^5J^{CH_3,F}_c + 0.5\ ^5J^{CH_3,F}_t = 0.956 \pm 0.009 \text{ Hz} \quad (43)$$

The magnitude and error of the coupling in (42) are the average, and the deviations from the average, respectively, of the two experimental values given in Table 4. The value of the coupling in (43) is the experimental value from Table 4, and the error is three times the standard deviation of the experimental value.

$^5J^{CH,H}_m$ in 2,6-difluoroisopropylbenzene is 0.292 ± 0.018 Hz, and is the average of the stereospecific coupling over the all-trans path, J_t, and the cis-trans coupling, J_c, which is presumably zero. Thus $^5J^{CH,H}_t$ is 0.584 ± 0.036 Hz (from (31) and (32)). In 2-isopropylphenol the sum of the two five-bond couplings is equal to $^5J^{CH,H}_t$, with a value of 0.628 ± 0.042 Hz.[3h] The two values are the same, within the limits of experimental error, and have an average value of 0.61 ± 0.06 Hz. As has been discussed, $^5J^{CH,H}_t$ is relatively insensitive to ring substituents, and is thus assumed to be unchanged in 2,6-diisopropylfluorobenzene. Thus in this compound we can write

$$p_{\underline{18}} = {}^5J^{CH,H}_m / {}^5J^{CH,H}_t = 0.420/0.606 = 0.69 \pm 0.08 \quad (44)$$

and $p_{\underline{19}} = 1 - p_{\underline{18}} = 0.31 \pm 0.08$, where $p_{\underline{18}}$ and $p_{\underline{19}}$ are the populations of conformers analogous to 18 and 19, respectively, for 2,6-diisopropylfluorobenzene.

The conformation of the isopropyl group in 3,5-dibromo-2-fluoroisopropylbenzene must be very similar to that in 2,6-diisopropylfluorobenzene. This follows as $^{4}J_{o}^{CH,H}$ and $^{5}J^{CH_3,F}$ are identical within experimental error in the two compounds (see Table 11). The differing values of $^{4}J_{o}^{CH,F}$ in the two compounds do not invalidate this argument. If, as has been suggested,[46] this coupling has a significant contribution from a through-space mechanism, then the coupling will be very sensitive to small changes in the $\underline{\alpha}$ proton to fluorine separation.* Thus the values of $p_{\underline{18}}$ and $p_{\underline{19}}$ are assumed to be identical in 2,6-diisopropylfluorobenzene and in 3,5-dibromo-2-fluoroisopropylbenzene.

Averaging the values for these two compounds given in Table 11, gives 0.50 ± 0.12 Hz and 0.50 ± 0.03 Hz for $^{4}J_{o}^{CH,F}$ and $^{5}J^{CH_3,F}$ respectively. Using the populations calculated above, we can write

$$^{4}J_{o}^{CH,F} = 0.69\ ^{4}J_{c}^{CH,F} + 0.31\ ^{4}J_{t}^{CH,F} = 0.50 \qquad (45)$$

and

$$^{5}J^{CH_3,F} = 0.69\ ^{5}J_{t}^{CH_3,F} + 0.31\ ^{5}J_{c}^{CH_3,F} = 0.50 \qquad (46)$$

Solving (42) and (45) gives values of -3.5 ± 1.0 Hz and 2.3 ± 1.0 Hz for $^{4}J_{t}^{CH,F}$ and $^{4}J_{c}^{CH,F}$ respectively; solving (43) and (46) gives -0.22 ± 0.40 Hz and 2.13 ± 0.40 Hz for $^{5}J_{t}^{CH_3,F}$ and $^{5}J_{c}^{CH_3,F}$ respectively.

---

* In 3,5-dichloro-2-hydroxythiophenol a change of 0.1 A in the O···H distance changes the through-space coupling, $^{5}J^{OH,SH}$ by 40 %.

The value of 2.1 Hz for $^{5}J_{CH_3,F}$ when the methyl protons and fluorine nucleus are proximate, 19, and the approximately zero coupling when these nuclei are distant, 18, suggests a through-space mechanism for the coupling. Such a mechanism has been proposed for $^{5}J_{CH_3,F}$ in some ethyl, isopropyl and t-butyl 2-fluorobenzene derivatives.[84] In these compounds, the coupling was only observed when the methyl carbon and the ring fluorine atoms were proximate, the observed coupling increasing very rapidly with the decreasing separation of these atoms. This sensitivity to the internuclear separation was taken as strong evidence for a predominantly through-space mechanism. In a number of 3-substituted 2,4,6-triisopropylfluorobenzenes, where the 3-substituent was considerably larger than the fluorine substituent, the conformation analogous to 19, with the methyl groups and the fluorine nucleus proximate, was predominant. In a series of these compounds, $^{5}J_{CH_3,F}$ was observed to lie between 1.68 and 1.94 Hz, although the sign of the coupling was not determined. If the sign is positive, these values are in good agreement with the value of $^{5}J_{c}^{CH_3,F}$ determined above. Thus it appears that $^{5}J_{CH_3,F}$ in 2-fluoroisopropylbenzenes is dominated by a positive, through-space coupling.

The value of $^{4}J_{o}^{CH,F}$ is 2.3 Hz for the conformation with the α-proton and the fluorine nucleus in a proximate orientation, 18, and is -3.5 Hz for the orientation in which they are distant, 19, in the 2-fluoroisopropylbenzenes studied in this work. For the former, the positive coupling suggests a contribution from a through-space mechanism, by analogy with the discussion for $^{5}J_{CH_3,F}$. However, the situation for $^{4}J_{o}^{CH,F}$ is much more complicated than this.

As Hutton and coworkers pointed out,[46] in cis-1-fluoropropene,[109a] pentafluorobenzaldehyde,[109b] pentafluorotoluene,[109b] 2-fluoro-4-iodo-5-nitrotoluene,[109c] and 2-fluoro-3-methylpyridine,[109d] $^4J_o^{CH,F}$ lies between +1 and +3 Hz. Previous studies[109c,d] had indicated a positive σ-π contribution to this coupling. However, the situation in 2-fluoro-5-chlorobenzal chloride, 20, 2-fluoro-3-nitro-6-chlorobenzal chloride, 21, and 2-fluoro-5-nitro-6-chlorobenzal chloride, 22, is different. For the

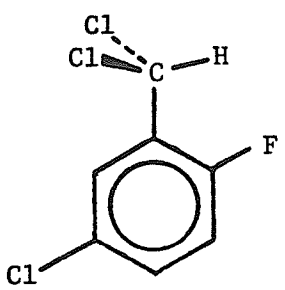

20

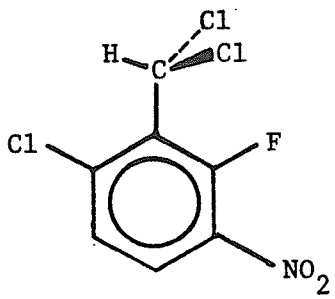

21

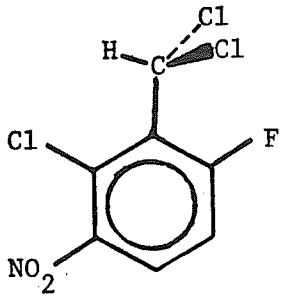

22

cisoid arrangement of the α-proton and the fluorine nucleus, 20, $^4J_o^{CH,F}$ is -0.3 Hz, and is -2.5 Hz in 21 and 22, where the two are in a transoid arrangement. The large negative value in 21 and 22 was explained in terms of a negative σ-contribution to the coupling, since in a planar configuration the π-contribution is small.* The small negative value of $^4J_o^{CH,F}$ for the cisoid arrangement, 20, was then accounted for by a

---

* The barrier to internal rotation of the dihalomethyl group in 20, 21 and 22 is presumably at least as large as the barrier of 2.2 kcal/mole in benzal chloride,[21] and thus conformations with the α-proton out of the benzene plane have only a small population.

positive through-space contribution. Alternate explanations of this reduction in the coupling invoked an angle dependence in the negative σ-contribution, or a larger torsional angle of the α C-H bond in 20, with a concomitant increase in the positive σ-π contribution in this molecule.

The coupling over the transoid arrangement in 21 and 22 is similar in magnitude and sign with that determined for this configuration in the present study. Apparently, the positive contribution in the cisoid arrangement for the isopropylbenzenes in the present study is larger than in benzal chloride, 20. This might be a result of the polarization of the α C-H bond by the two electronegative α chlorine substituents, causing a decrease in the proton-fluorine orbital overlap, and thus a reduction in the through-space coupling in 20.

INDO-FPT calculations on 2-fluorotoluene[56] are not in good agreement with these results. INDO predicts that $^{4}J_{o}^{CH,F}$ has a value of -0.24 Hz for the transoid configuration of the α C-H and C-F bonds, and -3.15 Hz for the cisoid configuration. Although the former agrees with the value of the coupling in 20, the latter is at variance with the values calculated in this study, as well as those in 21 and 22. The INDO results do, however, substantiate a large positive σ-π contribution for orientations with the α C-H bond out of plane. These calculations must be treated with circumspection, as it is not possible to reconcile their predictions with the small positive couplings observed in many 2-fluorotoluenes.*

---

* reference 56 and unpublished work in this laboratory

E. Summary and Conclusions

The barrier to internal rotation in α,α,2,6-tetrasubstituted toluenes arises from steric interactions between the α and ortho substituents. In the ground state conformation, the α C-H bond lies in the plane of the benzene ring, and in the transition state the bond is in a plane perpendicular to the ring. The exchange between the ground state and its mirror image is accompanied by exchange of the magnetic environment of the ortho substituents, and of the meta substituents, in a time short compared to the lifetime of the ground state conformer. The barrier to internal rotation in these molecules can thus be studied by dynamic nmr techniques.

In 2,6-difluoroisopropylbenzene the free energy, enthalpy and entropy of activation for internal rotation were determined by dnmr, observing the nmr spectrum of the ortho fluorine nuclei. A remarkably good correlation between the free energies, or the enthalpies, and a steric parameter, S, was found for this compound and a series of α,α,2,6-tetrasubstituted toluenes studied by other workers. S was given as the difference in the internuclear separation of the α and ortho substituents in the ground state, and in the transition state conformation, multiplied by the sum of the van der Waals volumes of the two substituents. For 2,6-difluoroisopropylbenzene it was not necessary to take a "gear effect" into account. Barrier heights in some α,α,2,6-tetrasubstituted toluenes were predicted from this relation.

Using the J method, the two-fold potential energy barrier to internal rotation was estimated in 2,6-difluoroisopropylbenzene. The barrier determined in this way was in agreement with that determined by

the dnmr method. This is an experimental verification of the J method for determining internal rotational barriers, with reference to the more established dnmr method.

The conformational dependence of the long-range nmr coupling constants, $^{4}J_{o}^{CH,F}$ and $^{5}J^{CH_3,F}$, in isopropylbenzenes was discussed, for conformations with the α C-H bond in the benzene ring plane. The mechanisms contributing to these couplings were also discussed. $^{5}J^{CH_3,F}$ has a small positive value for the configuration with the methyl protons and the fluorine nucleus proximate, and vanishes for the configuration with the nuclei distant. This coupling appears to be dominated by a through-space mechanism. Similarly, $^{4}J_{o}^{CH,F}$ is small and positive when the α C-H bond lies cis to the C-F bond, while the coupling is small and negative for the trans orientation of these bonds. A small positive through-space contribution appears to dominate the proximate orientation of the coupled nuclei, as with $^{5}J^{CH_3,F}$, while a negative σ-contribution, with an unknown angle dependence, was suggested to dominate for the trans orientation of the C-H and C-F bonds.

F. Suggestions for Future Research

A number of proposals for future research are suggested by the present work.

The barrier to rotation in 2,6-difluoroisopropylbenzene should be determinable by nmr measurements of relaxation in the rotating frame, $T_{1\rho}$, and could be compared with the barrier determined in this work.

It would be of interest to determine the barriers in benzal bromide and benzal iodide by the dnmr method, as the barriers predicted by the present study for some benzal halides differ from those estimated by the J method.

The relationship between the rotational barrier and the steric factor S is useful in predicting compounds that could be analyzed by the dnmr method. Thus the barriers in 2,6-difluorobenzal chloride and 2,6-difluorobenzal bromide should be determinable by the dnmr method.

As well, the dnmr determination of barriers in 2,6-dichloro, 2,6-dibromo and 2,6-diiodo isopropylbenzene is predicted to be possible, and should give further information on the importance of the "gear effect" for the methyl substituent.

It would also be useful to determine the magnitudes and signs of $^5J_{CH_3,F}$ and $^4J^{CH,F}_o$ in 2-fluoro-6-substituted isopropylbenzenes, where the 6-substituent is large. These studies might help to support the positive through-space contribution to these couplings. A study of 2,6-difluoroethylbenzene by the J method would also be useful. The values of the above couplings in this molecule, which has a ground state conformation with the $\underline{\alpha}$ C-H bonds at a 30° angle to the ring plane, might aid the assessment of the contributions of the various mechanisms to these

couplings. These latter two studies are presently in progress in this laboratory.

References

1.a) W. J. Orville-Thomas (ed.), Internal Rotation in Molecules (New York: Wiley, 1974)

b) E. L. Eliel, N. L. Allinger, S. J. Angyal and G. A. Morrison, Conformational Analysis (New York: Wiley, 1965)

c) N. Sheppard, Advances in Spectroscopy 1 288 (1959)

d) E. B. Wilson, Jr., Advances in Chemical Physics 2 367 (1959)

e) J. P. Lowe, Progress in Physical Organic Chemistry 6 1(1968)

f) R. A. Pethrick and E. Wyn-Jones, Quart. Rev. 23 301 (1969)

g) H. Kessler, Angew. Chem. Int. Ed. Engl. 9 219 (1970)

h) G. Binsch and H. Kessler, Angew. Chim. Int. Ed. Engl. 19 411 (1980)

i) J. B. Lambert, R. J. Nienhuis and J. W. Keepers, Angew. Chem. Int. Ed. Engl. 20 487 (1981)

j) R. Bucourt, Top. Stereochem. 8 159 (1974)

k) G. J. Karabatsos and D. J. Fenoglio, Top. Stereochem. 5 167 (1970)

L) W. J. E. Parr and T. Schaefer, Acc. Chem. Res. 13 400 (1980)

m) H. S. Aaron, Top. Stereochem. 11 1 (1979)

2. S. Forsén and B. Åkermark, Acta. Chem. Scand. 17 1712 (1963)

3.a) T. Schaefer and J. B. Rowbotham, Chem. Phys. Lett. 29 633 (1974)

b) J. B. Rowbotham and T. Schaefer, Can. J. Chem. 52, 3037 (1974)

c) J. B. Rowbotham, M. Smith and T. Schaefer, Can. J. Chem. 53 986 (1975)

d) T. Schaefer and J. B. Rowbotham, Can. J. Chem. 54 2243 (1976)

e) T. Schaefer and K. Chum, Can. J. Chem. 56 1788 (1978)

f) T. Schaefer and T. A.Wildman, Can. J. Chem. 57 450 (1979)

g) T. Schaefer, T. A. Wildman and S. R. Salman, J. Am. Chem. Soc. 102 107 (1980)

h) T. Schaefer, B. M. Addison, R. Sebastian and T. A. Wildman, Can. J. Chem. 59 1656 (1981)

i) T. Schaefer, R. Sebastian and T. A. Wildman, Can. J. Chem. 59 3021 (1981)

4.a) A. R. Quirt and J. S. Martin, J. Mag. Res. 5 318 (1971)
b) D. J. Loomes, R. K. Harris and P. Anstey, The NMR Program Library (Daresbury: Science Research Council, 1979) 3.98

5. R. Wasylishen and T. Schaefer, Can. J. Chem. 49 3216 (1971)

6. J. Peeling, T. Schaefer and C. M. Wong, Can. J. Chem. 48 2839 (1970)

7. J. Peeling, L. Ernst and T. Schaefer, Can. J. Chem. 52 849 (1974)

8. J. Peeling, J. B. Rowbotham, L. Ernst and T. Schaefer, Can. J. Chem. 52, 2414 (1974)

9.a) L. Radom, W. J. Hehre, J. A. Pople, G. L. Carlson and W. G. Fateley, J. Chem. Soc. Chem. Comm. 308 (1972)
b) C. R. Quade, J. Chem. Phys. 48 5490 (1968)
c) H. D. Bist, J. C. D. Brand and D. R. Williams, J. Mol. Spectrosc. 24 402 (1967)
d) E. Mathier, D. Welti, A. Bauder and Hs. H. Günthard, J. Mol. Spectrosc. 37 63 (1971)
e) H. Forset and B. P. Dailey, J. Chem. Phys. 45, 1736 (1966)

10.a) N. W. Larsen and F. M. Nicolaisen, J. Mol. Struct. 22 29 (1974)
b) W. J. E. Parr and T. Schaefer, J. Mag. Res. 25 171 (1977)

11. T. Schaefer and T. A. Wildman, Chem. Phys. Lett. 80 280 (1981)

12. R. Wasylishen and T. Schaefer, Can. J. Chem. 50 1852 (1972)

13. W. J. E. Parr and T. Schaefer, J. Mol. Spectrosc. 66 448 (1977)

14. T. Schaefer, L. Kruczynski and W. Niemczura, Chem. Phys. Lett. 38 498 (1976)

15. M. S. Farag, Diss. Abstr. Int. B35 1594 (1974)

16. A. Miller and D. W. Scott, J. Chem. Phys. 68 1317 (1978)

17. T. Schaefer, W. J. E. Parr and W. Danchura, J. Mag. Res. 25 167 (1977)

18. W. J. E. Parr and T. Schaefer, J. Am. Chem. Soc. 99 1033 (1977)

19. T. Schaefer, W. Niemczura and W. Danchura, Can. J. Chem. 57 355 (1979)

20. N. L. Bauld, C. E. Hudson and J. S. Hyde, J. Chem. Phys. 54 1834 (1971)

21. T. Schaefer, W. Danchura and W. Niemczura, Can. J. Chem. 56 36 (1978)

22. W. J. E. Parr and T. Schaefer, Can. J. Chem. 55 557 (1977)

23. T. Schaefer and W. J. E. Parr, Can. J. Chem. 55 3732 (1977)

24. T. Schaefer and W. J. E. Parr, Can. J. Chem. 57 1421 (1979)

25. R. A. Newmark and C. H. Sederholm, J. Chem. Phys. 43 602 (1965)

26. F. A. L. Anet and I. Yavari, J. Am. Chem. Soc. 99 6752 (1977)

27.a) A. Mannschreck, L. Ernst and E. Keck, Angew. Chem. Int. Ed. Engl. 9 806 (1970)

b) A. Mannschreck and L. Ernst, Chem. Ber. 104 228 (1971)

c) R. Price, G. Schilling, L. Ernst and A. Mannschreck, Tetrahedron Lett. 17 1689 (1972)

d) L. Ernst and A. Mannschreck, Chem. Ber. 110 3258 (1977)

28. B. Nilsson, P. Martinson, K. Olsson and R. E. Carter, J. Am. Chem. Soc. 96 3190 (1974)

29. A. Bondi, Physical Properties of Molecular Crystals, Liquids and Glasses, (New York: Wiley, 1968)

30. M. Charton and B. Charton, J. Am. Chem. Soc. 97 6472 (1975)

31. J. B. Rowbotham, A. F. Janzen, J. Peeling and T. Schaefer, Can. J. Chem. 52 481 (1974)

32. J. Peeling, Ph.D. Thesis, University of Manitoba, 1974

33. N. F. Ramsey and E. M. Purcell, Phys. Rev. 85 143 (1952)

34. J. Kowalewski, Progress in Nuclear Magnetic Resonance Spectroscopy 11. J. W. Emsley, J. Feeney and L. H. Sutcliffe (ed.) (Oxford: Pergamon Press, 1971)

35. N. F. Ramsey, Phys. Rev. 91 303 (1953)

36. D. B. O'Reilly, J. Chem. Phys. 36 274 (1962); 38 2583 (1963)

37.a) M. Barfield, J. Chem. Phys. 48 4458 (1968); 48 4463 (1968)
b) M. Barfield and B. Chakrabarti, J. Am. Chem. Soc. 91 4346 (1969)

38. T. J. Dougherty, T. Vladimiroff and S. T. Epstein, J. Chem. Phys. 45 1803 (1966)

39. J. A. Pople, J. W. McIver, Jr. and N. S. Ostlund, J. Chem. Phys. 49 2960 (1968)

40. J. A. Pople, J. W. McIver, Jr. and N. S. Ostlund, J. Chem. Phys. 49 2965 (1968)

41. J. A. Pople and D. L. Beveridge, Approximate Molecular Orbital Theory. (New York: McGraw-Hill, 1970)

42. J. A. Pople, D. P. Santry and G. A. Segal, J. Chem. Phys. 43 S129 (1965)

43. J. A. Pople, D. L. Beveridge and P. A. Dobosh, J. Chem. Phys. 47 2026 (1967)

44. D. G. de Kowalewski and V. J. Kowalewski, J. Chem. Phys. 37 1009 (1962)

45. G. J. Karabatsos and F. M. Vane, J. Am. Chem. Soc. 85 3886 (1963)

46. H. M. Hutton, J. B. Rowbotham, B. H. Barber and T. Schaefer, Can. J. Chem. 49 2033 (1971)

47.a) R. A. Hoffman, B. Gestblom, S. Gronowitz and S. Forsén J. Mol Spectrosc. 11 454 (1963)
b) S. Forsén, B. Gestblom, S. Gronowitz and R. A. Hoffman, Acta Chem. Scand. 18 313 (1964)
c) S. Forsén, T. Alm, B. Gestblom, S. Rodmar and R. A. Hoffman, J. Mol. Spectrosc. 17 13 (1965)

47.d) S. Rodmar, S. Forsén, B. Gestblom, S. Gronowitz and R. A. Hoffman, Acta Chem. Scand. 19 485 (1965)

48. S. Forsén, B. Akermark and T. Alm, Acta Chem. Scand. 18 2313 (1964)

49. R. A. Hoffman, Mol. Phys. 1 326 (1958)

50. R. Freeman, N. S. Bhacca and C. A. Reilly, J. Chem. Phys. 38 293 (1963)

51. S. Forsén and R. Hoffman, J. Mol. Spectrosc. 20 168 (1966)

52.a) T. Schaefer, R. Schwenk, C. J. Macdonald and W. F. Reynolds, Can. J. Chem. 46 2187 (1968)

b) M. Barfield, C. J. Macdonald, I. R. Peat and W. F. Reynolds, J. Am. Chem. Soc. 93 4195 (1971)

c) R. Wasylishen and T. Schaefer, Can. J. Chem. 50 274 (1972)

d) R. Wasylishen, J. B. Rowbotham, L. Ernst and T. Schaefer, Can. J. Chem. 50 2575 (1972)

e) J. B. Rowbotham and T. Schaefer, Can. J. Chem. 51 953 (1973)

f) I. R. Peat and W. F. Reynolds, Can. J. Chem. 51 2968 (1973)

g) J. B. Rowbotham and T. Schaefer, Can. J. Chem. 52 136 (1974)

h) W. Danchura, T. Schaefer, J. B. Rowbotham and D. J. Wood, Can. J. Chem. 52 3986 (1974)

53.a) M. Karplus and J. A. Pople, J. Chem. Phys. 38 2803 (1963)

b) J. A. Pople, Mol. Phys. 7 301 (1964)

54. J. Hilton and L. H. Sutcliffe, Progress in Nuclear Magnetic Resonance Spectroscopy 10 27. J. W. Emsley, J. Feeney and L. H. Sutcliffe (ed.) (Oxford: Pergamon Press, 1975)

55. M. Barfield and B. Chakrabarti, Chem. Rev. 69 757 (1969)

56. R. E. Wasylishen and M. Barfield, J. Am. Chem. Soc. 97 4545 (1975)

57. R. S. Mulliken, C. A. Rieke and W. G. Brown, J. Am. Chem. Soc. 63 41 (1941)

58. H. M. McConnell, J. Mol. Spectrosc. 1 11 (1957)

59.a) A. C. McLachlan, Mol. Phys. 1 233 (1958)
b) M. Karplus, J. Chem. Phys. 33 1842 (1960)
c) M. J. S. Dewar and R. C. Fahey, J. Am. Chem. Soc. 85 2704 (1963)
d) T. M. McKinney and T. H. Geske, J. Am. Chem. Soc. 89 2806 (1967)
e) D. B. Chesnut, J. Chem. Phys. 29 43 (1958)

60. C. Heller and H. M. McConnell, J. Chem. Phys. 32 1535 (1960)

61. R. A. Hoffman and S. Gronowitz, Acta Chem. Scand. 13 1477 (1959)

62. H. M. McConnell, J. Chem. Phys. 30 126 (1959)

63. T. Schaefer, J. B. Rowbotham and K. Chum, Can. J. Chem. 54 3666 (1976)

64. G. Kotowycz and T. Schaefer, Can. J. Chem. 44 2743 (1966)

65. C. J. MacDonald and W. F. Reynolds, Can. J. Chem. 48 1002 (1970)

66. J. M. Read, R. W. Crecely, R. S. Butler, J. E. Loemker and J. H. Goldstein, Tetrahedron Lett. 10 1215 (1968)

67. H. Pearson, J. Chem. Soc. Chem. Comm. 912 (1975)

68.a) R. A. Hoffman, Arkiv Kemi 17 1 (1961)
b) A. Forman, J. N. Murrell and L. E. Orgel, J. Chem. Phys. 31 1129 (1960)

69. D. J. Blears, S. S. Danyluk and T. Schaefer, Can. J. Chem. 46 654 (1968)

70. M. P. Williamson, R. J. Kostelnik and S. M. Costellano, J. Chem. Phys. 49 2218 (1968)

71. A. R. Engelmann, R. H. Contreras and J. C. Facelli, Theoret. Chim. Acta 59 17 (1981)

72.a) L. W. Reeves, Advances in Physical Organic Chemistry 3 187 (1965)
b) C. S. Johnson, Advances in Magnetic Resonance, 1 33 (1965)

72.c) G. Binsch, Top. Stereochem. 3 97 (1968)
d) I. O. Sutherland, Annual Reports on N.M.R. Spectroscopy 4 71 (1971)

73. F. Bloch, Phys. Rev. 70 460 (1946)

74.a) H. S. Gutowsky, D. W. McCall and C. P. Slichter, J. Chem. Phys. 21 279 (1953)
b) H. S. Gutowsky and A. Saika, J. Chem. Phys. 21 1688 (1953)
c) H. S. Gutowsky and C. H. Holm, J. Chem. Phys. 25 1228 (1956)

75. H. M. McConnell, J. Chem. Phys. 28 430 (1958)

76.a) L. W. Reeves and K. M. Shaw, Can. J. Chem. 48 3641 (1970)
b) E. A. Allan, M. G. Hogben, L. W. Reeves and K. N. Shaw, Pure and Applied Chemistry 32 9 (1972)

77.a) R. Kubo, Nuovo Cimento, Suppl. 6 1063 (1957)
b) R. A. Sack. Mol. Phys. 1 163 (1958)
c) C. S. Johnson, Jr., J. Chem. Phys. 41 3277 (1964)

78. P. W. Anderson, J. Phys. Soc. Japan 9 316 (1954)

79.a) A. Allerhand and H. S. Gutowsky, J. Chem. Phys. 41 2115 (1964)
b) A. Allerhand, H. S. Gutowsky, J. Jonas and R. A. Meinzer J. Am. Chem. Soc. 88 3185 (1966)
c) T. Drakenberg, K. Dalqvist and S. Forsén, Acta Chem. Scand. 24 694 (1970)
d) R. R. Shoup, E. D. Becker and M. L. McNeel, J. Phys. Chem. 76 71 (1972)
e) E. A. Allan , R. F. Hobson, L. W. Reeves and K. N. Shaw, J. Am. Chem. Soc. 94 6604 (1972)

80. A. Allerhand, F. Chen and H. S. Gutowsky, J. Chem. Phys. 42 3040 (1964)

81. F. A. L. Anet and A. J. R. Bourn, J. Am. Chem. Soc. 89 760 (1967)

82.a) H. S. Gutowsky, J. Jonas and T. H. Siddall, J. Am. Chem. Soc. 89 4300 (1967)

b) C. H. Bushweller, J. Golini, G. U. Rao, J. W. O'Neil, J. Am. Chem. Soc. 92 3055 (1970)

c) C. H. Bushweller, J. W. O'Neil, M. H. Halford and F. H. Bissett, J. Am. Chem. Soc. 93 1471 (1971)

d) A. Mannschreck, A. Mattheus and G. Rissmann, J. Mol. Spectrosc. 23 15 (1967)

83.a) H. A. Scheraga, Advances in Physical Organic Chemistry, 6 103 (1968)

b) J. E. Williams, P. J. Siang and P. v. R. Schleyer, Annual Review of Physical Chemistry, 19 531 (1968)

c) E. L. Eliel, N. L. Allinger, S. J. Angyal and G. A. Morrison, Conformational Analysis. (New York: Interscience Publishers, 1965) Chapter 7

84. P. C. Myhre, J. W. Edmonds,and J. D. Kruger, J. Am. Chem. Soc. 88 2459 (1966)

85. B. H. Barber and T. Schaefer, Can. J. Chem. 49 789 (1971)

86. A. Mannschreck and L. Ernst, Tetrahedron Lett. 17 5939 (1968)

87. A. F. Janzen and T. Schaefer, Can. J. Chem. 49 1818 (1971)

88. W. R. Snyder, H. D. Schreiber and J. N. Spencer, Spectrochim. Acta 29A 1225 (1973)

89. R. Adams and C. S. Marvel, Org. Syntheses, Coll. I 504 (1941)

90. R. Freeman and W. A. Anderson, J. Chem. Phys. 37 2053 (1962)

91. J. P. Maher and D. F. Evans, Proc. Chem. Soc. London 208 (1961)

92.a) S. Castellano and A. A. Bothner-By, J. Chem. Phys. 41 3863 (1964)

b) C. W. Haigh, Annual Reports on N.M.R. Spectroscopy 4 311 (1971)

93. J. A. Pople and M. Gordon, J. Am. Chem. Soc. 89 4253 (1967)

94. P. A. Dobosh, Quantum Chemistry Program Exchange 11 141 (1979)

95. R. Laatikainen, J. Mag. Res. 27 169 (1977)

96. T. Schaefer and R. Sebastian, J. Mag. Res. 41 395 (1980)

97. S. Castellano, R. Kostelnik and C. Sun, Tetrahedron Lett. 46 4635 (1967)

98. B. Richardson and T. Schaefer, Can. J. Chem. 46 2195 (1968)

99. C. E. Johnson, Jr. and F. A. Bovey, J. Chem. Phys. 29 1012 (1958)

100.a) T. Schaefer, Can. J. Chem. 39 1864 (1961)

b) G. J. Karabatsos and R. A. Taller, Tetrahedron 24 3347 (1968)

c) Z. W. Wolkowski, N. Thoai and J. Wiemann, Tetrahedron Lett. 1 93 (1970)

d) R. Wasylishen, T. Schaefer and R. Schwenk, Can. J. Chem. 48 2885 (1970)

101. L. C. Snyder and E. W. Anderson, J. Am. Chem. Soc. 86 5023 (1964)

102. T. A. Wildman, M.Sc. Thesis, University of Manitoba, 1978

103. T. Schaefer and W. J. E. Parr, Can. J. Chem. 55 552 (1977)

104. T. Schaefer, L. J. Kruczynski and W. J. E. Parr, Can. J. Chem. 54 3210 (1976)

105. M. Barfield and M. Karplus, J. Am. Chem. Soc. 91 1 (1969)

106.a) R. F. Zurcher, Progress in Nuclear Magnetic Resonance Spectroscopy 2. J. W. Emsley, J. Feeney and L. H. Sutcliffe (ed.) (Oxford: Pergamon Press, 1967)

b) A. D. Buckingham, Can. J. Chem. 38 300 (1960)

107. A. L. McClellan, Tables of Experimental Dipole Moments 2. (El Cerrito: Rahara Enterprises, 1974)

108. R. J. Abraham and E. Bretschneider, Internal Rotation in Molecules. W. J. Orville-Thomas (ed.) (New York: Wiley, 1974) Chapter 13

109.a) R. A. Beaudet and J. D. Baldeschwieler, J. Mol. Spectrosc. 9 30 (1962)

b) R. R. Dean and W. McFarlane, J. Chem. Soc. B 509 (1969)

c) D. J. Blears, S. S. Danyluk and T. Schaefer, J. Chem. Phys. 47 5037 (1967)

d) T. Schaefer, S. S. Danyluk and C. L. Bell, Can. J. Chem. 47 5107 (1969)

110. J. K. Krieger, Ph.D. Thesis, Massachusetts Institute of Technology, 1971

111. A. Steigel, J. Sauer, D. A. Kleier and G. Binsch, J. Am. Chem. Soc. 94 2770 (1972)

112. P. B. Ayscough, M. C. Brice and R. E. D. McClung, Mol. Phys. 20 41 (1971)

113.a) G. Govil and D. H. Whiffen, Mol. Phys. 12 449 (1967)

b) D. J. Loomes, R. K. Harris and P. Anstey, The NMR Program Library. (Daresbury: Science Research Council, 1979) 3.37

114. B. J. Fuhr, B. W. Goodwin, H. M. Hutton and T. Schaefer, Can. J. Chem. 48 1558 (1970)

115. A. Finch, A. N. Gates, K. Radcliffe, F. N. Dickson and F. F. Bentley, Chemical Applications of Far Infrared Spectroscopy. (London: Academic Press, 1970)) Chapter 4

116. C. Brot, Chem. Phys. Lett. 3 319 (1969)

117. T. D. Alger, H. S. Gutowsky and R. L. Vold, J. Chem. Phys. 47 3130 (1967)

118. L. E. Sutton (ed.), Tables of Interatomic Distances and Configuration of Molecules and Ions. (London: The Chemical Society) Special Publication 11 (1958); Special Publication 18 (1965)

119. T. Schaefer, J. B. Rowbotham, W. J. E. Parr, K. Marat and A. F. Janzen, Can. J. Chem. 54 1322 (1976)

120.a) D. S. Stephenson and G. Binsch, Quantum Chemistry Program Exchange 11 378 (1979)

b) D. S. Stephenson and G. Binsch, J. Mag. Res. 37 395 (1980); 37 409 (1980)

c) D. S. Stephenson and G. Binsch, Org. Mag. Res. 14 3 (1980)

121. J. Peeling, B. W. Goodwin, T. Schaefer and C. Wong, Can. J. Chem. 49 1489 (1971)

122. D. Malcolm, Introduction to Statistical Thermodynamics. (New York: Prentice-Hall, 1954)

Appendix

The Theory of Absolute Reaction Rates

Absolute reaction rate theory takes the potential energy of the interacting nuclei to be a known function of their relative positions. The potential energy of the configurations of nuclei may be represented as an n-dimensional surface in (n + 1)-dimensional space, where n is the number of independent variables that completely specifies these configurations. Note that this supposes an "adiabatic" approximation of fixed nuclei relative to the fast electron motion. There will be "valleys" in this potential surface. The bottom of these valleys are stable configurations for which the potential energy is in a local minimum.

Consider a system of nuclei with stable minimum energy configurations A and B. For the system to change from the A to the B configuration, it must pass through higher energy configurations. The motion of the system in (n + 1)-dimensional space will most probably be along the path with least requirement of energy. This path is called the reaction coordinate. The potential energy of the system for the change A→B can be plotted as a function of the "distance" along the reaction coordinate, as in Figure A. The region of highest potential energy along the reaction coordinate is the transition state, and the configuration of nuclei at this point is the activated complex.

To determine the rate of formation of B from A, it is assumed that there is an equilibrium between the reactant A and the activated complex, C

$$A \rightleftharpoons C \tag{1}$$

The equilibrium constant is

$$K^{\dagger} = \frac{[C]}{[A]} \tag{2}$$

Figure A

potential energy as a function of reaction coordinate for $A \rightarrow B$

A - reactant configuration

B - product configuration

C - transition state configuration

ZP - zero-point energy

E_o - activation energy at absolute zero

V - potential energy barrier

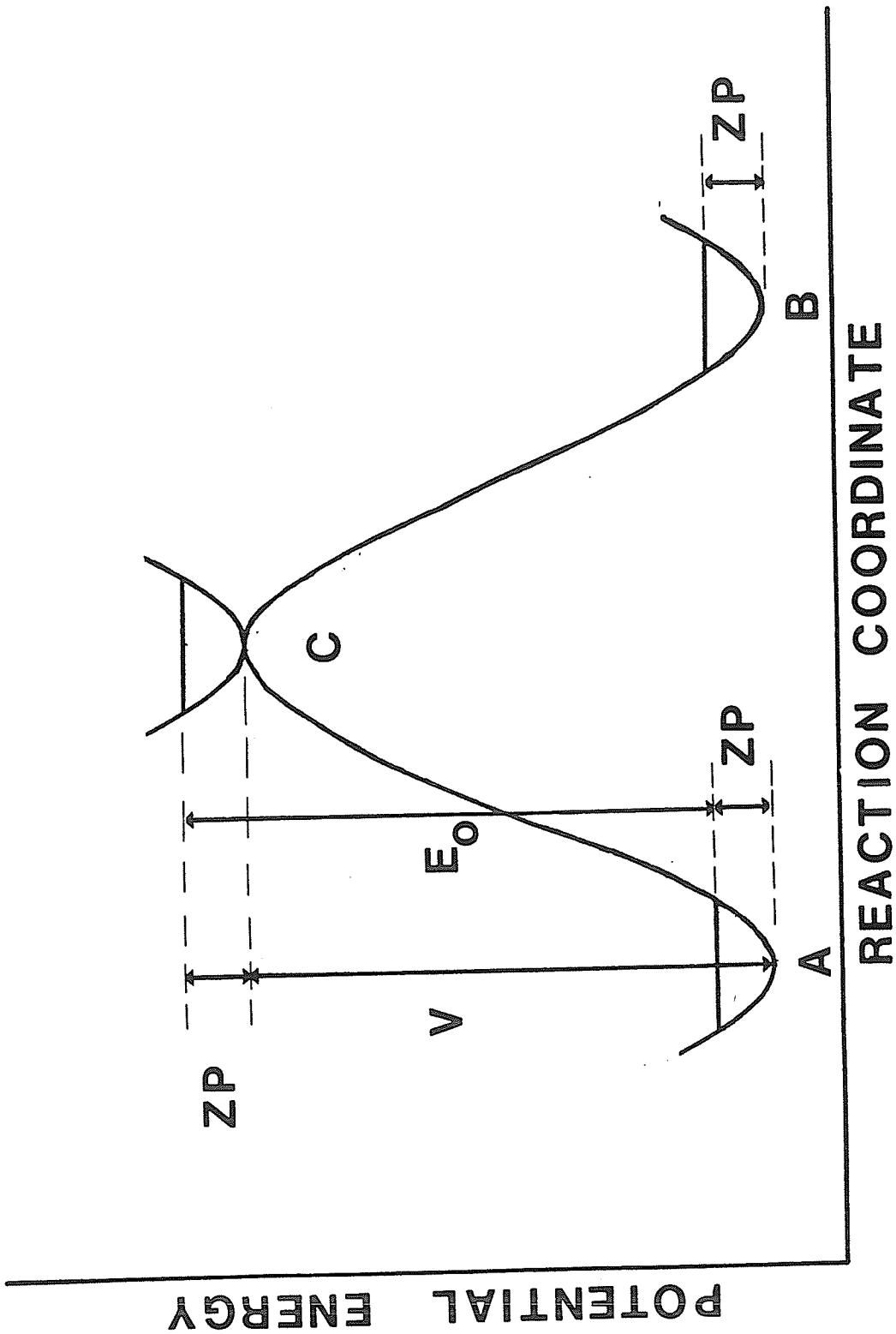
POTENTIAL ENERGY
REACTION COORDINATE
A
B
C
ZP
ZP
ZP
V
E_o

and the rate of product formation is

$$\text{rate} = k_r [A] \tag{3}$$

Using statistical mechanics, and the assumptions of absolute reaction rate theory, it can be shown that the rate constant is

$$k_r = \frac{\kappa kT}{h} \frac{Q_C^\cdot}{Q_A^\cdot} \exp(-E_o/RT) \tag{4}$$

where $Q_i^\cdot = Q_i/V$, the partition function for state i per unit volume, V. Note that $Q_C^\cdot$, the partition function for the activated complex has one less degree of vibrational freedom than $Q_A^\cdot$, that along the reaction coordinate. E_o is the potential energy difference at absolute zero between the lowest energy level of the activated and of the initial state (see Figure A). Thus the partition functions $Q_i^\cdot$ take the lowest energy level of state i as the zero of energy for that state. κ is the fraction of crossings through the transition state that lead to the product, B. It is taken to be equal to unity, except where quantum mechanical tunneling effects are significant, or where some peculiarity of the potential energy surface leads to deactivation of the activated complex without formation of the product.

Equation (4) can also be written as

$$k_r = \frac{\kappa kT}{h} K^\dagger \tag{5}$$

where $K^\dagger$ is defined by

$$K^\dagger = \frac{Q_C^\cdot}{Q_A^\cdot} \exp(-E_o/RT) \tag{6}$$

K is of the form of an equilibrium constant, therefore functions analogous to the thermodynamic functions for equilibrium constants are defined as

$$\Delta G^\dagger = -RT \ln K^\dagger \tag{7}$$

$$\Delta H^{\dagger} = RT^2 \frac{d \ln K^{\dagger}}{dT} \tag{8}$$

$$\Delta S^{\dagger} = \frac{\Delta H^{\dagger} - \Delta G^{\dagger}}{T} \tag{9}$$

where $\Delta G^{\dagger}$, $\Delta H^{\dagger}$ and $\Delta S^{\dagger}$ are the free energy, enthlapy and entropy of activation for standard states.

From (5), (7), (8) and (9) the rate constant can be written as

$$k_r = \frac{\kappa kT}{h} \exp\ (-\Delta G^{\dagger}/RT) \tag{10}$$

$$k_r = \frac{\kappa kT}{h} \exp\ (\Delta S^{\dagger}/R) \exp\ (-\Delta H^{\dagger}/RT) \tag{11}$$

Equation (10) or (11) is known as the Eyring equation. The Arrhenius equation, largely superseded by the Eyring equation, is given by

$$k_r = A \exp\ (-E_A/RT) \tag{12}$$

where A is a constant, and E_A is the Arrhenius activation energy.

For an ideal reaction in solution (11) and (12) can be written

$$\frac{d \ln k_r}{dT} = \frac{1}{T} + \frac{\Delta H^{\dagger}}{RT^2} \tag{13}$$

$$\frac{d \ln k_r}{dT} = \frac{E_A}{RT^2} \tag{14}$$

It has been assumed that $\Delta H^{\dagger}$, $\Delta S^{\dagger}$, E_A and A are temperature independent, with the choice of standard states that of unit concentration. Comparing (13) and (14) gives

$$E_A = \Delta H^{\dagger} + RT \tag{15}$$

Similarily (5) and (6) gives

$$\frac{d \ln k_r}{dT} = \frac{1}{T} + \frac{d}{dT}\left[\ln \frac{Q_C^{\cdot}}{Q_A^{\cdot}}\right] + \frac{E_o}{RT^2} \tag{16}$$

Comparing (16) and (13) gives

$$\Delta H^{\dagger} = RT^2 \frac{d}{dT}\left[\ln \frac{Q_C^{\cdot}}{Q_A^{\cdot}}\right] + E_o \qquad (17)$$

Thus without detailed knowledge of the temperature dependence of the partition functions on temperature we cannot evaluate $\Delta H^{\dagger}$ from E_o. However, if the experimental values for $\ln (k_r/T)$ are plotted versus $1/T$ and yield a linear plot, then from (5) and (6) this implies $d/dT \left[\ln (Q_C^{\cdot}/Q_A^{\cdot})\right] \simeq 0$. In this case we can write

$$\Delta H^{\dagger} = E_o \qquad (18)$$

The potential energy barrier, V, is

$$V = E_o + \Sigma \frac{1}{2} h\nu_C - \Sigma \frac{1}{2} h\nu_A \qquad (19)$$

from the definition of E_o and V in Figure A. The summation, $\Sigma\ 1/2\ h\nu_i$, is the sum of all contributions to the zero-point energy of configuration i.

Bibliography

S. Glasstone, K. J. Laidler and H. Eyring, The Theory of Rate Processes. (New York: McGraw-Hill, 1941) Chapter 4

A. A. Frost and R. G. Pearson, Kinetics and Mechanism. (New York: Wiley, 1961) Chapter 5